2019

On the Neumann boundary condition for the acoustic-wave Helmholtz equation, and the relationship between pressure and density fluctuations

Sattik Basu

ON THE NEUMANN BOUNDARY CONDITION FOR THE ACOUSTIC-WAVE HELMHOLTZ EQUATION, AND THE RELATIONSHIP BETWEEN PRESSURE AND DENSITY FLUCTUATIONS

by

SATTIK BASU

A THESIS

Submitted in partial fulfilment to the requirements for the degree of
Master of Science in Engineering
in
The Department of Mechanical and Aerospace Engineering
to
The School of Graduate Studies
of
The University of Alabama in Huntsville

HUNTSVILLE, ALABAMA
2019

In presenting this thesis in partial fulfillment of the requirements for a master's degree from The University of Alabama in Huntsville, I agree that the Library of this University shall make it freely available for inspection. I further agree that permission for extensive copying for scholarly purposes may be granted by my advisor or, in his absence, by the Chair of the Department or the Dean of the School of Graduate Studies. It is also understood that due recognition shall be given to me and to The University of Alabama in Huntsville in any scholarly use which may be made of any material in this thesis.

(student signature)

05/31/2019

(date)

THESIS APPROVAL FORM

Submitted by Sattik Basu in partial fulfillment of the requirements for the degree of Master of Science in Physics and accepted on behalf of the Faculty of the School of Graduate Studies by the thesis committee.

We, the undersigned members of the Graduate Faculty of The University of Alabama in Huntsville, certify that we have advised and/or supervised the candidate on the work described in this thesis. We further certify that we have reviewed the thesis manuscript and approve it in partial fulfillment of the requirements for the degree of Master of Science in Aerospace Engineering.

05/31/2019
Committee Chair

(Date)

05/31/2019

5/31/19

6/10/19
Department Chair

College Dean

7/10/19
Graduate Dean

TABLE OF CONTENTS

LIST OF FIGURES

Figure **Page**

ACKNOWLEDGEMENTS

I would first like to thank my advisor Dr. Sarma L. Rani from the Department of Mechanical and Aerospace Engineering (MAE) at The University of Alabama in Huntsville. The door to Dr. Rani's office was always open, be it regarding research or writing. He consistently allowed this paper to be my own work, relentlessly steering me in the right direction. I would also like to acknowledge him as the second reader of this thesis, and I am gratefully indebted to him for his very valuable comments on this thesis. Without his passionate participation and input, this study could not have been successfully conducted.

To Dr. Vijaya K. Rani, I take pride in acknowledging his insightful guidance. His words of motivation deeply impacted me and was pivotal towards the completion of the research. The 'Theory of Acoustics' course by Dr. Kader Frendi has been an eye-opener for me, and I deeply appreciate him taking time off his busy schedule to be in my committee. I also thank Dr. Sivaguru Ravindran for joining my committee.

I owe a special thanks to Vikram Ramanan, my undergraduate project guide, who ignited the fire in me to be the researcher I am today. His approach and attitude towards research impacted me heavily during my undergraduate days. He has been a constant lifeline during this period, helping me reach my goal faster.

I am forever grateful for the financial support from the Alabama Graduate Research Scholars Program (GRSP) funded through the Alabama Commission for Higher Education and administered by the Alabama EPSCoR.

Zeke Aguilera, the senior staff assistant for the Department of MAE, helped me with all the paperwork that I needed at the right time. His effort of getting me the date of the thesis defense within a short period does not go unappreciated. The same feeling is reciprocated towards Joseah Amai, a dear friend and a fellow research scholar, who sacrificed an entire week to help me prepare for the defense.

Finally, I must express my very profound gratitude to my family and all my friends for providing me with unfailing support and continuous encouragement throughout the period of this study and the process of researching and writing this thesis. This accomplishment would not have been possible without them.

Sattik Basu

ABSTRACT

The School of Graduate Studies

The University of Alabama in Huntsville

Degree Master of Science College/Dept. Engineering/Aerospace

Title On the Neumann Boundary Condition for the Acoustic-wave Helmholtz Equation, and the Relationship Between Pressure and Density Fluctuations

Acoustic wave propagation in a duct is governed by the Helmholtz equation, which can be derived from the fluctuating forms of the mass, momentum, and energy balance equations (after considering harmonic dependence on time). In one-dimensional (1-D) domains, the Helmholtz equation is a second-order ordinary differential equation (ODE), while the fluctuating balance equations are all first-order ODEs. As a result, one needs two boundary conditions for the spatial pressure fluctuation $\hat{p}(x)$ in order to solve the Helmholtz equation, while only one boundary condition each is needed for $\hat{\rho}$, $\hat{u}$ and $\hat{p}$ in case of the fluctuating balance equations. Accordingly, this study was motivated by two principal objectives. The first was to develop the exact Neumann (or derivative) boundary condition at the inlet to a quasi 1-D duct needed to solve the Helmholtz equation. Such an exact boundary condition would ensure that the spatial pressure fluctuations $\hat{p}(x)$ obtained by solving the Helmholtz equation are identical to the $\hat{p}(x)$ obtained through the solution of the fluctuating balance equations. The second principal objective was to determine the exact relationship between the density and pressure fluctuations, $\hat{\rho}$ and $\hat{p}$ respectively, so that the $\hat{\rho}(x)$ calculated using the Helmholtz-equation $\hat{p}(x)$ is again identical to the $\hat{\rho}(x)$ obtained by solving the fluctuating balance equations. The exact $\hat{\rho}$-$\hat{p}$ relation is also compared with the "classical" relation, namely $\hat{\rho} = \hat{p}/\bar{c}^2$, enabling us to evaluate the accuracy of the latter. The Neumann boundary conditions and the $\hat{\rho}$-$\hat{p}$ relations were developed for five cases with axially uniform and non-uniform duct cross-sectional areas, as well

as homogeneous and inhomogeneous mean flow properties such as the velocity, temperature, density and pressure. It is seen that the $\hat{\rho} = \hat{p}/\bar{c}^2$ relation is valid only for the cases with uniform cross-sectional area and homogeneous mean properties. For the cases with uniform cross-section, inhomogeneous mean properties (with zero or uniform mean flow), the "classical" $\hat{\rho}$ relation suffers from significant errors both in amplitude and phase.

Committee Chair (Date)

Department Chair

Graduate Dean

Chapter 1

Introduction

The study of duct acoustics has various applications. Of these, one that is of utmost significance is the exhaust noise from internal combustion engines. A well designed muffler can reduce this noise either by dissipating the acoustic energy into heat or reflecting it back by area discontinuities [1].

1.1 Motivation

The behaviour of one-dimensional acoustic fields in ducts with a mean temperature gradient is a problem of considerable scientific and practical interest. For instance, there is a need to develop an understanding of the manner in which a mean axial temperature gradient affects the propagation of sound waves and the stability of small amplitude disturbances in a duct [2]. Acoustic wave propagation in a duct is governed by the Helmholtz equation, which can be derived from the fluctuating forms of the mass, momentum, and energy balance equations (after considering harmonic dependence on time) [3]. However, deriving the Helmholtz (or wave) equation from the equations of the vibrating string [4] has been one of the earliest practices and still finds its importance [5, 6, 7] a century later.

In one-dimensional (1-D) domains, the Helmholtz equation is a second-order ordinary differential equation (ODE), while the fluctuating balance equations are all first-order ODEs. Any three acoustic variable could be used to solve the fluc-

tuating governing equations. Dowling et al. [8] used acoustic entropy instead of pressure and Mawardi [9] used impedance and admittance instead of acoustic variable. The three acoustic variables chosen in this study are acoustic pressure, density and velocity. As a result, one needs two boundary conditions for the spatial pressure fluctuation $\hat{p}(x)$ in order to solve the Helmholtz equation, while only one boundary condition each is needed for $\hat{\rho}$, $\hat{u}$ and $\hat{p}$ in case of the fluctuating balance equations.

1.2 Objectives

This study was motivated by two principal objectives. The first was to develop the exact Neumann (or derivative) boundary condition at the inlet to a quasi 1-D duct needed to solve the Helmholtz equation. Such an exact boundary condition would ensure that the spatial pressure fluctuations $\hat{p}(x)$ obtained by solving the Helmholtz equation are identical to the $\hat{p}(x)$ obtained through the solution of the fluctuating balance equations. The second principal objective was to determine the exact relationship between the density and pressure fluctuations, $\hat{\rho}$ and $\hat{p}$ respectively, so that the $\hat{\rho}(x)$ calculated using the Helmholtz-equation $\hat{p}(x)$ is again identical to the $\hat{\rho}(x)$ obtained by solving the fluctuating balance equations. The exact $\hat{\rho}$-$\hat{p}$ relation is also compared with the "classical" relation, namely $\hat{\rho} = \hat{p}/\bar{c}^2$, enabling us to evaluate the accuracy of the latter. Five mean flow and duct geometry cases are investigated.

I Uniform Mean Properties with No Mean Flow

II Uniform Mean Properties with Mean Flow

III Non-Uniform Mean Properties with No Mean Flow

IV Non-Uniform Mean Properties with Uniform Mean Flow

V Non-Uniform Mean Properties with Non-Uniform Mean Flow

Non-uniform temperature gradient has been the focus on several studies [10, 11, 12, 13, 14, 15], but none as extensive as this, where all properties having non-uniformities is also considered.

1.3 Outline of the thesis

Chapter 2 introduces the quasi 1-D balance equations. These are decomposed into the mean and fluctuating forms. The equation of state is also defined in the differential form. The mean balance equations in addition to the mean equation of the state dictates the mean properties, namely pressure $\bar{p}$, density $\bar{\rho}$, velocity $\bar{u}$ and the cross-sectional area S.

Chapters 3 and 4 examines the two cases concerning uniform mean properties. Chapter 3 has zero velocity while chapter 4 considers a spatially uniform velocity. It was found that the fluctuating pressure-density relation for both the cases is $\hat{p} = \hat{\rho}c^2$. This is the same as the well-defined Classical relation that was discussed earlier.

Chapters 5, 6 and 7 investigates the non-uniform mean properties. User-defined non-uniform mean temperature profiles (both linear and non-linear) are considered. A linear temperature profile : $T(x) = mx + c$ has been considered based on the works done by Rani et al. [3] and Sujith et al. [2]. The non-linear profile considered is: $T(x) = (ax+b)^{\frac{4}{3}}$, also called the four-thirds profile which is known to result in solutions for a travelling wave as shown by Subrahmanyam et al. [16].

Chapter 5 assumes zero mean velocity, while chapter 6 assumes a uniform mean velocity. Chapter 7 is the most generalized case with no assumptions. In these cases, consisting of non-uniform mean properties, the exact $\hat{\rho}$-$\hat{p}$ relation differs from the Classical relation. Due to this, the percentage of error from considering the Classical $\hat{\rho}$ instead of the exact derived $\hat{\rho}$ is also investigated. The error for each of the cases is tabulated in table 8.1.

Chapter 2

Governing Equations

In this study, the following basic assumptions are made regarding the propagation of acoustic waves.

- The medium is isentropic (and hence adiabatic).
- Viscous dissipation losses are neglected.
- There is no heat generation due to processes such as chemical reactions.

With these assumptions, the governing mass, momentum, and energy balance equations, respectively, are [3]

$$\frac{\partial(S\rho)}{\partial t} + \frac{\partial(S\rho u)}{\partial x} = 0 \tag{2.1}$$

$$\rho\left(\frac{\partial u}{\partial t} + u\frac{\partial u}{\partial x}\right) + \frac{\partial p}{\partial x} = 0 \tag{2.2}$$

$$\frac{\partial(Sp)}{\partial t} + Su\frac{\partial p}{\partial x} + \gamma p\frac{\partial(Su)}{\partial x} = 0 \tag{2.3}$$

where p is the fluid pressure, ρ is the density, u is the axial velocity, and $S(x)$ is the local cross-sectional area. Decomposing flow variables into the respective mean and fluctuating components [e.g., $p(x,t) = \bar{p}(x)+p'(x,t)$, where $p'(x,t)/\bar{p}(x) \ll 1$],

the mean governing equations are

$$\begin{aligned} S\bar{u}\frac{\mathrm{d}\bar{\rho}}{\mathrm{d}x} + S\bar{\rho}\frac{\mathrm{d}\bar{u}}{\mathrm{d}x} + \bar{\rho}\bar{u}\frac{\mathrm{d}S}{\mathrm{d}x} &= 0 \\ \bar{\rho}\bar{u}\frac{\mathrm{d}\bar{u}}{\mathrm{d}x} + \frac{\mathrm{d}\bar{p}}{\mathrm{d}x} &= 0 \\ S\bar{u}\frac{\mathrm{d}\bar{p}}{\mathrm{d}x} + \gamma S\bar{p}\frac{\mathrm{d}\bar{u}}{\mathrm{d}x} + \gamma\bar{p}\bar{u}\frac{\mathrm{d}S}{\mathrm{d}x} &= 0 \end{aligned} \tag{2.4}$$

and the linearized fluctuating balance equations are

$$\begin{aligned} S\frac{\partial\rho'}{\partial t} + S\bar{u}\frac{\partial\rho'}{\partial x} + S\frac{\mathrm{d}\bar{\rho}}{\mathrm{d}x}u' + S\bar{\rho}\frac{\partial u'}{\partial x} + S\frac{\mathrm{d}\bar{u}}{\mathrm{d}x}\rho' + \bar{\rho}\frac{\mathrm{d}S}{\mathrm{d}x}u' + \bar{u}\frac{\mathrm{d}S}{\mathrm{d}x}\rho' &= 0 \\ \bar{\rho}\frac{\partial u'}{\partial t} + \bar{u}\frac{\mathrm{d}\bar{u}}{\mathrm{d}x}\rho' + \bar{\rho}\bar{u}\frac{\partial u'}{\partial x} + \bar{\rho}\frac{\mathrm{d}\bar{u}}{\mathrm{d}x}u' + \frac{\partial p'}{\partial x} &= 0 \\ S\frac{\partial p'}{\partial t} + S\bar{u}\frac{\partial p'}{\partial x} + S\frac{\mathrm{d}\bar{p}}{\mathrm{d}x}u' + \gamma S\bar{p}\frac{\partial u'}{\partial x} + \gamma S\frac{\mathrm{d}\bar{u}}{\mathrm{d}x}p' + \gamma\bar{p}\frac{\mathrm{d}S}{\mathrm{d}x}u' + \gamma\bar{u}\frac{\mathrm{d}S}{\mathrm{d}x}p' &= 0 \end{aligned} \tag{2.5}$$

In addition to the mean and the fluctuating equations, we also consider the equation of state given by

$$p = \rho R_{air} T \tag{2.6}$$

The mean sound speed is related to the mean temperature through $\bar{c} = \sqrt{\gamma R_{air}\bar{T}}$. Using this relation, the mean equation of state can be written as

$$\gamma\bar{p} = \bar{\rho}\bar{c}^2 \tag{2.7}$$

which in the differential form is

$$\gamma\frac{\mathrm{d}\bar{p}}{\mathrm{d}x} = \bar{c}^2\frac{\mathrm{d}\bar{\rho}}{\mathrm{d}x} + 2\bar{c}\bar{\rho}\frac{\mathrm{d}\bar{c}}{\mathrm{d}x} \tag{2.8}$$

For the five cases considered in the study, we now present the derivation of the Neumann boundary condition for the Helmholtz equation, as well as the relation between the density and pressure fluctuations.

Chapter 3

CASE I: Uniform Mean Properties with No Mean Flow

We start with the most simplified case. We present the mean properties, followed by the fluctuating properties. The Helmholtz equation is then derived followed by the derivation of the exact $\hat{\rho}$-$\hat{p}$ relation pertaining to this case.

3.1 Mean properties

Case I is the most simplified case with maximum restrictions on the mean properties—temperature $\bar{T}(x)$, pressure $\bar{p}(x)$ and density $\bar{\rho}(x)$—i.e., they are all uniform across the duct. This case is further simplified by assuming no mean flow, hence the velocity, $\bar{u}(x)$ is zero. Therefore, the assumptions are

$$\bar{u}(x) = 0; \quad \frac{\mathrm{d}\bar{T}}{\mathrm{d}x} = 0; \quad \frac{\mathrm{d}\bar{p}}{\mathrm{d}x} = 0; \quad \frac{\mathrm{d}\bar{\rho}}{\mathrm{d}x} = 0; \tag{3.1}$$

These assumptions (3.1) when applied to the mean balance equations (2.4) and the differential equation of state (2.8) returns

$$\frac{\mathrm{d}S}{\mathrm{d}x} = 0; \quad \frac{\mathrm{d}\bar{c}}{\mathrm{d}x} = 0$$

Thus with the assumptions (3.1), it is found that the cross-sectional area S, and the mean sound speed $\bar{c}$, are both uniform across the length of the duct. Since all the properties are spatially uniform, the functionality of 'x' has been dropped from the properties. The mean properties are thus all algebraic relations

$$\bar{\rho} = \rho_0; \quad \bar{T} = T_0; \quad \bar{c} = \sqrt{\gamma R_{air} \bar{T}}; \quad \bar{p} = \bar{\rho} R_{air} \bar{T};$$

where the mean density $\bar{\rho}$ is considered to be 1 kg/m^3 and the mean temperature $\bar{T}$ is 2000 K. The ratio of the specific heats γ and the specific gas constant R_{air} are taken as 1.4 and 287 J/kg-K respectively.

3.2 Fluctuating balance equations

Using the assumptions (3.1) for Case I in equations (2.5), the balance equations for the fluctuating properties reduces to

$$\frac{\partial \rho'}{\partial t} + \bar{\rho} \frac{\partial u'}{\partial x} = 0 \tag{3.2}$$

$$\bar{\rho} \frac{\partial u'}{\partial t} + \frac{\partial p'}{\partial x} = 0 \tag{3.3}$$

$$\frac{\partial p'}{\partial t} + \gamma \bar{p} \frac{\partial u'}{\partial x} = 0 \tag{3.4}$$

Considering the harmonic temporal dependence of the three acoustic variables $p' = \hat{p} e^{i\omega t}$, $u' = \hat{u} e^{i\omega t}$ and $\rho' = \hat{\rho} e^{i\omega t}$, the fluctuating balance equations become

$$i\omega \hat{\rho} + \bar{\rho} \frac{\mathrm{d}\hat{u}}{\mathrm{d}x} = 0 \tag{3.5}$$

$$i\omega \bar{\rho} \hat{u} + \frac{\mathrm{d}\hat{p}}{\mathrm{d}x} = 0 \tag{3.6}$$

$$i\omega \hat{p} + \bar{\rho} \bar{c}^2 \frac{\mathrm{d}\hat{u}}{\mathrm{d}x} = 0 \tag{3.7}$$

The above sets of equations can be solved with the following inlet boundary

condition

$$\hat{p}(0) = \hat{p}_0; \quad \hat{u}(0) = \hat{u}_0; \quad \hat{\rho}(0) = \frac{\hat{p}_0}{\bar{c}^2}; \tag{3.8}$$

where $\hat{p}_0$=1 Pa and $\hat{u}_0 = 0.01$ m/s. Any arbitrary value should not be considered for the fluctuating inlet density, $\hat{\rho}(0)$. This is due to $\hat{\rho}$ and $\hat{p}$ having an algebraic relation (this will be shown in the derivation of the exact $\hat{\rho}$-$\hat{p}$ relation (3.12) in section 3.4).

The $\hat{\rho}$ and $\hat{p}$ obtained from the solution of equations (3.5)-(3.7) will be used as the benchmark to validate the $\hat{p}$ from the Helmholtz equation and the $\hat{\rho}$ from the exact $\hat{\rho}$-$\hat{p}$ relation.

3.3 Helmholtz equation for $\hat{p}$

For the development of the Helmholtz equation, we start by deriving the wave equation. This process involves $\frac{\partial}{\partial x}$[equation (3.3)] $- \frac{1}{\bar{c}^2}\frac{\partial}{\partial t}$[equation (3.4)], giving

$$\frac{\partial^2 p'}{\partial x^2} - \frac{1}{\bar{c}^2}\frac{\partial^2 p'}{\partial t^2} = 0 \tag{3.9}$$

The Helmholtz equation is obtained by removing the temporal dependence in the wave equation (i.e., $p' = \hat{p}e^{i\omega t}$).

$$\frac{\mathrm{d}^2\hat{p}}{\mathrm{d}x^2} + \frac{\omega^2}{\bar{c}^2}\hat{p} = 0 \tag{3.10}$$

The Dirichlet boundary condition for the Helmholtz equation is identical to that of the fluctuating balance equations ($\hat{p}(0) = \hat{p}_0$). The Neumann boundary condition can be obtained effortlessly from Equation (3.6).

$$\left.\frac{\mathrm{d}\hat{p}}{\mathrm{d}x}\right|_{x=0} = -i\omega\bar{\rho}\hat{u}_0 \tag{3.11}$$

The boundary condition (BC) in (3.11) is the exact Neumann BC for the

Helmholtz equation. We now derive the exact relation between $\hat{\rho}$ and $\hat{p}$.

3.4 Exact relation between $\hat{\rho}$ and $\hat{p}$

Now, to get the exact relationship between $\hat{p}$ and $\hat{\rho}$, we manipulate the fluctuating balnce equations. The process involves $\frac{1}{\bar{c}^2}$[equation (3.7)] − [equation (3.5)]. The following relation is developed.

$$\hat{\rho} = \frac{\hat{p}}{\bar{c}^2} \tag{3.12}$$

Having obtained the exact relation between $\hat{p}$ and $\hat{\rho}$, we now solve for $\hat{p}$ using two approaches. The first involves solving the Helmholtz equation for $\hat{p}$, and the second consists of solving the fluctuating balance equations (3.5)-(3.7). The latter serves as the benchmark for the former.

This relation will be referred to as the "Classical" relation between $\hat{\rho}$ and $\hat{p}$ throughout this study. This relation also sets the basis for comparison for the cases involving Non-Uniform Mean Properties.

3.5 Fluctuating Property Plots

We present the pressure and density fluctuations, $\hat{p}$ and $\hat{\rho}$, obtained by solving the fluctuating balnce equations (3.5)-(3.7), as well as the Helmholtz equation (4.10) in figure 3.1. These equations are solved at a frequency $\omega = 500$ rad/s. All fluctuating profiles have been non-dimensionalized with its respective mean property to removes any specificity towards a particular initial mean value.

In figure 3.1a, we compare two $\hat{p}$ profiles. The $\hat{p}$ profile labelled "Helmholtz" is obtained from solving the Helmholtz equation (3.10). The $\hat{p}$ profile labelled "Conservation" is obtained by directly solving the fluctuating balnce equations (3.5)-(3.7). These two solutions are essentially identical, validating the Helmholtz equation solution. In figure 3.1b, we compare the Helmholtz and the Conservation $\hat{\rho}$. The Helmholtz $\hat{\rho}$ is essentially solving equation (3.12) using the $\hat{p}$ obtained from

solving the Helmholtz equation (3.10). Both the $\hat{\rho}$ profiles are indistinguishable and perfectly coincide with each other.

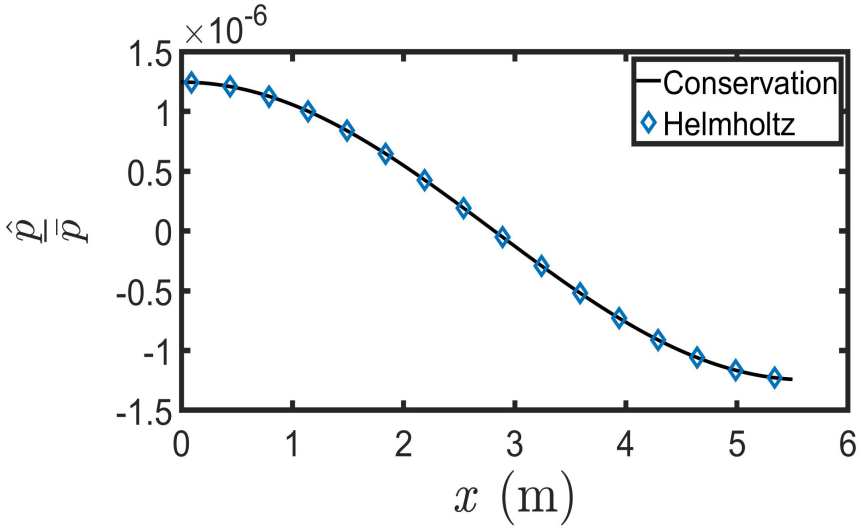

(a) Non-Dimensionalized Fluctuating Pressure Profile

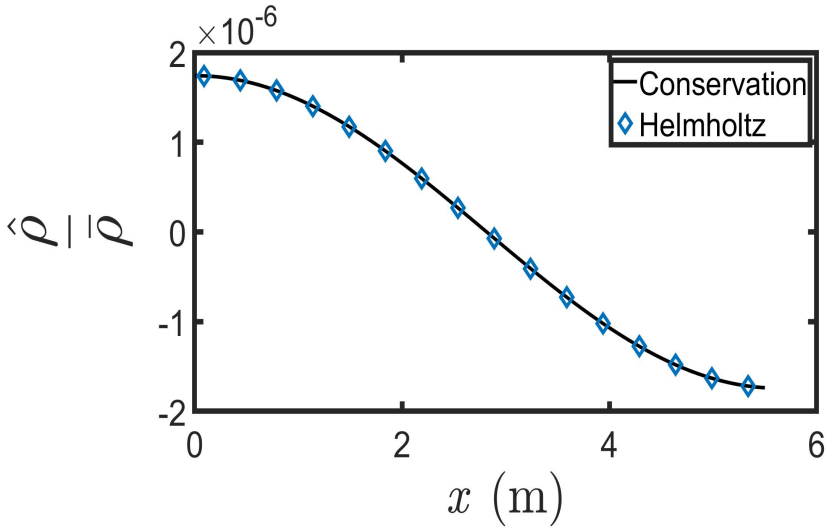

(b) Non-Dimensionalized Fluctuating Density Profile

Figure 3.1: Fluctuating Property Profiles of Case I

Chapter 4

CASE II: Uniform Mean Properties with Uniform Mean Flow

Case II is the final case investigating uniform mean properties. We begin by presenting the mean properties, followed by the fluctuating properties. The Helmholtz equation is then derived followed by the derivation of the exact $\hat{\rho}$-$\hat{p}$ relation pertaining to this case.

4.1 Mean properties

The assumptions made in Case II affects all the mean properties—temperature $\bar{T}(x)$, velocity $\bar{u}(x)$, pressure $\bar{p}(x)$ and density $\bar{\rho}(x)$—i.e., they are all uniform across the duct. Case II differs from Case I in one assumption, i.e., the mean velocity is uniform in this case, whereas it was zero in Case II. The assumptions are listed below

$$\frac{\mathrm{d}\bar{u}}{\mathrm{d}x} = 0; \quad \frac{\mathrm{d}\bar{T}}{\mathrm{d}x} = 0; \quad \frac{\mathrm{d}\bar{p}}{\mathrm{d}x} = 0; \quad \frac{\mathrm{d}\bar{\rho}}{\mathrm{d}x} = 0; \tag{4.1}$$

These assumptions (4.1) when applied to the mean governing equations (2.4) and the differential equation of state (2.8) gives

$$\frac{\mathrm{d}S}{\mathrm{d}x} = 0; \quad \frac{\mathrm{d}\bar{c}}{\mathrm{d}x} = 0$$

Thus with the assumptions (4.1), it is found that the cross-sectional area S,

and the mean sound speed $\bar{c}$, are both uniform across the length of the duct. Since all the properties are spatially uniform, the functionality of 'x' has been dropped from the properties. The mean properties are thus all algebraic relations

$$\bar{\rho} = \rho_0; \qquad \bar{T} = T_0; \qquad \bar{M} = M_0;$$
$$\bar{c} = \sqrt{\gamma R_{air} \bar{T}}; \qquad \bar{p} = \bar{\rho} R_{air} \bar{T}; \qquad \bar{u} = M_0 \bar{c};$$

where the mean density $\bar{\rho}$ is considered to be 1 kg/m^3, mean temperature $\bar{T}$ is 2000 K and the inlet Mach number is taken to be 0.3.

4.2 Fluctuating balance equations

Using the assumptions (4.1) for Case II, the fluctuating balance equations (2.5) reduces to

$$\frac{\partial \rho'}{\partial t} + \bar{u}\frac{\partial \rho'}{\partial x} + \bar{\rho}\frac{\partial u'}{\partial x} = 0 \tag{4.2}$$
$$\bar{\rho}\frac{\partial u'}{\partial t} + \bar{\rho}\bar{u}\frac{\partial u'}{\partial x} + \frac{\partial p'}{\partial x} = 0 \tag{4.3}$$
$$\frac{\partial p'}{\partial t} + \bar{u}\frac{\partial p'}{\partial x} + \gamma\bar{p}\frac{\partial u'}{\partial x} = 0 \tag{4.4}$$

Considering the harmonic temporal dependence of the three acoustic variables $p' = \hat{p}e^{i\omega t}$, $u' = \hat{u}e^{i\omega t}$ and $\rho' = \hat{\rho}e^{i\omega t}$, the fluctuating balance equations become

$$i\omega\hat{\rho} + \bar{u}\frac{\mathrm{d}\hat{\rho}}{\mathrm{d}x} + \bar{\rho}\frac{\mathrm{d}\hat{u}}{\mathrm{d}x} = 0 \tag{4.5}$$
$$i\omega\bar{\rho}\hat{u} + \bar{\rho}\bar{u}\frac{\mathrm{d}\hat{u}}{\mathrm{d}x} + \frac{\mathrm{d}\hat{p}}{\mathrm{d}x} = 0 \tag{4.6}$$
$$i\omega\hat{p} + \bar{u}\frac{\mathrm{d}\hat{p}}{\mathrm{d}x} + \bar{\rho}\bar{c}^2\frac{\mathrm{d}\hat{u}}{\mathrm{d}x} = 0 \tag{4.7}$$

The above sets of equations can be solved with the following inlet boundary

condition

$$\hat{p}(0) = \hat{p}_0; \quad \hat{u}(0) = \hat{u}_0; \quad \hat{\rho}(0) = \frac{\hat{p}_0}{\bar{c}^2}; \tag{4.8}$$

where $\hat{p}_0 = 1$ Pa and $\hat{u}_0 = 0.01$ m/s. Any arbitrary value should not be considered for the fluctuating inlet density, $\hat{\rho}(0)$. This is due to $\hat{\rho}$ and $\hat{p}$ having an algebraic relation (this will be shown in the derivation of the exact $\hat{\rho}$-$\hat{p}$ relation (4.14) in section 4.4).

The $\hat{\rho}$ and $\hat{p}$ obtained from the solution of equations (4.5)-(4.7) will be used as the benchmark to validate the $\hat{p}$ from the Helmholtz equation and the $\hat{\rho}$ from the exact $\hat{\rho}$-$\hat{p}$ relation.

4.3 Helmholtz equation for $\hat{p}$

For the development of the Helmholtz equation, we start by deriving the wave equation. This process involves $\frac{\partial}{\partial x}$[equation (4.3)] $- \frac{1}{\bar{c}^2}\frac{\partial}{\partial t}$[equation (4.4)], giving

$$(1 - \bar{M}^2)\frac{\partial^2 p'}{\partial x^2} - \frac{1}{\bar{c}^2}\frac{\partial^2 p'}{\partial t^2} - \frac{2\bar{M}}{\bar{c}}\frac{\partial^2 p'}{\partial t \partial x} = 0 \tag{4.9}$$

The Helmholtz Equation is obtained by removing the temporal dependence in the Wave Equation (i.e., $p' = \hat{p}e^{i\omega t}$).

$$(1 - \bar{M}^2)\frac{\mathrm{d}^2\hat{p}}{\mathrm{d}x^2} - \frac{2i\omega\bar{M}}{\bar{c}}\frac{\mathrm{d}\hat{p}}{\mathrm{d}x} + \frac{\omega^2}{\bar{c}^2}\hat{p} = 0 \tag{4.10}$$

The Dirichlet boundary condition for the Helmholtz equation is identical to that of the fluctuating balance equations ($\hat{p}(0) = \hat{p}_0$). The Neumann boundary condition can be obtained from Equation (4.6).

$$\frac{\mathrm{d}\hat{p}}{\mathrm{d}x} = -i\omega\bar{\rho}\hat{u} - \bar{\rho}\bar{u}\frac{\mathrm{d}\hat{u}}{\mathrm{d}x} \tag{4.11}$$

Equation (4.11) consists of a $\frac{\mathrm{d}\hat{u}}{\mathrm{d}x}$ term that needs to be replaced by $\hat{p}$ and $\hat{u}$. This

process removes the necessity to calculate derivatives to solve for the Neumann boundary condition. $\frac{1}{\bar{u}}$[equation (4.7)] − [equation (4.6)] provides the necessary relation.

$$\frac{\mathrm{d}\hat{u}}{\mathrm{d}x} = \frac{i\omega\bar{M}^2}{(\bar{M}^2-1)\bar{u}}\left(\frac{\hat{p}}{\bar{\rho}\bar{u}} - \hat{u}\right) \tag{4.12}$$

Substituting the $\frac{\mathrm{d}\hat{u}}{\mathrm{d}x}$ relation (4.12) in equation (4.11), we get the Neumann boundary condition for the Helmholtz equation (4.10).

$$\left.\frac{\mathrm{d}\hat{p}}{\mathrm{d}x}\right|_{x=0} = \frac{i\bar{\rho}_0\omega}{(\bar{M}_0^2-1)}\hat{u}_0 - \frac{i\omega\bar{M}_0^2}{(\bar{M}_0^2-1)\bar{u}_0}\hat{p}_0 \tag{4.13}$$

The boundary condition (BC) in (4.13) is the exact Neumann BC for the Helmholtz equation. We now derive the exact relation between $\hat{\rho}$ and $\hat{p}$.

4.4 Exact relation between $\hat{\rho}$ and $\hat{p}$

To get the exact relationship between $\hat{p}$ and $\hat{\rho}$, we manipulate the fluctuating balance equations. The process involves $\frac{1}{\bar{c}^2}$[equation (4.7)] − [equation (4.5)]. The following relation is developed.

$$\hat{\rho} = \frac{\hat{p}}{\bar{c}^2} \tag{4.14}$$

This is the exact relation between the fluctuating density and pressure for Case II. Using the $\hat{p}$ profile from the Helmholtz equation, the "Helmholtz" density profile can now be obtained. It should be noted that the $\hat{\rho}$-$\hat{p}$ relation for Cases I and II are identical.

4.5 Fluctuating Property Plots

We present the pressure and density fluctuations, $\hat{p}$ and $\hat{\rho}$, obtained by solving the fluctuating balance equations (4.5)-(4.7), as well as the Helmholtz equation (4.10) in figure 4.1. These equations are solved at a frequency $\omega = 500$ rad/s.

In figure 4.1a, we compare two $\hat{p}$ profiles. The $\hat{p}$ profile labelled "Helmholtz"

is obtained from solving the Helmholtz equation (4.10). The $\hat{p}$ profile labelled "Conservation" is obtained by directly solving the fluctuating balance equations (4.5)-(4.7). These two solutions are identical, validating the Helmholtz equation solution. In figure 4.1b, we compare the Helmholtz and the Conservation $\hat{\rho}$. The Helmholtz $\hat{\rho}$ is essentially solving equation (4.14) using the $\hat{p}$ obtained from solving the Helmholtz equation (4.10). Both the $\hat{\rho}$ profiles are also identical.

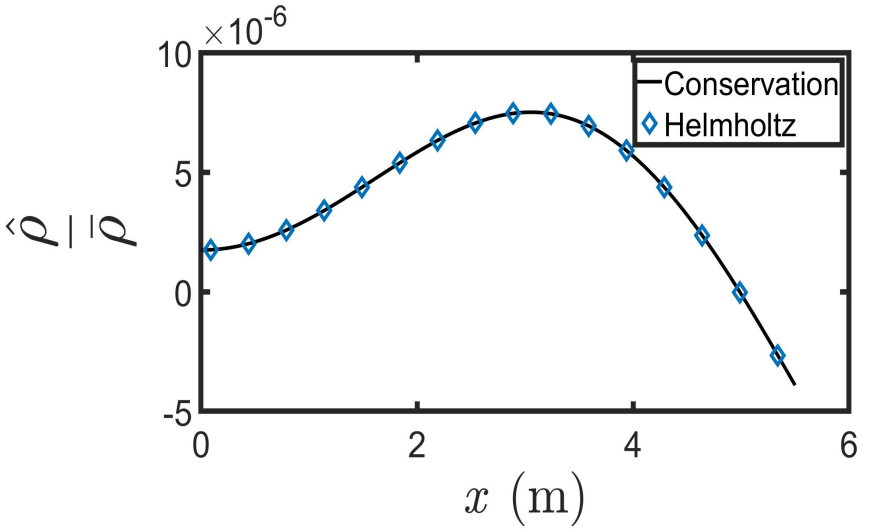

(a) Non-Dimensionalized Fluctuating Pressure Profile

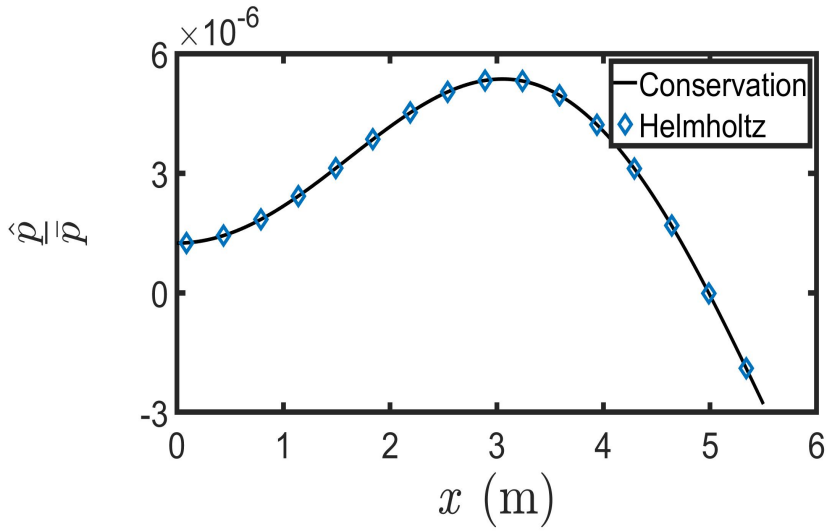

(b) Non-Dimensionalized Fluctuating Density Profile

Figure 4.1: Fluctuating Property Plots for Case II

Chapter 5

CASE III: Non-Uniform Mean Properties with No Mean Flow

As we transition to the non-uniformities in the mean properties, we start with a rather simplifying assumption of no mean flow. We begin by presenting the mean properties, followed by the fluctuating properties. The Helmholtz equation is then derived followed by the derivation of the exact $\hat{\rho}$-$\hat{p}$ relation pertaining to this case.

5.1 Mean properties

Case III is the first case to deal with non-uniformities in mean quantities—temperature $\bar{T}(x)$ and density $\bar{\rho}(x)$. Here, we are still restricting the mean velocity of the medium. We also assume a uniform cross-sectional area profile. Thus the assumptions in this case are

$$\bar{u} = 0; \quad \frac{\mathrm{d}\bar{\rho}}{\mathrm{d}x} \neq 0; \quad \frac{\mathrm{d}S}{\mathrm{d}x} = 0; \quad \frac{\mathrm{d}\bar{T}}{\mathrm{d}x} \neq 0; \tag{5.1}$$

Using the above mentioned assumptions (5.1), the mean conservation equations (2.4) returns

$$\frac{\mathrm{d}\bar{p}}{\mathrm{d}x} = 0 \tag{5.2}$$

Now applying (5.1) and (5.2) to the differential equation of state (2.8), we get the mean density profile.

$$\frac{1}{\bar{\rho}}\frac{\mathrm{d}\bar{\rho}}{\mathrm{d}x} = -\frac{2}{\bar{c}}\frac{\mathrm{d}\bar{c}}{\mathrm{d}x}$$

In the above equations, the speed of sound is obtained using $\bar{c}(x) = \sqrt{\gamma R_{gas}\bar{T}(x)}$ and the inlet boundary condition to solve the ODE is $\bar{\rho}_0 = 1$ kg/m^3. Two profiles of $\bar{T}(x)$ have been considered, which are

- Linear profile, $\bar{T}(x) = \bar{T}_0 + mx$, and
- Power law profile, $\left(\bar{T}_0^{\frac{3}{4}} + bx\right)^{\frac{4}{3}}$

Here, we considered $\bar{T}_0 = 2000$ K with $m = -25$ K/m for the linear case, and $\bar{T}_0 = 1000$ K with $b = -1$ K$^{\frac{3}{4}}$/m for the non-linear case. Every other mean property is defined by algebraic relations which are derived from the mean conservation equations using the above assumptions. The properties are thus

$$\bar{c}(x) = \sqrt{\gamma R_{gas}\bar{T}(x)}; \quad \bar{p} = \frac{\bar{\rho}\bar{c}^2}{\gamma}; \quad \bar{u} = 0;$$

Figure 5.1 presents the mean property profiles obtained for the linear mean temperature case. The linear temperature profile considered in Case III is shown figure 5.1a, where we see a temperature decrease of $\sim$7% over a duct length of 5.5 m. Figure 5.1b shows the uniformity of mean pressure along the duct length. The mean density, shown in figure 5.1c, increases along the duct, while an increase is exhibited by the sound speed profile in figure 5.1d. Both the trends are weakly non-linear.

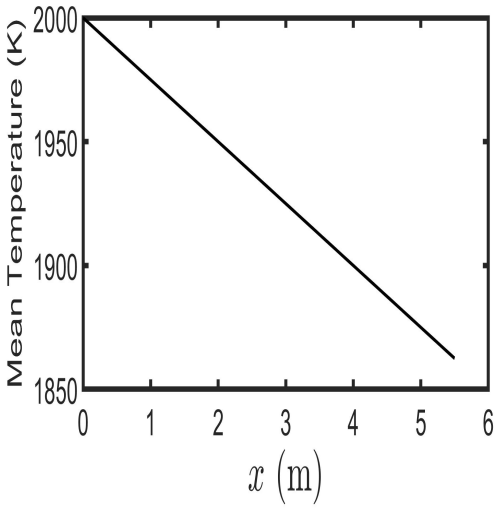

(a) Mean Temperature Profile

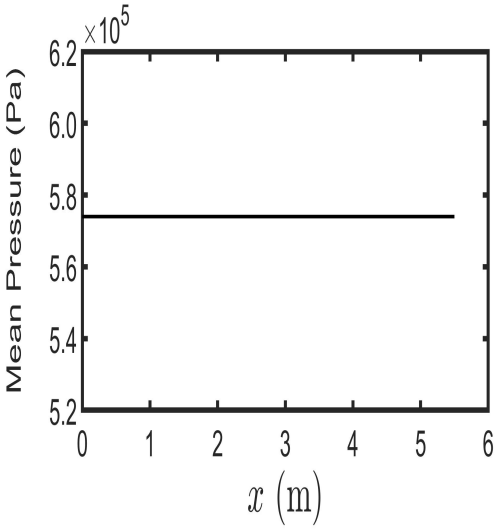

(b) Mean Pressure Profile

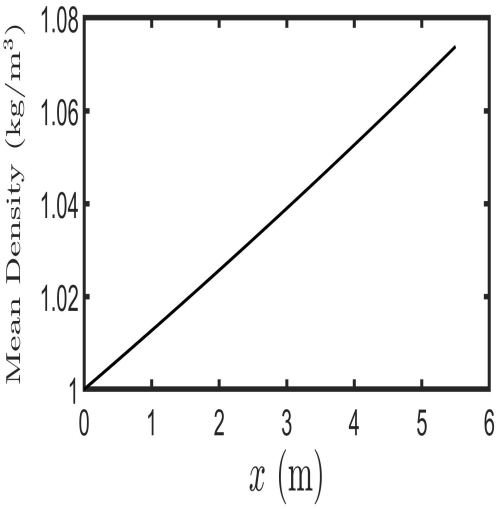

(c) Mean Density Profile

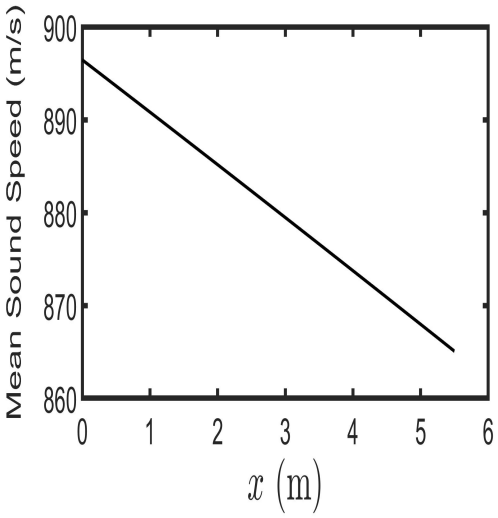

(d) Mean Sound Speed Profile

Figure 5.1: Mean Quantity Profiles

5.2 Fluctuating balance equations

The mean properties dictate the coefficients of the conservation equations for the fluctuating properties. Applying equations (5.1) and (5.2) on the the fluctuating conservation equations (2.5), we get

$$\frac{\partial \rho'}{\partial t} + \frac{\mathrm{d}\bar{\rho}}{\mathrm{d}x}u' + \bar{\rho}\frac{\partial u'}{\partial x} = 0 \tag{5.3}$$

$$\bar{\rho}\frac{\partial u'}{\partial t} + \frac{\partial p'}{\partial x} = 0 \tag{5.4}$$

$$\frac{\partial p'}{\partial t} + \gamma\bar{p}\frac{\partial u'}{\partial x} = 0 \tag{5.5}$$

Considering the harmonic temporal dependence of the three acoustic variables $p' = \hat{p}e^{i\omega t}$, $u' = \hat{u}e^{i\omega t}$ and $\rho' = \hat{\rho}e^{i\omega t}$, the fluctuating conservation equations become

$$i\omega\hat{\rho} + \frac{\mathrm{d}\bar{\rho}}{\mathrm{d}x}\hat{u} + \bar{\rho}\frac{\mathrm{d}\hat{u}}{\mathrm{d}x} = 0 \tag{5.6}$$

$$i\omega\bar{\rho}\hat{u} + \frac{\mathrm{d}\hat{p}}{\mathrm{d}x} = 0 \tag{5.7}$$

$$i\omega\hat{p} + \bar{\rho}\bar{c}^2\frac{\mathrm{d}\hat{u}}{\mathrm{d}x} = 0 \tag{5.8}$$

The boundary conditions necessary to solve the above equations are

$$\hat{p}(0) = \hat{p}_0; \quad \hat{u}(0) = \hat{u}_0; \quad \hat{\rho}(0) = \frac{\hat{p}_0}{\bar{c}_0^2} + \frac{i}{\omega}\frac{\mathrm{d}\bar{\rho}}{\mathrm{d}x}\bigg|_{x=0}\hat{u}_0; \tag{5.9}$$

where $\hat{p}_0 = 1$ Pa and $\hat{u}_0 = 0.01$ m/s. Any arbitrary value should not be considered for the fluctuating inlet density, $\hat{\rho}(0)$. This is due to $\hat{\rho}$ and $\hat{p}$ having an algebraic relation (this will be shown in the derivation of the exact $\hat{\rho}$-$\hat{p}$ relation (5.14) in section 5.4).

The $\hat{\rho}$ and $\hat{p}$ obtained from the solution of equations (5.6)-(5.8) will be used as the benchmark to validate the $\hat{p}$ from the Helmholtz equation and the $\hat{\rho}$ from the exact $\hat{\rho}$-$\hat{p}$ relation.

5.3 Helmholtz equation for $\hat{p}$

The wave equation for Case III is obtained from equations (5.4) and (5.5). This process involves $\frac{\partial}{\partial x}$[equation (5.4)] $- \frac{1}{\bar{c}^2}\frac{\partial}{\partial t}$[equation (5.5)], giving

$$\frac{\partial^2 p'}{\partial x^2} - \frac{1}{\bar{c}^2}\frac{\partial^2 p'}{\partial t^2} + \frac{\mathrm{d}\bar{\rho}}{\mathrm{d}x}\frac{\partial u'}{\partial t} = 0 \tag{5.10}$$

The Helmholtz equation is obtained by substituting into the wave equation $p' = \hat{p}e^{i\omega t}$, $u' = \hat{u}e^{i\omega t}$ and $\rho' = \hat{\rho}e^{i\omega t}$.

$$\frac{\mathrm{d}^2\hat{p}}{\mathrm{d}x^2} + i\omega\frac{\mathrm{d}\bar{\rho}}{\mathrm{d}x}\hat{u} + \frac{\omega^2}{\bar{c}^2}\hat{p} = 0. \tag{5.11}$$

Substituting Equation (5.7) for the $\hat{u}$ term, we get the final Helmholtz Equation in terms of only $\hat{p}$, which is

$$\frac{\mathrm{d}^2\hat{p}}{\mathrm{d}x^2} - \frac{1}{\bar{\rho}}\frac{\mathrm{d}\bar{\rho}}{\mathrm{d}x}\frac{\mathrm{d}\hat{p}}{\mathrm{d}x} + \frac{\omega^2}{\bar{c}^2}\hat{p} = 0 \tag{5.12}$$

This equation has the same form that was derived by Sujith et al. [2] for non-uniform temperature profiles.

The Dirichlet boundary condition for the Helmholtz equation is identical to that of the fluctuating conservation equations ($\hat{p}(0) = \hat{p}_0$). The Neumann boundary condition can be obtained quite effortlessly from Equation (5.7).

$$\left.\frac{\mathrm{d}\hat{p}}{\mathrm{d}x}\right|_{x=0} = -i\omega\bar{\rho}_0\hat{u}_0 \tag{5.13}$$

The boundary condition (BC) in (5.13) is the exact Neumann BC for the Helmholtz equation. We now derive the exact relation between $\hat{\rho}$ and $\hat{p}$.

5.4 Exact relation between $\hat{\rho}$ and $\hat{p}$

We first divide equation (5.8) by $\bar{c}^2$ and then subtract equation (5.6) from it. The following relation is developed.

$$\hat{\rho} = \frac{\hat{p}}{\bar{c}^2} + \frac{i}{\omega}\frac{\mathrm{d}\bar{\rho}}{\mathrm{d}x}\hat{u} \tag{5.14}$$

From Equation (5.7), we get an expression of $\hat{u}$ in terms of $\hat{p}$

$$\hat{u} = -\frac{1}{i\omega\bar{\rho}}\frac{\mathrm{d}\hat{p}}{\mathrm{d}x} \tag{5.15}$$

Thus the final relation, after substituting equation (5.15) to (5.14), is summarized below

$$\hat{\rho} = \frac{\hat{p}}{\bar{c}^2} - \frac{1}{\omega^2\bar{\rho}}\frac{\mathrm{d}\bar{\rho}}{\mathrm{d}x}\frac{\mathrm{d}\hat{p}}{\mathrm{d}x} \tag{5.16}$$

A very similar $\hat{\rho}$-$\hat{p}$ relation has been derived (replacing the mean density, $\bar{\rho}$ with other mean properties) in various studies [17, 2, 18]. As can be seen, equation (5.16) is no longer the "Classical" $\hat{\rho}$-$\hat{p}$ relation ($\hat{\rho} = \hat{p}/\bar{c}^2$) and this calls for a comparative study between the Helmholtz and the Classical $\hat{\rho}$ profiles.

5.5 Fluctuating Property Plots

We present the pressure and density fluctuations, $\hat{p}$ and $\hat{\rho}$, obtained by solving the fluctuating conservation equations, as well as the Helmholtz equation. These equations are solved at frequencies ω ranging from 50 rad/s to 2000 rad/s. However, the plots presented are for $\omega = 150$ rad/s only. The corresponding plots at the other ω values may be found in Appendix A. Study with various values of ω was done to observe how much the "Classical" $\hat{\rho}$ deviated from the "Helmholtz" $\hat{\rho}$.

Two mean temperature profiles — linear and power-law profiles — were considered to calculate the mean properties and the duct cross-sectional area, which

are needed as parameters to solve the fluctuating conservation equations and the Helmholtz equation. Thus, the $\hat{p}$ and $\hat{\rho}$ plots are presented for the two mean temperature cases.

We present the fluctuation plots first for the linear temperature profile, and then for the power law profile. We finish this section with an error plot as a function of ω. The error is defined as

$$\text{Absolute Percentage Error} = \left| \frac{\hat{\rho}_{\text{exact}} - \hat{\rho}_{\text{classical}}}{\hat{\rho}_{\text{exact}}} \right| \times 100\% \tag{5.17}$$

and this definition is referred back to in the rest of the non-uniform mean properties cases IV and V.

5.5.1 Linear Temperature Profile: $\bar{T}(x) = \bar{T}_0 + mx$

The spatial profiles of the pressure and density fluctuations, $\hat{p}$ and $\hat{\rho}$, are shown in figure 5.2. In figure 5.2a, we compare the $\hat{p}$ profiles obtained by solving the Helmholtz equation and the fluctuating conservation equations. The two solutions are essentially identical. In figure 5.2b, we compare three profiles of $\hat{\rho}$. The $\hat{\rho}$ profile labeled "Helmholtz" is obtained from the exact $\hat{p}$-$\hat{\rho}$ relation (5.16), with $\hat{p}$ from the Helmholtz equation. The $\hat{\rho}$ profile labeled "Conservation" is obtained by directly solving the fluctuating conservation equations (5.6)-(5.8). Finally, the "Classical" profile is calculated from $\hat{\rho} = \hat{p}/\bar{c}^2$, with the Helmholtz $\hat{p}$. First, we see in figure 5.2b that the Helmholtz $\hat{\rho}$ is indistinguishable from the Conservation $\hat{\rho}$, thereby validating the former. However, we see that the Classical $\hat{\rho}$ profile shows negligible differences with these two. The errors in the Classical $\hat{\rho}$ are quantified as a function of frequency ω in figure 5.3. We observe that the peak error is $\sim$5%. The error initially increases till $\omega = 300$ rad/s, then monotonically decreases till $\omega = 1000$ rad/s. The error subsequently reduces to $\sim$0.5% for higher values of ω. It can be deduced that in Case III, for the linear temperature profile, the Classical approximation performs accurately across higher values of ω.

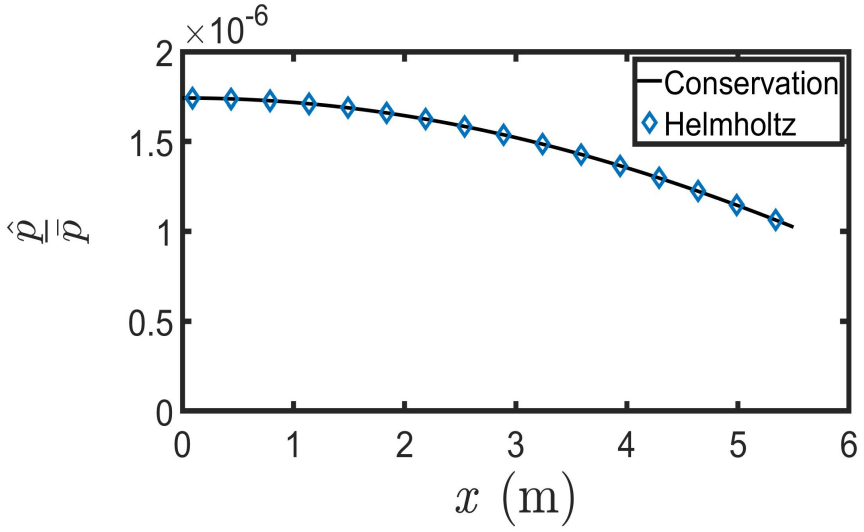

(a) Non-Dimensionalized Fluctuating Pressure Profile

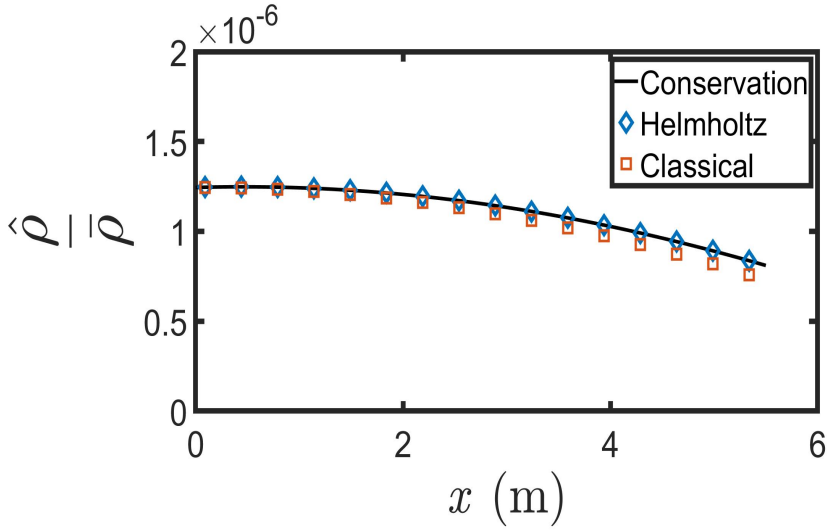

(b) Non-Dimensionalized Fluctuating Density Profile

Figure 5.2: Fluctuating Properties for linear temperature distribution in Case III

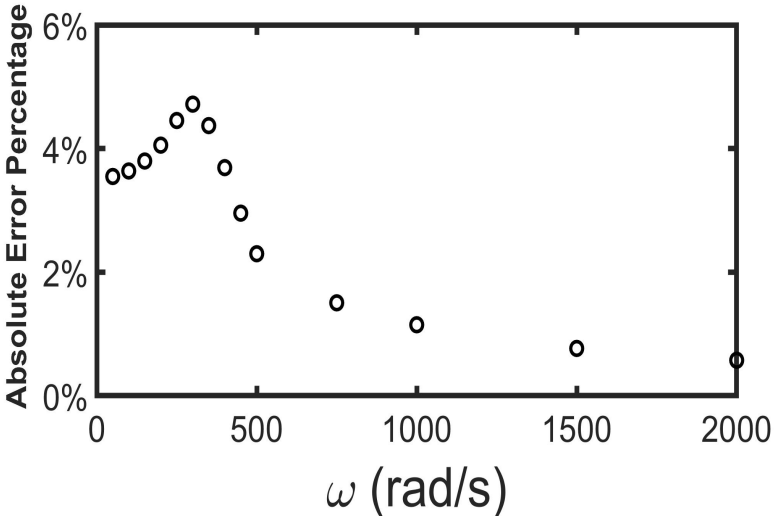

Figure 5.3: Error for Linear Temperature Profile

5.5.2 Non-Linear Temperature Profile : $\bar{T}(x) = \left(\bar{T}_0^{\frac{3}{4}} + bx\right)^{\frac{4}{3}}$

For the power-law profile, figure 5.4 illustrates the fluctuating properties, $\hat{p}$ and $\hat{\rho}$. Figure 5.4a shows that the Helmholtz and Conservation $\hat{p}$ are in excellent agreement. In figure 5.4b, the Helmholtz and the Conservation $\hat{\rho}$ are indistinguishable as well. The Classical $\hat{\rho}$ is also is excellent agreement.

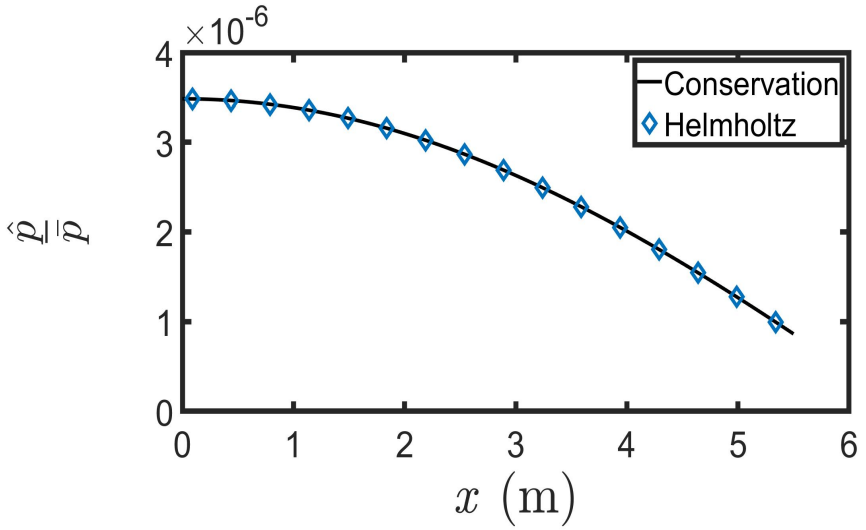

(a) Non-Dimensionalized Fluctuating Pressure Profile

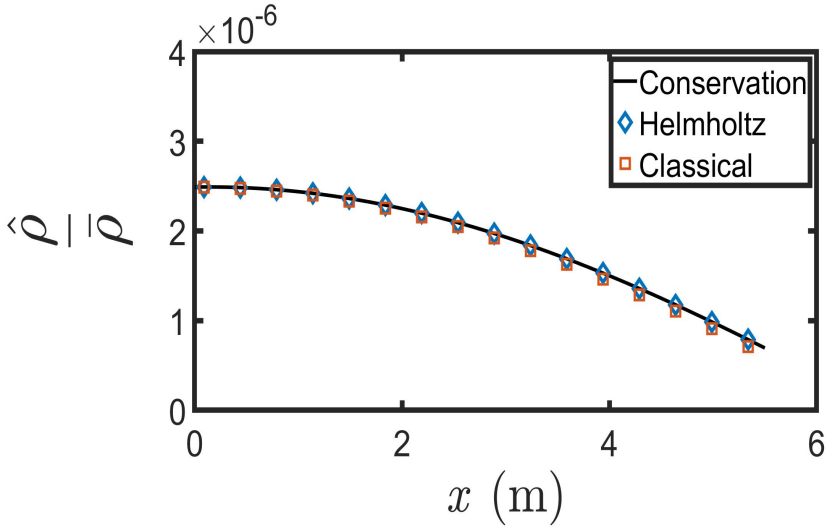

(b) Non-Dimensionalized Fluctuating Density Profile

Figure 5.4: Fluctuating Properties for four-thirds temperature distribution

The errors between the Classical and Helmholtz $\hat{\rho}$ are presented as a function of ω in figure 5.5. The peak error is ~3% at $\omega = 200$ rad/s and reduces to ~0.25% over our range of ω considered in this study. It can thus be stated that

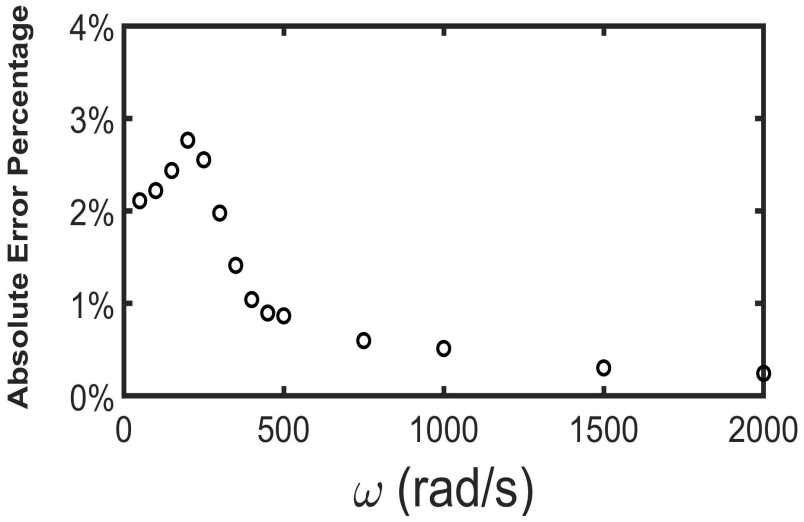

Figure 5.5: Error for power law temperature profiles

the Classical approximation performs accurately across all values of ω.

Chapter 6

CASE IV: Non-Uniform Mean Properties with Uniform Mean Flow

As we continue with the non-uniform mean properties, we add a mean medium velocity, albeit uniform, in addition to the rest of the conditions considered in Case III. We begin by presenting the mean properties, followed by the fluctuating properties. The Helmholtz equation is then derived followed by the derivation of the exact $\hat{\rho}$-$\hat{p}$ relation pertaining to this case.

6.1 Mean properties

Case IV investigates the effect of an uniform mean medium velocity $\bar{u}$, in addition to the non-uniformities in mean temperature $\bar{T}(x)$ and density $\bar{\rho}(x)$. Thus the assumptions in this case are

$$\frac{\mathrm{d}\bar{u}}{\mathrm{d}x} = 0; \quad \frac{\mathrm{d}\bar{\rho}}{\mathrm{d}x} \neq 0; \quad \frac{\mathrm{d}\bar{T}}{\mathrm{d}x} \neq 0; \tag{6.1}$$

Using the above assumptions in the mean conservation equations (2.4), we find that the mean pressure and the cross-sectional area are also uniform across the duct.

$$\frac{\mathrm{d}\bar{p}}{\mathrm{d}x} = 0; \quad \frac{\mathrm{d}S}{\mathrm{d}x} = 0; \tag{6.2}$$

Now applying (6.1) and (6.2) to the differential equation of state (2.8), we get the mean density profile.

$$\frac{1}{\bar{\rho}}\frac{\mathrm{d}\bar{\rho}}{\mathrm{d}x} = -\frac{2}{\bar{c}}\frac{\mathrm{d}\bar{c}}{\mathrm{d}x}$$

In the above equations, the speed of sound is obtained using $\bar{c}(x) = \sqrt{\gamma R_{gas}\bar{T}(x)}$ and the inlet boundary condition to solve the ODE is $\bar{\rho}_0 = 1$ kg/m^3. Two profiles of $\bar{T}(x)$ have been considered in Case III. These are

- Linear profile, $\bar{T}(x) = \bar{T}_0 + mx$, and
- Power law profile, $\left(\bar{T}_0^{\frac{3}{4}} + bx\right)^{\frac{4}{3}}$

Here, we considered $\bar{T}_0 = 2000$ K with $m = -25$ K/m for the linear case, and $\bar{T}_0 = 1000$ K with $b = -1$ K$^{\frac{3}{4}}$/m for the non-linear case. Every other mean property is defined by algebraic relations which are derived from the mean conservation equations using the above assumptions. The properties are

$$\bar{c}(x) = \sqrt{\gamma R\bar{T}(x)}; \quad \bar{p} = \frac{\rho_0\bar{c}_0^2}{\gamma}; \quad \bar{u} = \bar{M}_0\bar{c}_0; \quad \bar{M}(x) = \frac{\bar{u}}{\bar{c}(x)};$$

Figure 6.1 presents the mean property profiles obtained for the linear mean temperature case. The linear temperature profile considered in Case IV is shown figure 6.1a, where we see a temperature decrease of $\sim$7% over a duct length of 5.5 m. Figure 6.1b and 6.1c shows the uniformity in mean pressure and velocity along the duct length. The mean density, shown in figure 6.1d, increases along the duct, similar to that of Case III. A decrease in the mean sound speed is observed along the duct in figure 6.1e. Due to the decrease in sound speed and the uniformity in the medium velocity, the Mach number profile increases along the duct, as seen in figure 6.1f. The profiles in figures 6.1d,6.1e and 6.1f are weakly non-linear.

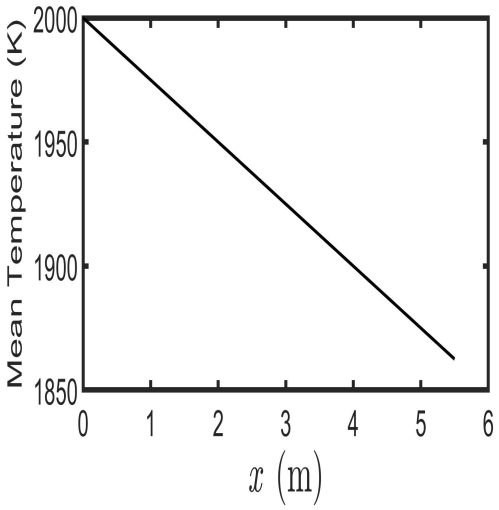

(a) Mean Temperature Profile

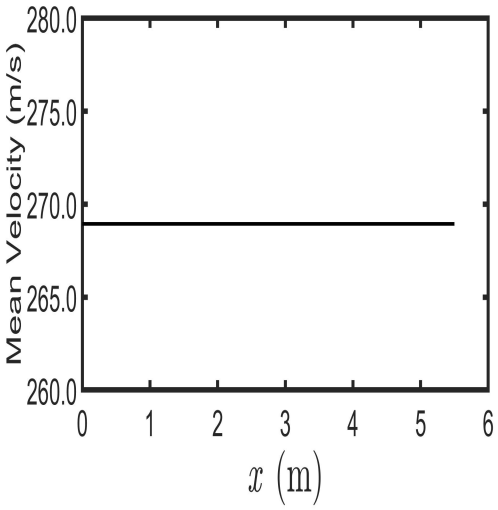

(b) Mean Velocity Profile

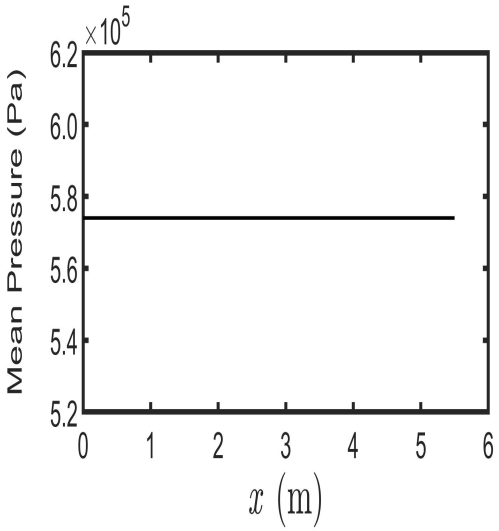

(c) Mean Pressure Profile

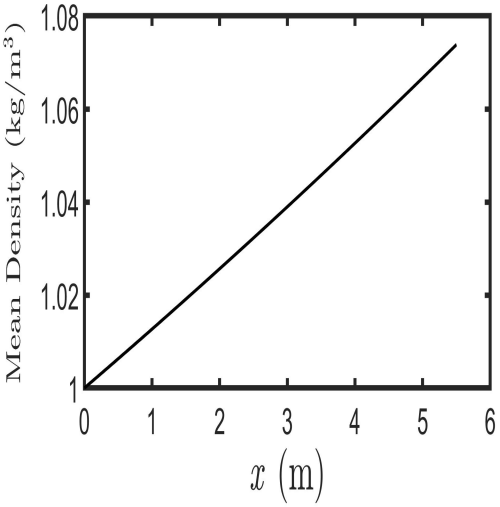

(d) Mean Density Profile

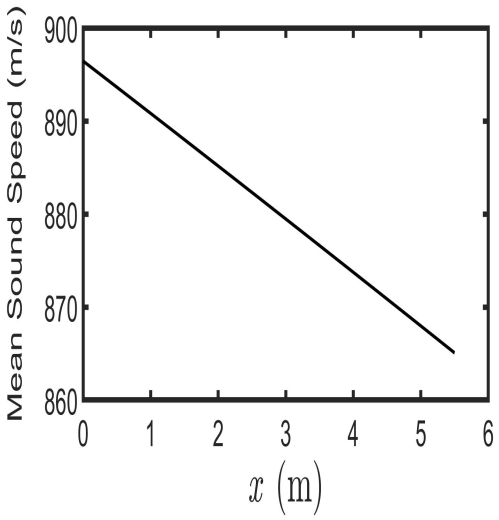

(e) Mean Sound Speed Profile

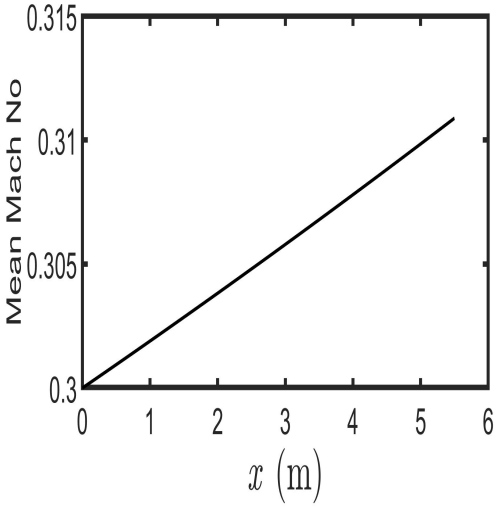

(f) Mach Number Profile

Figure 6.1: Mean Quantity Profiles

6.2 Fluctuating balance equations

The conservation equations for the fluctuating properties, i.e. equations (2.5), are reproduced below

$$\frac{\partial \rho'}{\partial t} + \bar{u}\frac{\mathrm{d}\hat{\rho}}{\mathrm{d}x} + \frac{\mathrm{d}\bar{\rho}}{\mathrm{d}x}u' + \bar{\rho}\frac{\partial u'}{\partial x} = 0 \tag{6.3}$$

$$\bar{\rho}\frac{\partial u'}{\partial t} + \bar{\rho}\bar{u}\frac{\partial u'}{\partial x} + \frac{\partial p'}{\partial x} = 0 \tag{6.4}$$

$$\frac{\partial p'}{\partial t} + \bar{u}\frac{\partial p'}{\partial x} + \gamma\bar{p}\frac{\partial u'}{\partial x} = 0 \tag{6.5}$$

Considering the harmonic temporal dependence of the three acoustic variables $p' = \hat{p}e^{i\omega t}$, $u' = \hat{u}e^{i\omega t}$ and $\rho' = \hat{\rho}e^{i\omega t}$, the fluctuating conservation equations become

$$i\omega\hat{\rho} + \bar{u}\frac{\mathrm{d}\hat{\rho}}{\mathrm{d}x} + \frac{\mathrm{d}\bar{\rho}}{\mathrm{d}x}\hat{u} + \bar{\rho}\frac{\mathrm{d}\hat{u}}{\mathrm{d}x} = 0 \tag{6.6}$$

$$i\omega\bar{\rho}\hat{u} + \bar{\rho}\bar{u}\frac{\mathrm{d}\hat{u}}{\mathrm{d}x} + \frac{\mathrm{d}\hat{p}}{\mathrm{d}x} = 0 \tag{6.7}$$

$$i\omega\hat{p} + \bar{u}\frac{\mathrm{d}\hat{p}}{\mathrm{d}x} + \bar{\rho}\bar{c}^2\frac{\mathrm{d}\hat{u}}{\mathrm{d}x} = 0 \tag{6.8}$$

The inlet boundary conditions for the fluctuating conservation equations are

$$\hat{p}(0) = \hat{p}_0; \quad \hat{u}(0) = \hat{u}_0; \quad \hat{\rho}(0) = \hat{\rho}_0; \tag{6.9}$$

where $\hat{p}_0 = 1$ Pa, $\hat{u}_0 = 0.1$ m/s and $\hat{\rho}_0 = 0.0001$ kg/m^3. The $\hat{\rho}$ and $\hat{p}$ obtained from the solution of equations (6.6)-(6.8) will be used as the benchmark to validate the solution to the Helmholtz equation.

6.3 Helmholtz equation for $\hat{p}$

The wave equation for Case IV is obtained from equations (6.4) and (6.5). This process involves $\frac{\partial}{\partial x}$[equation (6.4)] $-\frac{1}{\bar{c}^2}\frac{\partial}{\partial t}$[equation (6.5)], giving

$$\frac{\partial^2 p'}{\partial x^2} - \frac{1}{\bar{c}^2}\frac{\partial^2 p'}{\partial t^2} + \frac{\mathrm{d}\bar{\rho}}{\mathrm{d}x}\frac{\partial u'}{\partial t} + \bar{\rho}\bar{u}\frac{\partial^2 u'}{\partial x^2} + \bar{u}\frac{\mathrm{d}\bar{\rho}}{\mathrm{d}x}\frac{\partial u'}{\partial x} - \frac{\bar{u}}{\bar{c}^2}\frac{\partial^2 p'}{\partial x \partial t} = 0 \tag{6.10}$$

The Helmholtz equation is obtained by substituting into the wave equation $p' = \hat{p}e^{i\omega t}$, $u' = \hat{u}e^{i\omega t}$ and $\rho' = \hat{\rho}e^{i\omega t}$.

$$\frac{\mathrm{d}^2\hat{p}}{\mathrm{d}x^2} - \frac{i\omega\bar{M}}{\bar{c}}\frac{\mathrm{d}\hat{p}}{\mathrm{d}x} + \frac{\omega^2}{\bar{c}^2}\hat{p} + \bar{\rho}\bar{u}\frac{\mathrm{d}^2\hat{u}}{\mathrm{d}x^2} + \bar{u}\frac{\mathrm{d}\bar{\rho}}{\mathrm{d}x}\frac{\mathrm{d}\hat{u}}{\mathrm{d}x} + i\omega\frac{\mathrm{d}\bar{\rho}}{\mathrm{d}x}\hat{u} = 0 \tag{6.11}$$

We still need to eliminate $\hat{u}$ and its derivatives so as to obtain the Helmholtz equation in terms of $\hat{p}$ alone. We start by finding $\hat{u}$. This requires the following process: $\frac{1}{\bar{u}}$[equation (6.7)] – $\frac{1}{\bar{c}^2}$[equation (6.8)]

$$\hat{u} = \frac{\bar{M}}{\bar{\rho}\bar{c}}\hat{p} + \frac{i(1-\bar{M}^2)}{\bar{\rho}\omega}\frac{\mathrm{d}\hat{p}}{\mathrm{d}x} \tag{6.12}$$

The expression for $\frac{\mathrm{d}\hat{u}}{\mathrm{d}x}$ is obtained from rearranging equation (6.8) which is

$$\frac{\mathrm{d}\hat{u}}{\mathrm{d}x} = -\frac{i\omega}{\bar{\rho}\bar{c}^2}\hat{p} - \frac{\bar{u}}{\bar{\rho}\bar{c}^2}\frac{\mathrm{d}\hat{p}}{\mathrm{d}x} \tag{6.13}$$

$\frac{\mathrm{d}^2\hat{u}}{\mathrm{d}x^2}$ can be found by taking the derivative of above equation.

$$\frac{\mathrm{d}^2\hat{u}}{\mathrm{d}x^2} = \frac{d}{dx}\left[-\frac{i\omega}{\bar{\rho}\bar{c}^2}\hat{p} - \frac{\bar{u}}{\bar{\rho}\bar{c}^2}\frac{\mathrm{d}\hat{p}}{\mathrm{d}x}\right] \tag{6.14}$$

Thus once these expressions, i.e., equation (6.12), (6.13) and (6.14) are substituted into equation (6.11), we get the Helmholtz equation only in terms of $\hat{p}$

$$\alpha_1\frac{\mathrm{d}^2\hat{p}}{\mathrm{d}x^2} + \alpha_2\frac{\mathrm{d}\hat{p}}{\mathrm{d}x} + \alpha_3\hat{p} = 0 \tag{6.15}$$

where α_1, α_2 and α_3 are all complicated functions of x. The analytical forms of these coefficients are rather long and involved, and are not presented here.

The Dirichlet boundary condition for the Helmholtz equation (6.15) is identical to that of the fluctuating conservation equations ($\hat{p}(0) = \hat{p}_0$). The Neumann boundary condition $\frac{\mathrm{d}\hat{p}}{\mathrm{d}x}$ is obtained from equation (6.12).

$$\left.\frac{\mathrm{d}\hat{p}}{\mathrm{d}x}\right|_{x=0} = \frac{1}{1-\bar{M}_0^2}\left(\frac{i\bar{M}_0}{\bar{c}_0}\hat{p}_0 - i\omega\bar{\rho}_0\hat{u}_0\right) \tag{6.16}$$

The boundary condition (BC) in (6.16) is the exact Neumann BC for the Helmholtz equation. We now derive the exact relation between $\hat{\rho}$ and $\hat{p}$.

6.4 Exact relation between $\hat{\rho}$ and $\hat{p}$

We first divide equation (6.8) by $\bar{c}^2$ and subtract equation (6.6) from it, which gives

$$i\omega\hat{\rho} + \bar{u}\frac{\mathrm{d}\hat{\rho}}{\mathrm{d}x} + \frac{\mathrm{d}\bar{\rho}}{\mathrm{d}x}\hat{u} = \frac{i\omega}{\bar{c}^2}\hat{p} + \frac{\bar{u}}{\bar{c}^2}\frac{\mathrm{d}\hat{p}}{\mathrm{d}x} \tag{6.17}$$

To eliminate $\hat{u}$ from the above equation, we use the fluctuating momentum equation (6.7)

$$\hat{u} = \frac{i\bar{u}}{\omega}\frac{\mathrm{d}\hat{u}}{\mathrm{d}x} + \frac{i}{\omega\bar{\rho}}\frac{\mathrm{d}\hat{p}}{\mathrm{d}x} \tag{6.18}$$

where $\frac{\mathrm{d}\hat{u}}{\mathrm{d}x}$ from equation (6.8) is

$$\frac{\mathrm{d}\hat{u}}{\mathrm{d}x} = -\frac{i\omega}{\bar{\rho}\bar{c}^2}\hat{p} - \frac{\bar{u}}{\bar{\rho}\bar{c}^2}\frac{\mathrm{d}\hat{p}}{\mathrm{d}x} \tag{6.19}$$

Substitution of the resulting $\hat{u}$ and $\frac{\mathrm{d}\hat{u}}{\mathrm{d}x}$ into equation (6.17) yields the desired relationship between $\hat{p}$ and $\hat{\rho}$.

$$i\omega\hat{\rho} + \bar{u}\frac{\mathrm{d}\hat{\rho}}{\mathrm{d}x} = \left(\frac{i\omega}{\bar{c}^2} - \frac{\bar{M}}{\bar{\rho}\bar{c}}\frac{\mathrm{d}\bar{\rho}}{\mathrm{d}x}\right)\hat{p} + \left(\frac{\bar{M}}{\bar{c}} - \frac{i(1-\bar{M}^2)}{\bar{\rho}\omega}\frac{\mathrm{d}\bar{\rho}}{\mathrm{d}x}\right)\frac{\mathrm{d}\hat{p}}{\mathrm{d}x} \tag{6.20}$$

Having obtained the exact relation between $\hat{p}$ and $\hat{\rho}$, we now solve for $\hat{p}$ using two approaches. The first involves solving the Helmholtz equation for $\hat{p}$, and the

second consists of solving the fluctuating balance equations (6.6)-(6.8). The latter serves as the benchmark for the former.

6.5 Fluctuating Property Plots

We present the pressure and density fluctuations, $\hat{p}$ and $\hat{\rho}$, obtained by solving the fluctuating conservation equations, as well as the Helmholtz equation. These equations are solved at frequencies ω ranging from 50 rad/s to 2000 rad/s. However, the plots presented are for $\omega = 150$ rad/s only. The corresponding plots at the other ω values may be found in Appendix B.

Two mean temperature profiles — linear and power-law profiles — were considered to calculate the mean properties and the duct cross-sectional area, which are needed as parameters to solve the fluctuating conservation equations and the Helmholtz equation. Thus, the $\hat{p}$ and $\hat{\rho}$ plots are presented for the two mean temperature cases.

We present the fluctuation plots first for the linear temperature profile, and then for the power law profile.

6.5.1 Linear Temperature Profile: $\bar{T}(x) = \bar{T}_0 + mx$

The spatial profiles of the pressure and density fluctuations, $\hat{p}$ and $\hat{\rho}$, are shown in figure 6.2. In figure 6.2a, we compare the $\hat{p}$ profiles obtained by solving the Helmholtz equation and the fluctuating conservation equations. The two solutions are essentially identical, validating the Helmholtz equation solution. In figure 6.2b, we compare three profiles of $\hat{\rho}$. The $\hat{\rho}$ profile labeled "Helmholtz" is obtained from the exact $\hat{p}$ and $\hat{\rho}$ relation (6.20), with $\hat{p}$ from the Helmholtz equation. The $\hat{\rho}$ profile labeled "Conservation" is obtained by directly solving the fluctuating conservation equations (6.6)-(6.8). Finally, the "Classical" profile is calculated from $\hat{\rho} = \hat{p}/\bar{c}^2$, with the Helmholtz $\hat{p}$. First, we see in figure 6.2b that the "Helmholtz" $\hat{\rho}$ is indistinguishable from the "Conservation" $\hat{\rho}$, thereby validating the former.

However, we see that the "Classical" $\hat{\rho}$ profile shows significant differences with these two, both in amplitude and phase. The errors in the Classical $\hat{\rho}$ are quantified as a function of frequency ω using equation (5.17) in figure 6.3. We observe that the peak error is $\sim$175%. For $\omega \lesssim 500$, the error decreases monotonically with ω, and subsequently oscillates around $\sim$2.5%, eventually asymptoting to this value. Thus, we deduce that in Case IV for linear mean temperature profiles, the "Classical" approximation performs better at higher frequencies just like in Case III.

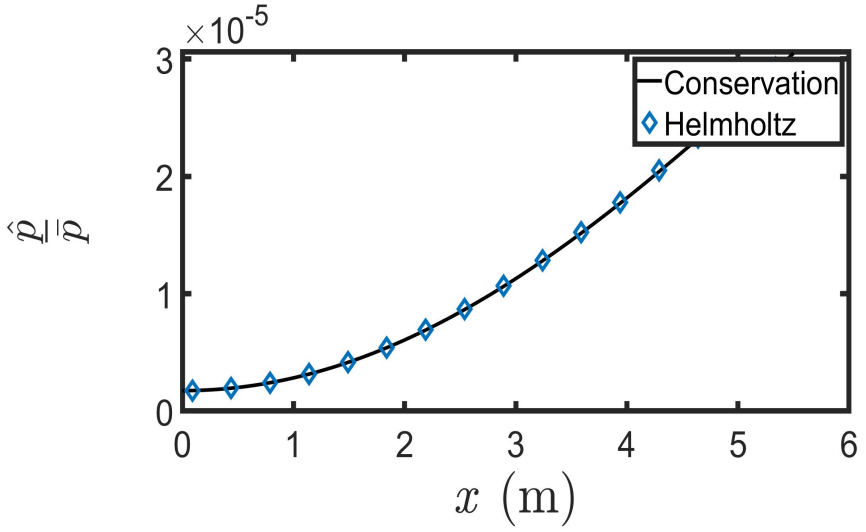

(a) Non-Dimensionalized Fluctuating Pressure Profile

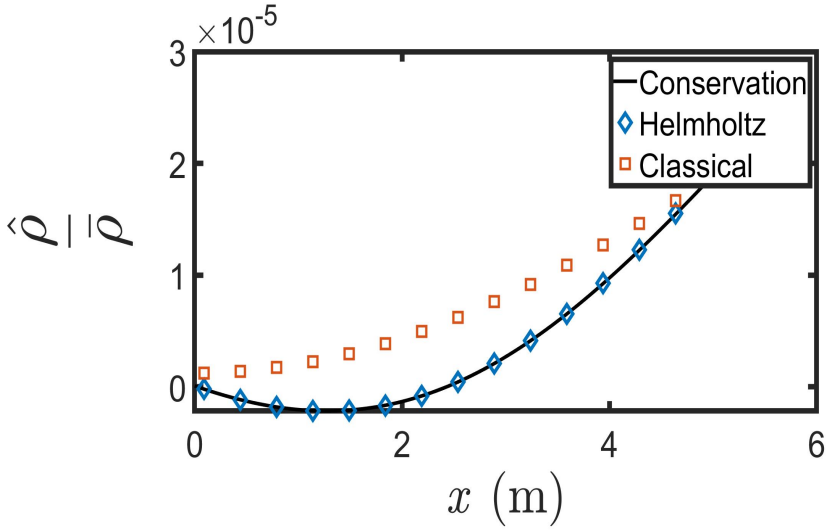

(b) Non-Dimensionalized Fluctuating Density Profile

Figure 6.2: Fluctuating Properties for linear temperature distribution

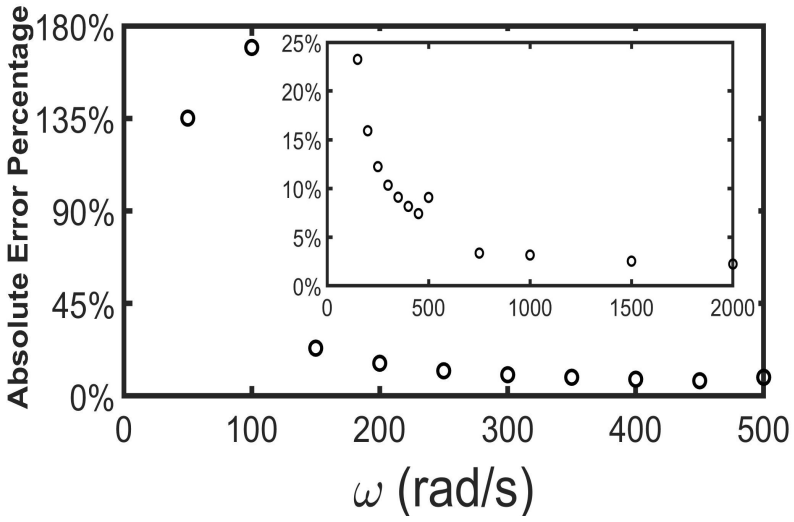

Figure 6.3: Error for Linear Temperature Profile

6.5.2 Non-Linear Temperature Profile : $\bar{T}(x) = \left(\bar{T}_0^{\frac{3}{4}} + bx\right)^{\frac{4}{3}}$

For the power-law profile, figure 6.4 illustrates the fluctuating properties, $\hat{p}$ and $\hat{\rho}$. Figure 6.4a shows that the Helmholtz and Conservation $\hat{p}$ are in excellent agreement. In figure 6.4b, the Helmholtz and the Conservation $\hat{\rho}$ are indistinguishable as well. The Classical $\hat{\rho}$ is however, in complete disagreement with the other two profiles for $\omega = 500$ rad/s. The errors between the Classical and Helmholtz $\hat{\rho}$ are presented as a function of ω using equation (5.17) in figure 6.5. The peak error for the power law profile is $\sim$150% for $\omega \sim 150$ rad/s. The error reduces monotonically till $\omega \sim 500$ rad/s. Post $\omega > 1000$ rad/s the error asymptotes at $\sim$60%. This shows that the Classical assumption can yield incorrect $\hat{\rho}$ profiles.

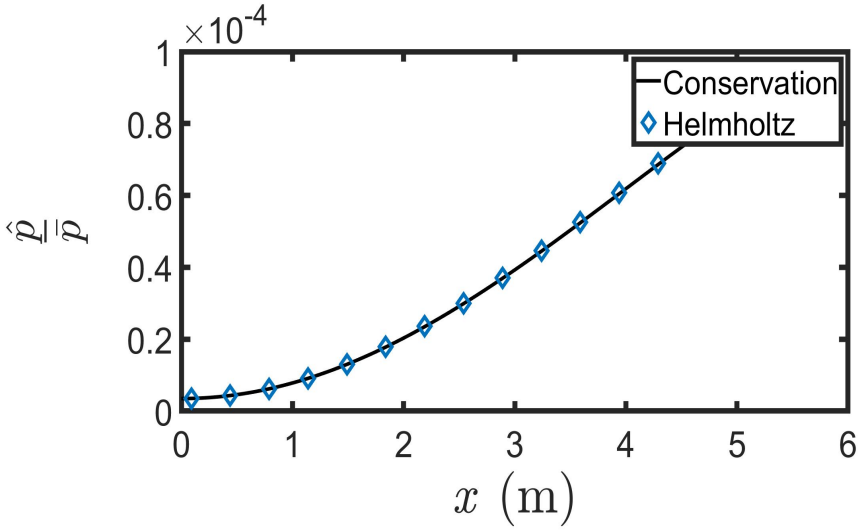

(a) Non-Dimensionalized Fluctuating Pressure Profile

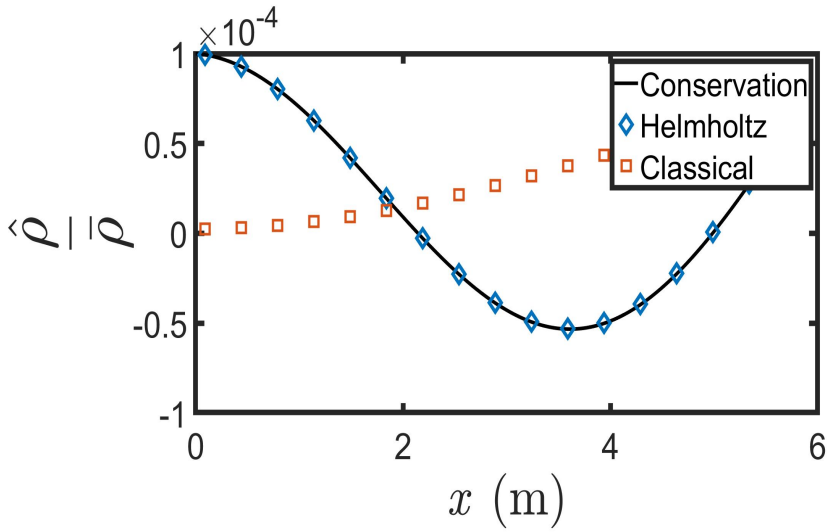

(b) Non-Dimensionalized Fluctuating Density Profile

Figure 6.4: Fluctuating Properties for four-thirds temperature distribution

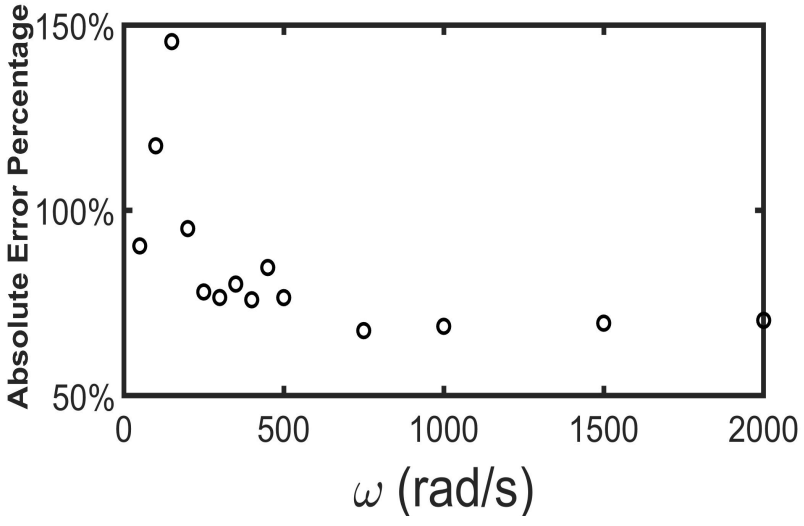

Figure 6.5: Error for non-linear Temperature Profile

Chapter 7

CASE V: Non-Uniform Mean Properties with Non-Uniform Mean Flow

We begin by presenting the details of the spatially varying mean properties, followed by the analysis of the fluctuating properties.

7.1 Mean properties

Case V is the most generalized case with no simplifying assumptions made regarding the mean property profiles — $\bar{\rho}(x)$, $\bar{u}(x)$, $\bar{p}(x)$, and $\bar{T}(x)$. The duct cross-sectional area, $S(x)$, is also regarded as an arbitrary function of axial location x. Therefore, we have

$$\frac{\mathrm{d}\bar{\rho}}{\mathrm{d}x} \neq 0; \quad \frac{\mathrm{d}\bar{u}}{\mathrm{d}x} \neq 0; \quad \frac{\mathrm{d}\bar{p}}{\mathrm{d}x} \neq 0; \quad \frac{\mathrm{d}\bar{T}}{\mathrm{d}x} \neq 0; \quad \frac{\mathrm{d}S}{\mathrm{d}x} \neq 0 \tag{7.1}$$

As in Cases III and IV, two profiles of mean temperature $\bar{T}(x)$ are considered. These are

- Linear profile, $\bar{T}(x) = \bar{T}_0 + mx$, and
- Power law profile, $\left(\bar{T}_0^{\frac{3}{4}} + bx\right)^{\frac{4}{3}}$

Having specified $\bar{T}(x)$, the profiles of the remaining mean properties and of the duct cross-sectional area can be determined uniquely by solving the mean

conservation equations (2.4) coupled with the differential form of the equation of state (2.8). The four governing equations are reproduced below.

$$\begin{aligned} S\bar{u}\frac{\mathrm{d}\bar{\rho}}{\mathrm{d}x} + S\bar{\rho}\frac{\mathrm{d}\bar{u}}{\mathrm{d}x} + \bar{\rho}\bar{u}\frac{\mathrm{d}S}{\mathrm{d}x} &= 0 \\ \bar{\rho}\bar{u}\frac{\mathrm{d}\bar{u}}{\mathrm{d}x} + \frac{\mathrm{d}\bar{p}}{\mathrm{d}x} &= 0 \\ S\bar{u}\frac{\mathrm{d}\bar{p}}{\mathrm{d}x} + \gamma S\bar{p}\frac{\mathrm{d}\bar{u}}{\mathrm{d}x} + \gamma\bar{p}\bar{u}\frac{\mathrm{d}S}{\mathrm{d}x} &= 0 \\ \gamma\frac{\mathrm{d}\bar{p}}{\mathrm{d}x} - \bar{c}^2\frac{\mathrm{d}\bar{\rho}}{\mathrm{d}x} - 2\bar{c}\bar{\rho}\frac{\mathrm{d}\bar{c}}{\mathrm{d}x} &= 0 \end{aligned} \tag{7.2}$$

In the above equations, the speed of sound is obtained using $\bar{c}(x) = \sqrt{\gamma R_{gas}\bar{T}(x)}$. The following inlet boundary conditions are used for solving the system of mean equations.

$$\bar{c}_0 = \sqrt{\gamma R_{gas} T_0}; \qquad \bar{M}_0 = 0.3; \quad \bar{u}(0) = \bar{M}_0\bar{c}_0; \tag{7.3}$$

$$\bar{\rho}(0) = \bar{\rho}_0 = 1 \text{ kg/m}^3; \qquad \bar{p}(0) = \frac{\bar{\rho}_0\bar{c}_0^2}{\gamma}; \quad S(0) = 0.2 \text{ m}^2; \tag{7.4}$$

It should be noted that for a given inlet temperature $\bar{T}_0$, not all values of m and b in the two $\bar{T}(x)$ profiles will yield smooth and continuous mean properties. Here, we considered $\bar{T}_0 = 2000$ K with $m = -25$ K/m for the linear case, and $\bar{T}_0 = 1000$ K with $b = -1$ K$^{\frac{3}{4}}$/m for the non-linear case. The relatively high inlet temperatures were also considered so as to obtain stable solutions to the mean governing equations (however, it should be mentioned that an exhaustive investigation of the $\bar{T}_0$ values necessary for a stable solution was not undertaken). We now present the mean property profiles obtained through a numerical solution of equations (7.2), performed using Mathematica®.

Figure 7.1 presents the mean property and cross-sectional area profiles obtained for the linear mean temperature case. The linear profile considered in Case V is shown figure 7.1a, where we see a temperature decrease of ∼7% over a duct length of 5.5 m. Figure 7.1b shows the mean pressure variation along the duct length. We observe a significant decrease of ∼22% in the mean pressure. Furthermore, this

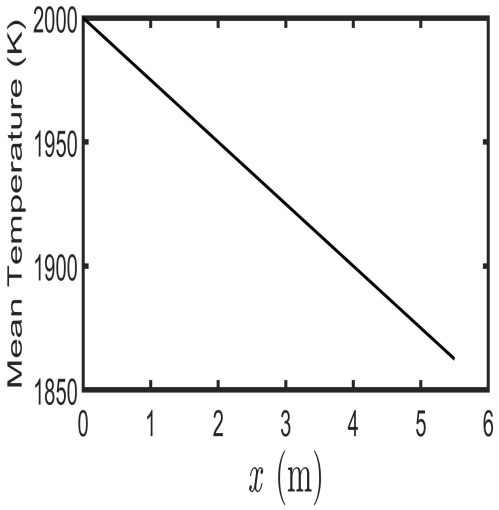

(a) Mean Temperature Profile

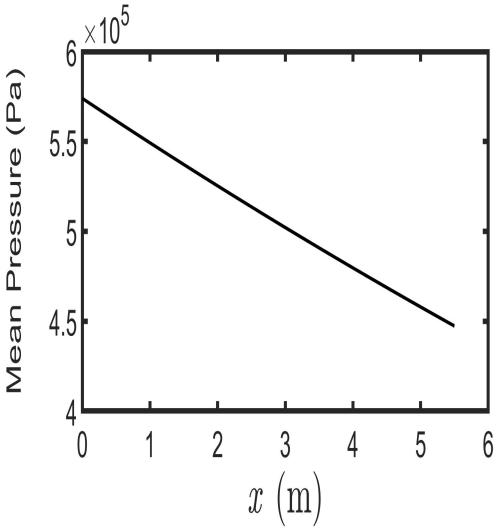

(b) Mean Pressure Profile

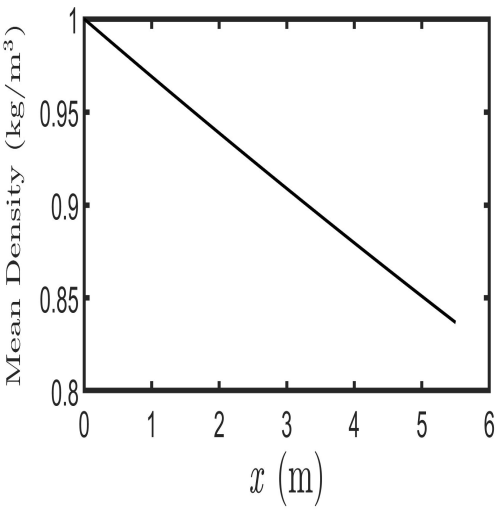

(c) Mean Density Profile

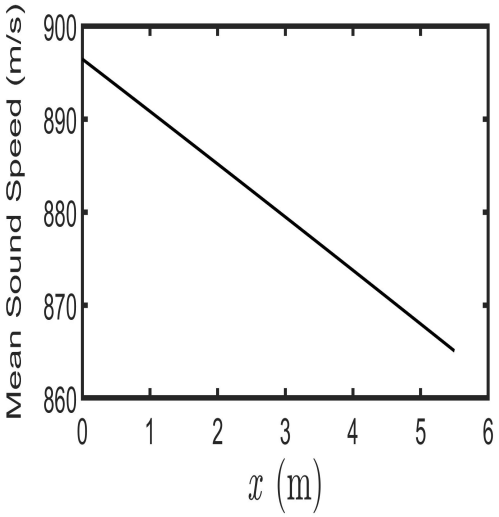

(d) Mean Sound Speed Profile

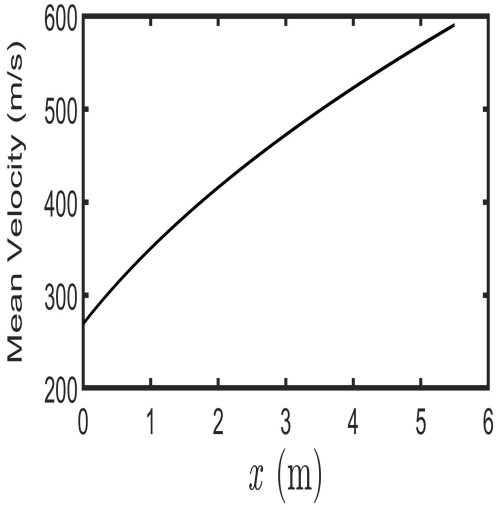

(e) Mean Velocity Profile

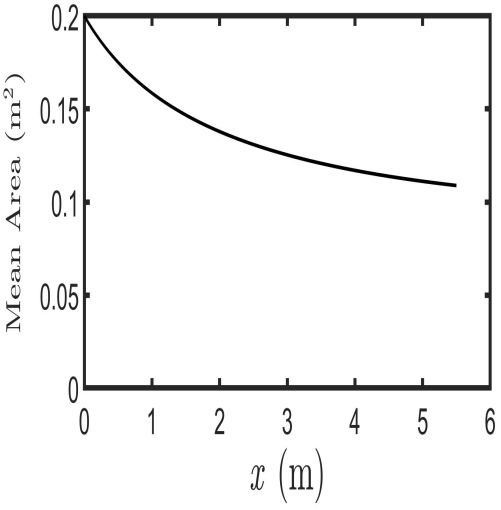

(f) Mean Area Profile

Figure 7.1: Mean Quantity Profiles

is the only case (in Cases I through V) where the mean pressure varies along the duct. The mean density, shown in figure 7.1c, decreases along the duct, as opposed to cases III and IV in which density decreases. The variation of mean pressure and density with x is only weakly non-linear. The variation in cross-sectional area and mean velocity, shown in figures 7.1e and Figure 7.1f, is evidently non-linear. The decrease in the mean velocity is in accordance with the increasing mean pressure along the duct.

7.2 Fluctuating balance equations

The governing equations for the fluctuating properties, i.e. equations (2.5), are reproduced below.

$$S\frac{\partial \rho'}{\partial t} + S\bar{u}\frac{\partial \rho'}{\partial x} + S\frac{\mathrm{d}\bar{\rho}}{\mathrm{d}x}u' + S\bar{\rho}\frac{\partial u'}{\partial x} + S\frac{\mathrm{d}\bar{u}}{\mathrm{d}x}\rho' + \bar{\rho}\frac{\mathrm{d}S}{\mathrm{d}x}u' + \bar{u}\frac{\mathrm{d}S}{\mathrm{d}x}\rho' = 0 \tag{7.5}$$

$$\bar{\rho}\frac{\partial u'}{\partial t} + \bar{u}\frac{\mathrm{d}\bar{u}}{\mathrm{d}x}\rho' + \bar{\rho}\bar{u}\frac{\partial u'}{\partial x} + \bar{\rho}\frac{\mathrm{d}\bar{u}}{\mathrm{d}x}u' + \frac{\partial p'}{\partial x} = 0 \tag{7.6}$$

$$S\frac{\partial p'}{\partial t} + S\bar{u}\frac{\partial p'}{\partial x} + S\frac{\mathrm{d}\bar{p}}{\mathrm{d}x}u' + \gamma S\bar{p}\frac{\partial u'}{\partial x} + \gamma S\frac{\mathrm{d}\bar{u}}{\mathrm{d}x}p' + \gamma\bar{p}\frac{\mathrm{d}S}{\mathrm{d}x}u' + \gamma\bar{u}\frac{\mathrm{d}S}{\mathrm{d}x}p' = 0 \tag{7.7}$$

Considering the harmonic temporal dependence of the three acoustic variables $p' = \hat{p}e^{i\omega t}$, $u' = \hat{u}e^{i\omega t}$ and $\rho' = \hat{\rho}e^{i\omega t}$, the fluctuating conservation equations become

$$S\bar{u}\frac{\mathrm{d}\hat{\rho}}{\mathrm{d}x} + \left(i\omega S + S\frac{\mathrm{d}\bar{u}}{\mathrm{d}x} + \bar{u}\frac{\mathrm{d}S}{\mathrm{d}x}\right)\hat{\rho} + S\bar{\rho}\frac{\mathrm{d}\hat{u}}{\mathrm{d}x} + \left(S\frac{\mathrm{d}\bar{\rho}}{\mathrm{d}x} + \bar{\rho}\frac{\mathrm{d}S}{\mathrm{d}x}\right)\hat{u} = 0 \tag{7.8}$$

$$\frac{\mathrm{d}\hat{p}}{\mathrm{d}x} + \bar{\rho}\bar{u}\frac{\mathrm{d}\hat{u}}{\mathrm{d}x} + \left(i\omega\bar{\rho} + \bar{\rho}\frac{\mathrm{d}\bar{u}}{\mathrm{d}x}\right)\hat{u} + \bar{u}\frac{\mathrm{d}\bar{u}}{\mathrm{d}x}\hat{\rho} = 0 \tag{7.9}$$

$$\gamma S\bar{p}\frac{\mathrm{d}\hat{u}}{\mathrm{d}x} + \left(S\frac{\mathrm{d}\bar{p}}{\mathrm{d}x} + \gamma\bar{p}\frac{\mathrm{d}S}{\mathrm{d}x}\right)\hat{u} + S\bar{u}\frac{\mathrm{d}\hat{p}}{\mathrm{d}x} + \left(i\omega S + \gamma S\frac{\mathrm{d}\bar{u}}{\mathrm{d}x} + \gamma\bar{u}\frac{\mathrm{d}S}{\mathrm{d}x}\right)\hat{p} = 0 \tag{7.10}$$

The inlet boundary conditions for the fluctuating conservation equations are

$$\hat{p}(0) = \hat{p}_0; \quad \hat{u}(0) = \hat{u}_0; \quad \hat{\rho}(0) = \hat{\rho}_0 \tag{7.11}$$

where $\hat{p}_0 = 1$ Pa, $\hat{u}_0 = 0.1$ m/s and $\hat{\rho}_0 = 0.0001$ kg/m^3. The $\hat{\rho}$ and $\hat{p}$ obtained from the solution of equations (7.8)-(7.10) will be used as the benchmark to validate the solution to the Helmholtz equation.

7.3 Helmholtz equation for $\hat{p}$

The wave equation for Case V is obtained from equations (7.6) and (7.7). This process involves $\frac{\partial}{\partial x}$[equation (7.6)] $- \frac{1}{\bar{c}^2}\frac{\partial}{\partial t}$[equation (7.7)], giving

$$\frac{\partial^2 p'}{\partial x^2} - \frac{1}{\bar{c}^2}\frac{\partial^2 p'}{\partial t^2} + \left(\frac{\mathrm{d}\bar{\rho}}{\mathrm{d}x} - \frac{1}{\bar{c}^2}\frac{\mathrm{d}\bar{p}}{\mathrm{d}x} - \frac{\bar{\rho}}{S}\frac{\mathrm{d}S}{\mathrm{d}x}\right)\frac{\partial u'}{\partial t} + \left(\bar{u}\frac{\mathrm{d}\bar{\rho}}{\mathrm{d}x} + 2\bar{\rho}\frac{\mathrm{d}\bar{u}}{\mathrm{d}x}\right)\frac{\partial u'}{\partial x} + \bar{\rho}\bar{u}\frac{\partial^2 u'}{\partial x^2} - \frac{\bar{u}}{\bar{c}^2}\frac{\partial^2 p'}{\partial x \partial t} + \bar{u}\frac{\mathrm{d}\bar{u}}{\mathrm{d}x}\frac{\partial \rho'}{\partial x} - \left(\frac{\gamma}{\bar{c}^2}\frac{\mathrm{d}\bar{u}}{\mathrm{d}x} + \frac{\gamma\bar{u}}{S\bar{c}^2}\frac{\mathrm{d}S}{\mathrm{d}x}\right)\frac{\partial p'}{\partial t} = 0 \tag{7.12}$$

The Helmholtz equation is obtained by substituting into the wave equation $p' = \hat{p}e^{i\omega t}$, $u' = \hat{u}e^{i\omega t}$ and $\rho' = \hat{\rho}e^{i\omega t}$.

$$\frac{\mathrm{d}^2\hat{p}}{\mathrm{d}x^2} - \frac{i\omega\bar{M}}{\bar{c}}\frac{\mathrm{d}\hat{p}}{\mathrm{d}x} + \left(\frac{\omega^2}{\bar{c}^2} - \frac{i\omega\gamma}{\bar{c}^2}\frac{\mathrm{d}\bar{u}}{\mathrm{d}x} - \frac{i\omega\gamma\bar{u}}{S\bar{c}^2}\frac{\mathrm{d}S}{\mathrm{d}x}\right)\hat{p} + \bar{\rho}\bar{u}\frac{\partial^2\hat{u}}{\partial x^2} + \left(\bar{u}\frac{\mathrm{d}\bar{\rho}}{\mathrm{d}x} + 2\bar{\rho}\frac{\mathrm{d}\bar{u}}{\mathrm{d}x}\right)\frac{\partial\hat{u}}{\partial x} + \left(i\omega\frac{\mathrm{d}\bar{\rho}}{\mathrm{d}x} - \frac{i\omega}{\bar{c}^2}\frac{\mathrm{d}\bar{p}}{\mathrm{d}x} - \frac{i\omega\bar{\rho}}{S}\frac{\mathrm{d}S}{\mathrm{d}x} + \bar{\rho}\frac{\mathrm{d}^2\bar{u}}{\mathrm{d}x^2} + \frac{\mathrm{d}\bar{\rho}}{\mathrm{d}x}\frac{\mathrm{d}\bar{u}}{\mathrm{d}x}\right)\hat{u} + \bar{u}\frac{\mathrm{d}\bar{u}}{\mathrm{d}x}\frac{\mathrm{d}\hat{\rho}}{\mathrm{d}x} + \left(\left[\frac{\mathrm{d}\bar{u}}{\mathrm{d}x}\right]^2 + \bar{u}\frac{\mathrm{d}^2\bar{u}}{\mathrm{d}x^2}\right)\hat{\rho} = 0 \tag{7.13}$$

We still need to eliminate $\hat{\rho}$ and $\hat{u}$ so as to obtain the Helmholtz equation in terms of $\hat{p}$ alone. We start by finding $\hat{u}$. This requires the following process: [equation (7.9)] – [$\frac{\bar{u}}{S\bar{c}^2}$ × equation (7.10)]

$$\hat{u} = \frac{(1-\bar{M}^2)\frac{\mathrm{d}\hat{p}}{\mathrm{d}x} + \bar{u}\frac{\mathrm{d}\bar{u}}{\mathrm{d}x}\hat{\rho} - \left(\frac{i\omega\bar{M}}{\bar{c}} + \frac{\gamma\bar{M}}{\bar{c}}\frac{\mathrm{d}\bar{u}}{\mathrm{d}x} + \frac{\gamma\bar{M}^2}{S}\frac{\mathrm{d}S}{\mathrm{d}x}\right)\hat{p}}{\left(\frac{\bar{M}}{\bar{c}}\frac{\mathrm{d}\bar{p}}{\mathrm{d}x} + \frac{\bar{\rho}\bar{u}}{S}\frac{\mathrm{d}S}{\mathrm{d}x} - i\omega\bar{\rho} - \bar{\rho}\frac{\mathrm{d}\bar{u}}{\mathrm{d}x}\right)} \tag{7.14}$$

The expression for $\frac{\mathrm{d}\hat{u}}{\mathrm{d}x}$ is obtained by dividing equation (7.10) by $\gamma S\bar{p}$ as follows.

$$\frac{\mathrm{d}\hat{u}}{\mathrm{d}x} = \frac{-\left(i\omega S + \gamma S\frac{\mathrm{d}\bar{u}}{\mathrm{d}x} + \gamma\bar{u}\frac{\mathrm{d}S}{\mathrm{d}x}\right)\hat{p} - S\bar{u}\frac{\mathrm{d}\hat{p}}{\mathrm{d}x} - \left(S\frac{\mathrm{d}\bar{p}}{\mathrm{d}x} + \gamma\bar{p}\frac{\mathrm{d}S}{\mathrm{d}x}\right)\hat{u}}{\gamma S\bar{p}} \tag{7.15}$$

To obtain $\frac{\mathrm{d}^2\hat{u}}{\mathrm{d}x^2}$, we first use $\hat{u}$ from (7.14) in (7.15) and then take a derivative, which yields the following expression.

$$\frac{\mathrm{d}^2\hat{u}}{\mathrm{d}x^2} = \frac{d}{dx}\left[\frac{-\left(i\omega S + \gamma S\frac{\mathrm{d}\bar{u}}{\mathrm{d}x} + \gamma\bar{u}\frac{\mathrm{d}S}{\mathrm{d}x}\right)\hat{p} - S\bar{u}\frac{\mathrm{d}\hat{p}}{\mathrm{d}x} - \left(S\frac{\mathrm{d}\bar{p}}{\mathrm{d}x} + \gamma\bar{p}\frac{\mathrm{d}S}{\mathrm{d}x}\right)\hat{u}}{\gamma S\bar{p}}\right] \tag{7.16}$$

In equation (7.14), the expression for $\hat{u}$ contains $\hat{\rho}$ on the right-hand side, which needs to be eliminated as well. However, an explicit expression relating $\hat{\rho}$ to $\hat{p}$ cannot be obtained for Case V due to the presence of the $\bar{u}\frac{\mathrm{d}\bar{u}}{\mathrm{d}x}\frac{\mathrm{d}\hat{\rho}}{\mathrm{d}x}$ term in equation (7.13) [note, however, that we could accomplish this for the less general Cases I-IV]. To make further analytical progress, we are obliged to use an approximate relation, which in our study is

$$\hat{\rho} = \frac{\hat{p}}{\bar{c}^2} \tag{7.17}$$

This is the only assumption made in deriving the Helmholtz equation for Case V, and is, in fact, the only simplification used for the fluctuating properties among all five cases. It will be seen that this assumption does not significantly affect the fluctuating pressure profile as the fluctuating density is over five orders of magnitude smaller than the fluctuating pressure.

Now substituting equations (7.14)-(7.17) into (7.13), we get the Helmholtz Equation in the desired form, shown below.

$$\xi_1\frac{\mathrm{d}^2\hat{p}}{\mathrm{d}x^2} + \xi_2\frac{\mathrm{d}\hat{p}}{\mathrm{d}x} + \xi_3\hat{p} = 0 \tag{7.18}$$

where ξ_1, ξ_2 and ξ_3 are all complicated functions of x.

The Dirichlet boundary condition for the Helmholtz equation (7.18) is identical to that of the fluctuating conservation equations ($\hat{p}(0) = \hat{p}_0$). The Neumann boundary condition $\frac{\mathrm{d}\hat{p}}{\mathrm{d}x}$ is obtained from equation (7.14).

$$\begin{aligned}\left.\frac{\mathrm{d}\hat{p}}{\mathrm{d}x}\right|_{x=0} =& \frac{1}{(1-\bar{M}_0^2)}\left[\left(\frac{\bar{M}_0}{\bar{c}_0}\left.\frac{\mathrm{d}\bar{p}}{\mathrm{d}x}\right|_{x=0} + \frac{\bar{\rho}_0\bar{u}_0}{S_0}\left.\frac{\mathrm{d}S}{\mathrm{d}x}\right|_{x=0} - i\omega\bar{\rho}_0 - \bar{\rho}_0\left.\frac{\mathrm{d}\bar{u}}{\mathrm{d}x}\right|_{x=0}\right)\hat{u}_0 - \right.\\ &\left.\bar{u}_0\left.\frac{\mathrm{d}\bar{u}}{\mathrm{d}x}\right|_{x=0}\hat{\rho}_0 + \left(\frac{i\omega\bar{M}_0}{\bar{c}_0} + \frac{\gamma\bar{M}_0}{\bar{c}_0}\left.\frac{\mathrm{d}\bar{u}}{\mathrm{d}x}\right|_{x=0} + \frac{\gamma\bar{M}_0^2}{S_0}\left.\frac{\mathrm{d}S}{\mathrm{d}x}\right|_{x=0}\right)\hat{p}_0\right]\end{aligned} \tag{7.19}$$

The inlet pressure, velocity and density fluctuations $\hat{p}_0$, $\hat{u}_0$ and $\hat{\rho}_0$ are identical to those in equation (7.11). The boundary condition (BC) in (7.19) is the exact Neumann BC for the Helmholtz equation.

We now derive the exact relation between $\hat{\rho}$ and $\hat{p}$.

7.4 Exact relation between $\hat{\rho}$ and $\hat{p}$

We first divide equation (7.10) by $\bar{c}^2$ and subtract equation (7.8) from it, which gives

$$\left(i\omega S + S\frac{\mathrm{d}\bar{u}}{\mathrm{d}x} + \bar{u}\frac{\mathrm{d}S}{\mathrm{d}x}\right)\hat{\rho} + S\bar{u}\frac{\mathrm{d}\hat{\rho}}{\mathrm{d}x} + \left(S\frac{\mathrm{d}\bar{\rho}}{\mathrm{d}x} - \frac{S}{\bar{c}^2}\frac{\mathrm{d}\bar{p}}{\mathrm{d}x}\right)\hat{u} = \left(\frac{i\omega S}{\bar{c}^2} + \frac{\gamma S}{\bar{c}^2}\frac{\mathrm{d}\bar{u}}{\mathrm{d}x} + \frac{\gamma\bar{u}}{\bar{c}^2}\frac{\mathrm{d}S}{\mathrm{d}x}\right)\hat{p} + \frac{S\bar{u}}{\bar{c}^2}\frac{\mathrm{d}\hat{p}}{\mathrm{d}x} \tag{7.20}$$

To eliminate $\hat{u}$ from the above equation, we multiply (7.8) with $\frac{\bar{u}}{S}$, and subtract it from (7.9). This gives us

$$\hat{u} = \frac{\frac{\mathrm{d}\hat{p}}{\mathrm{d}x} - \bar{u}^2\frac{\mathrm{d}\hat{\rho}}{\mathrm{d}x} - \left(i\omega\bar{u} + \frac{\bar{u}^2}{S}\frac{\mathrm{d}S}{\mathrm{d}x}\right)\hat{\rho}}{\bar{u}\frac{\mathrm{d}\bar{\rho}}{\mathrm{d}x} + \frac{\bar{\rho}\bar{u}}{S}\frac{\mathrm{d}S}{\mathrm{d}x} - i\omega\bar{\rho} - \bar{\rho}\frac{\mathrm{d}\bar{u}}{\mathrm{d}x}} \tag{7.21}$$

Substitution of the resulting $\hat{u}$ into equation (7.20) yields the desired relationship between $\hat{p}$ and $\hat{\rho}$.

$$\beta_1\frac{\mathrm{d}\hat{\rho}}{\mathrm{d}x} + \beta_2\hat{\rho} = \beta_3\frac{\mathrm{d}\hat{p}}{\mathrm{d}x} + \beta_4\hat{p} \tag{7.22}$$

where the coefficients β_1, β_2,β_3 and β_4 are all functions of x. The analytical forms of these coefficients are rather long and involved, and are not presented here.

Having obtained the exact relation between $\hat{p}$ and $\hat{\rho}$, we now solve for $\hat{p}$ using two approaches. The first involves solving the Helmholtz equation for $\hat{p}$, and the second consists of solving the fluctuating balance equations (7.8)-(7.10). The latter serves as the benchmark for the former.

7.5 Fluctuating Property Plots

We present the pressure and density fluctuations, $\hat{p}$ and $\hat{\rho}$, obtained by solving the fluctuating balance equations, as well as the Helmholtz equation. These equations are solved at frequencies ω ranging from 50 rad/s to 2000 rad/s. However, the plots presented are for $\omega = 150$ rad/s only. The corresponding plots at the other ω values may be found in Appendix C.

Two mean temperature profiles — linear and power-law profiles — were considered to calculate the mean properties and the duct cross-sectional area, which are needed as parameters to solve the fluctuating balance equations and the Helmholtz equation. Thus, the $\hat{p}$ and $\hat{\rho}$ plots are presented for the two mean temperature cases.

We present the fluctuation plots first for the linear temperature profile, and then for the power law profile.

7.5.1 Linear Temperature Profile: $\bar{T}(x) = \bar{T}_0 + mx$

The spatial profiles of the pressure and density fluctuations, $\hat{p}$ and $\hat{\rho}$, are shown in figure 7.2. In figure 7.2a, we compare the $\hat{p}$ profiles obtained by solving the Helmholtz equation and the fluctuating balance equations. The two solutions are essentially identical, validating the Helmholtz equation solution. We can also deduce that the approximation $\hat{\rho} = \hat{p}/\bar{c}^2$ used to derive the Helmholtz equation in Case V has negligible effect on the accuracy of the $\hat{p}$ solution. In figure 7.2b, we compare three profiles of $\hat{\rho}$. The $\hat{\rho}$ profile labeled "Helmholtz" is obtained from the exact $\hat{p}$ and $\hat{\rho}$ relation (7.22), with $\hat{p}$ from the Helmholtz equation. The $\hat{\rho}$ profile labeled "Conservation" is obtained by directly solving the fluctuating balance equations (7.8)-(7.10). Finally, the "Classical" profile is calculated from $\hat{\rho} = \hat{p}/\bar{c}^2$, with the Helmholtz $\hat{p}$. First, we see in figure 7.2b that the "Helmholtz" $\hat{\rho}$ is indistinguishable from the "Conservation" $\hat{\rho}$, thereby validating the former. However, we see that the "Classical" $\hat{\rho}$ profile shows small differences with these

two, both in amplitude and phase. The errors in the Classical $\hat{\rho}$ are quantified as a function of frequency ω in figure 7.3. We observe that the peak error is $\sim$150%. For $\omega \lesssim 1000$, the error decreases monotonically with ω, and subsequently asymptotes at around $\sim$60%. Thus, we deduce that in Case V, the "Classical" approximation does not perform well in the range of ω considered.

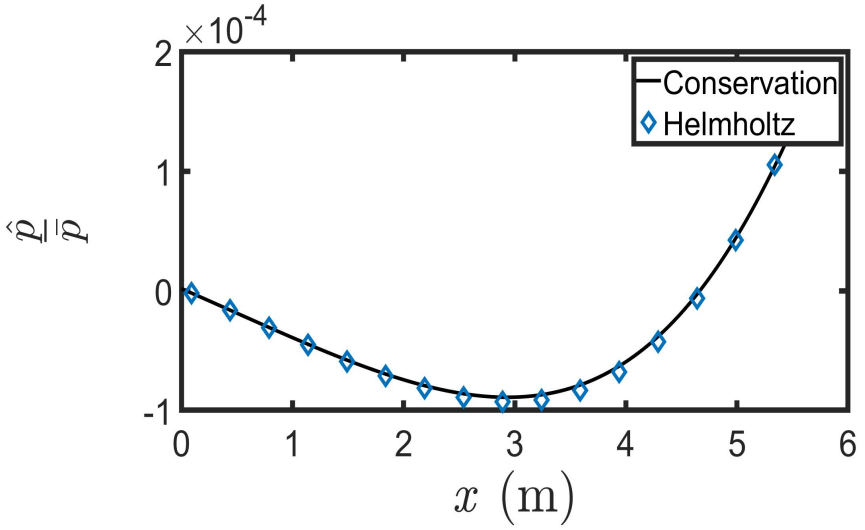

(a) Non-Dimensionalized Fluctuating Pressure Profile

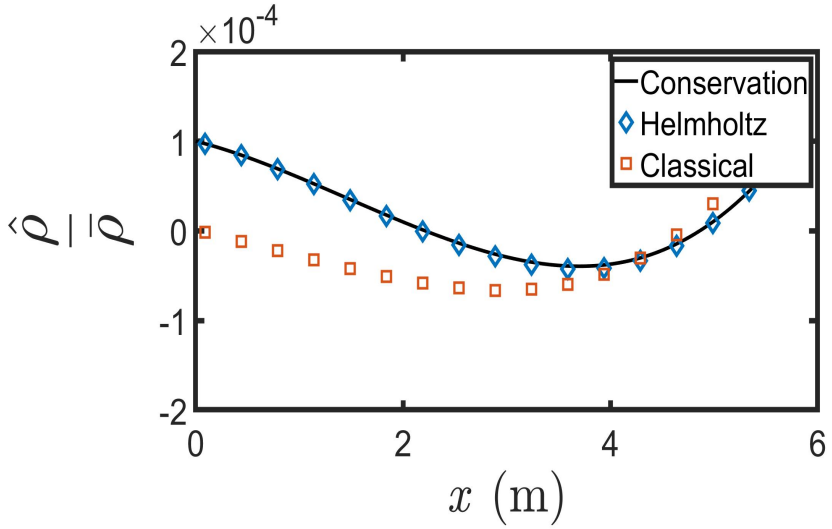

(b) Non-Dimensionalized Fluctuating Density Profile

Figure 7.2: Fluctuating Properties for linear temperature distribution

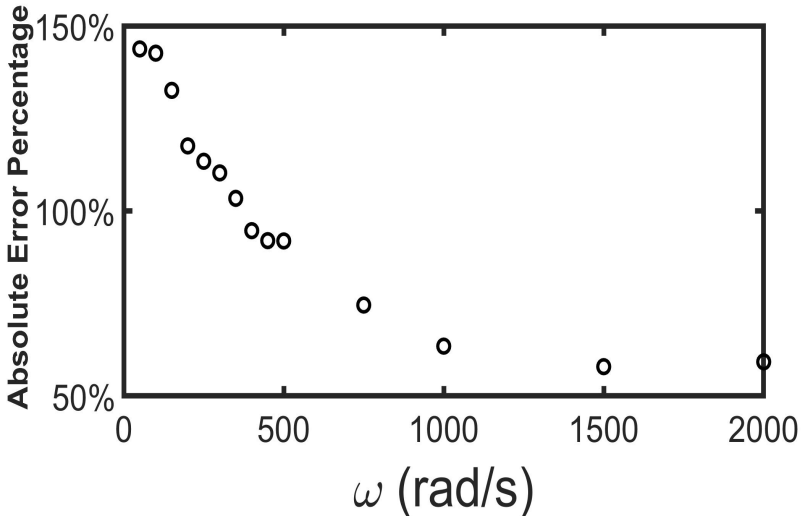

Figure 7.3: Error for Linear Temperature Profile

7.5.2 Non-Linear Temperature Profile : $\bar{T}(x) = \left(\bar{T}_0^{\frac{3}{4}} + bx\right)^{\frac{4}{3}}$

For the power-law profile, figure 7.4 illustrates the fluctuating properties, $\hat{p}$ and $\hat{\rho}$. Figure 7.4a shows that the Helmholtz and Conservation $\hat{p}$ are in excellent agreement. This further demonstrates that the simplification $\hat{\rho} = \hat{p}/\bar{c}^2$ made in deriving the Helmholtz equation for Case V does not significantly affect the accuracy of the Helmholtz $\hat{p}$. In figure 7.4b, the Helmholtz and the Conservation $\hat{\rho}$ are indistinguishable as well. The Classical $\hat{\rho}$ is in reasonably good agreement with the other two profiles for $\omega = 500$ rad/s. The errors between the Classical and Helmholtz $\hat{\rho}$ are presented as a function of ω in figure 7.5. The peak error is $\sim$180% for $\omega \lesssim 500$, and for large ω oscillates about $\sim$45%. Here too, like the linear temperature profile, the Classical relation doesn't perform well over the entire range of ω.

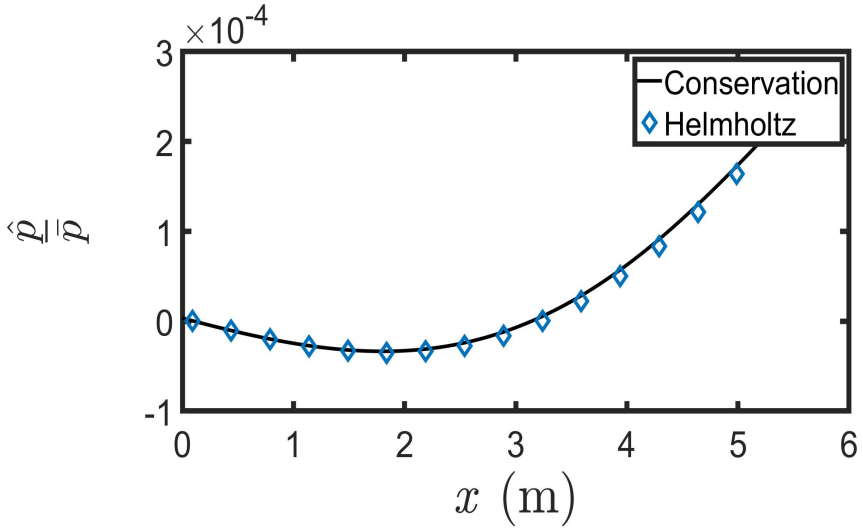

(a) Non-Dimensionalized Fluctuating Pressure Profile

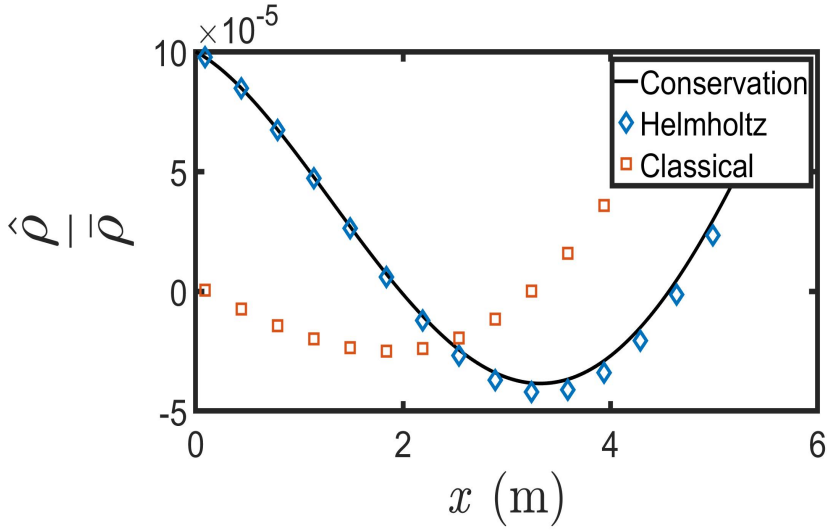

(b) Non-Dimensionalized Fluctuating Density Profile

Figure 7.4: Fluctuating Properties for four-thirds temperature distribution

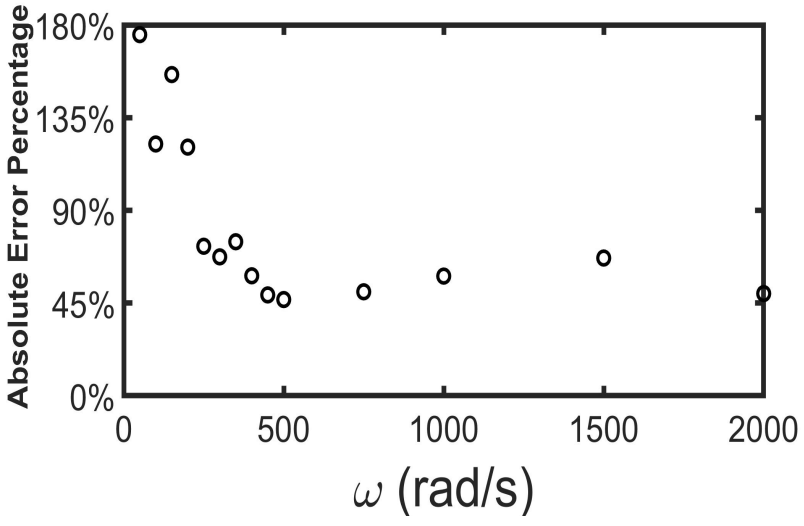

Figure 7.5: Error for Non-Linear Temperature Profile

Chapter 8

Conclusions

The two principal objectives of this thesis were the derivation of

- Neumann (derivative) boundary condition for pressure fluctuations at the inlet to a duct.
- Exact relation between density and pressure fluctuations.

As indicated in Table 8.1, five 1-D ducts were considered with axially uniform and non-uniform cross-sectional areas, as well as homogeneous and inhomogeneous mean flow properties such as the velocity, temperature, density and pressure. For each case, the acoustic-wave Helmholtz equation was derived from the fluctuating forms of the mass, momentum and the energy balance equations. The spatial pressure fluctuations $\hat{p}(x)$ were obtained using two approaches — by solving the fluctuating balance equations, and the Helmholtz equation. For each of the five cases, the exact $\hat{\rho}$-$\hat{p}$ relation was used to calculate $\hat{\rho}$, where $\hat{p}$ was obtained from the Helmholtz equation (it may be noted that the $\hat{p}(x)$ obtained using the aforementioned two approaches are practically identical). The "exact" $\hat{\rho}$ was then compared with that obtained using the "classical" definition $\hat{\rho} = \hat{p}/\bar{c}^2$.

Cases I and II have the same uniform mean flow properties, but differ in that the former has zero mean velocity, while the latter has a non-zero uniform mean velocity. For these cases, the exact $\hat{\rho}$ is seen to be identical to the classical $\hat{\rho}$.

In Cases III, IV and V, the mean temperature and density are both axially varying. Case III has zero mean flow and uniform mean pressure. Case IV has

uniform mean flow and uniform mean pressure, while Case V has non-uniform mean flow and mean pressure. Cases III and IV have uniform cross-section, but Case V has an axially varying cross-sectional area. For these three cases, the exact $\hat{\rho}$ was found to be a function of ω as well. The exact and classical $\hat{\rho}$ profiles were compared with $\hat{\rho}$ obtained by solving the fluctuating balance equations. For Case III (with both linear and non-linear mean temperature profiles), we observe that the error in the classical $\hat{\rho}$ relative to the exact $\hat{\rho}$ varies inversely as the frequency ω. In the range of ω values considered ($50 \leq \omega \leq 2000$ rad/s), the maximum error is $\sim$5% for the linear case, and $\sim$3% for the non-linear case. For both temperature profiles, the error initially increases, before decreasing monotonically with ω, asymptoting to $\sim$0.5% for the linear profile, and $\sim$0.25% for the power-law profile of temperature, at higher values of ω. It can be deduced that in Case III, the classical $\hat{\rho}$-$\hat{p}$ relation performs reasonably well across all ω for both the temperature profiles considered.

For Case IV (with both linear and non-linear mean temperature profiles), we observe that the error in the classical $\hat{\rho}$ relative to the exact $\hat{\rho}$ again varies inversely as the frequency ω. The maximum error at $\omega = 150$ rad/s is $\sim$175% for the linear case, and $\sim$150% for the non-linear case. For the linear temperature profile, the error asymptotes to to $\sim$2.5%, while for the non-linear temperature profile, the error asymptotes to $\sim$50%. Thus, we see that in Case IV, the classical $\hat{\rho}$ is significantly different from the exact $\hat{\rho}$ for the non-linear temperature profile.

For Case V, we observe that the peak error is $\sim$150% for the linear temperature profile and $\sim$180% for the non linear temperature profile at $\omega = 50$ rad/s. For the linear temperature profile, the error reaches $\sim$50%, while for the non-linear temperature profile, the error oscillates around $\sim$50% for large ω. Thus, in Case V, the classical $\hat{\rho}$-$\hat{p}$ performs better at higher frequencies for both linear and the non-linear mean temperature profiles.

Table 8.1: Comparison of each case

CASE	**TITLE**	**ERROR (∼%)**			
		$\bar{T}(x) = 2000 - 25x$		$\bar{T}(x) = \left(1000^{\frac{3}{4}} - x\right)^{\frac{4}{3}}$	
		Lowest	Highest	Lowest	Highest
I	Uniform Mean Properties with No Mean Flow	NA			
II	Uniform Mean Properties with Uniform Mean Flow	NA			
III	Non-Uniform Mean Properties with No Mean Flow	0.5	5	0.25	3
IV	Non-Uniform Mean Properties with Uniform Mean Flow	2.5	175	70	150
V	Non-Uniform Mean Properties with Non-Uniform Mean Flow	60	150	50	180

Appendix A

Supporting Plots for CASE III

A.1 Linear Temperature Profile

A.1.1 Pressure fluctuations across the duct

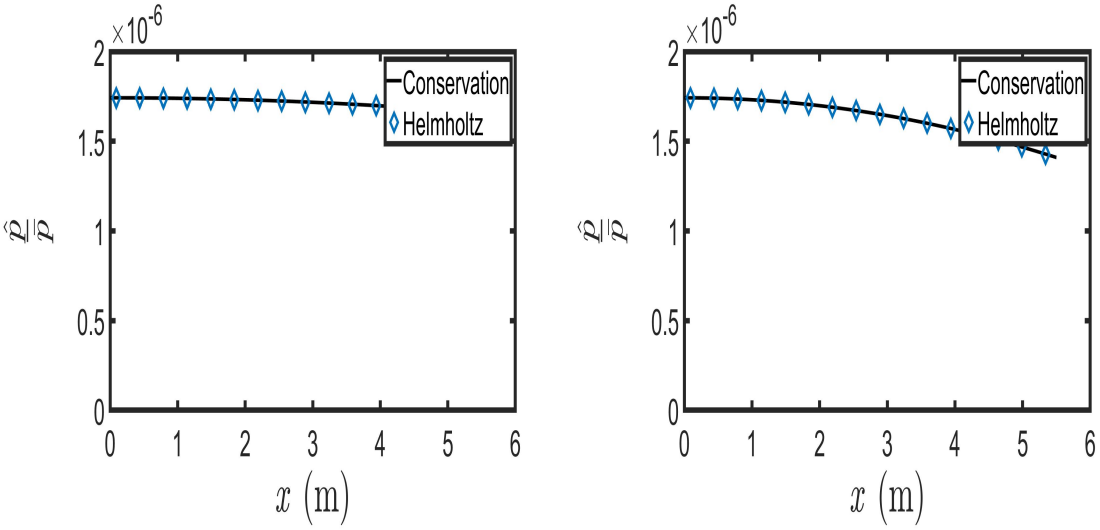

(a) $\omega = 50$ rad/s (b) $\omega = 100$ rad/s

Figure A.1: Pressure Fluctuations for linear profile - case III

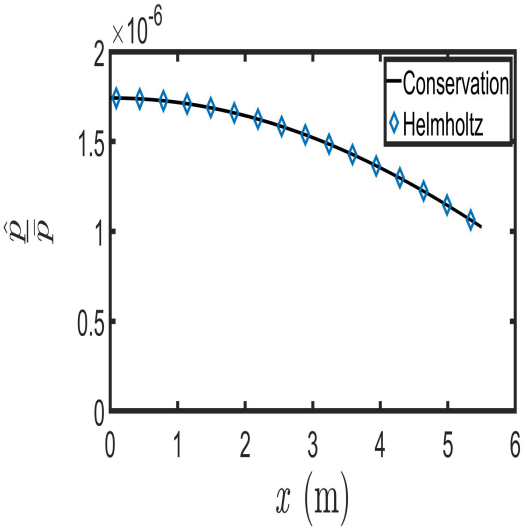

(c) $\omega = 150$ rad/s

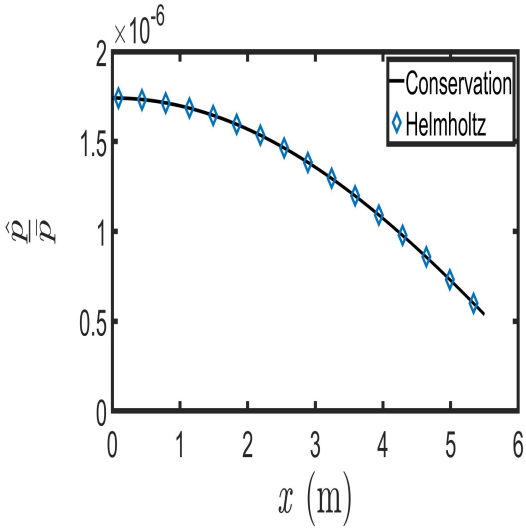

(d) $\omega = 200$ rad/s

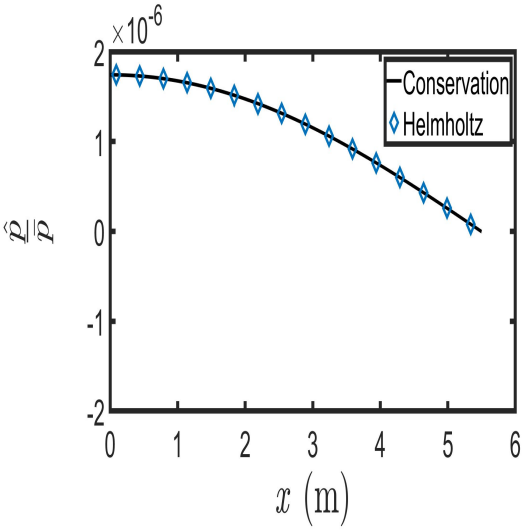

(e) $\omega = 250$ rad/s

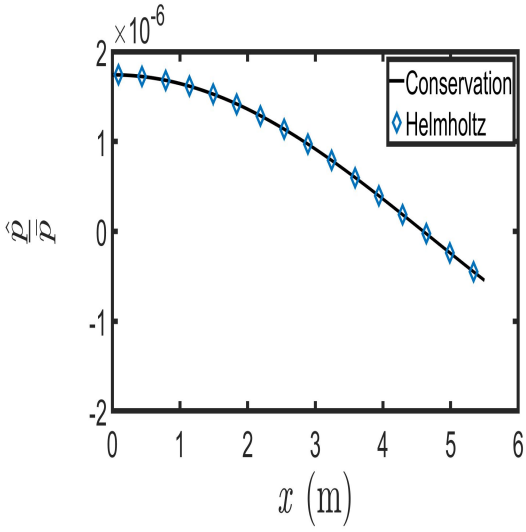

(f) $\omega = 300$ rad/s

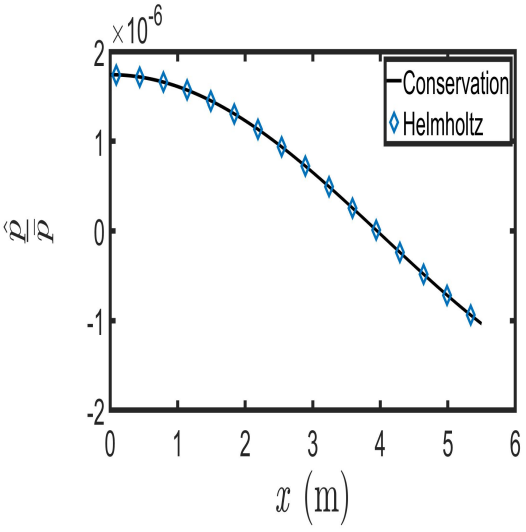

(g) $\omega = 350$ rad/s

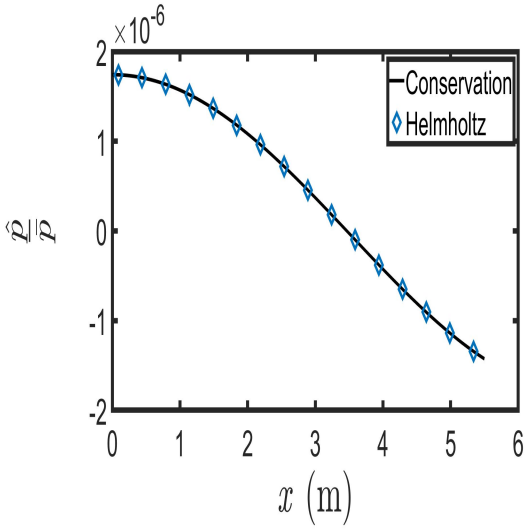

(h) $\omega = 400$ rad/s

Figure A.1: Pressure Fluctuations for linear profile - case III

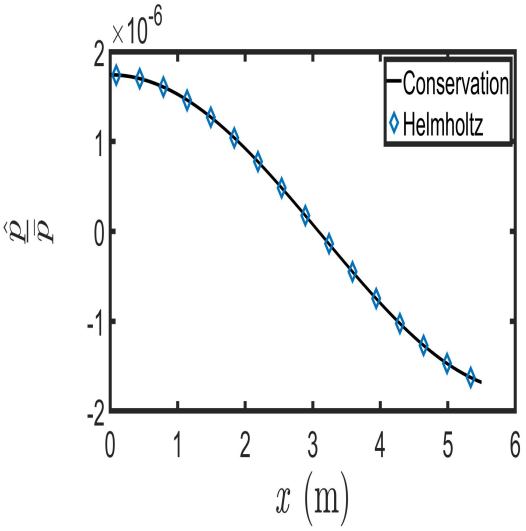

(i) $\omega = 450$ rad/s

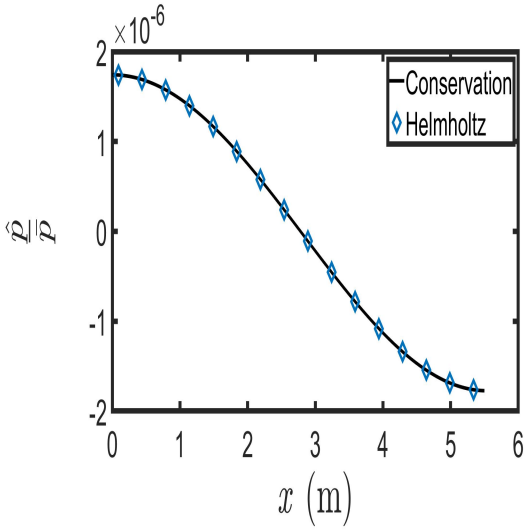

(j) $\omega = 500$ rad/s

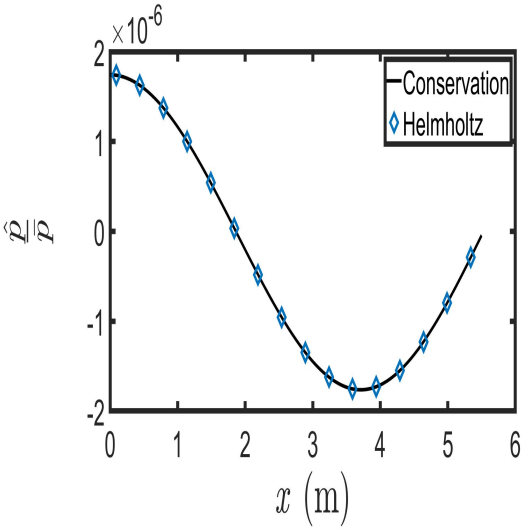

(k) $\omega = 750$ rad/s

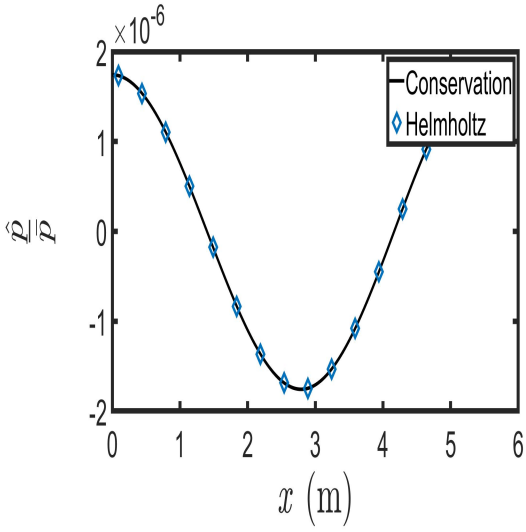

(l) $\omega = 1000$ rad/s

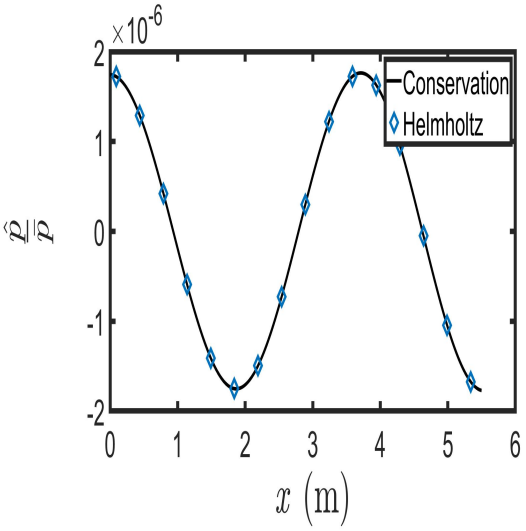

(m) $\omega = 1500$ rad/s

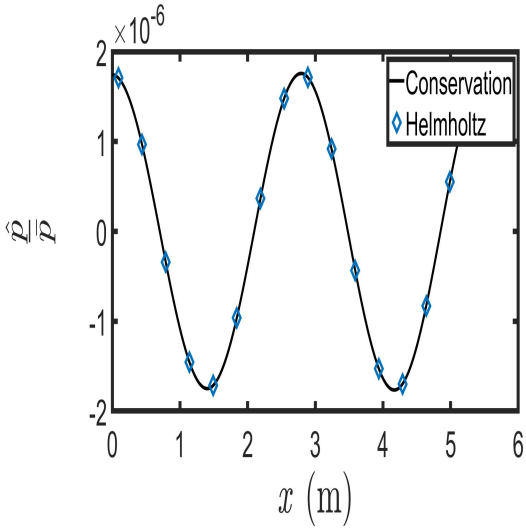

(n) $\omega = 2000$ rad/s

Figure A.1: Pressure Fluctuations for linear profile - case III

A.1.2 Density fluctuations across the duct

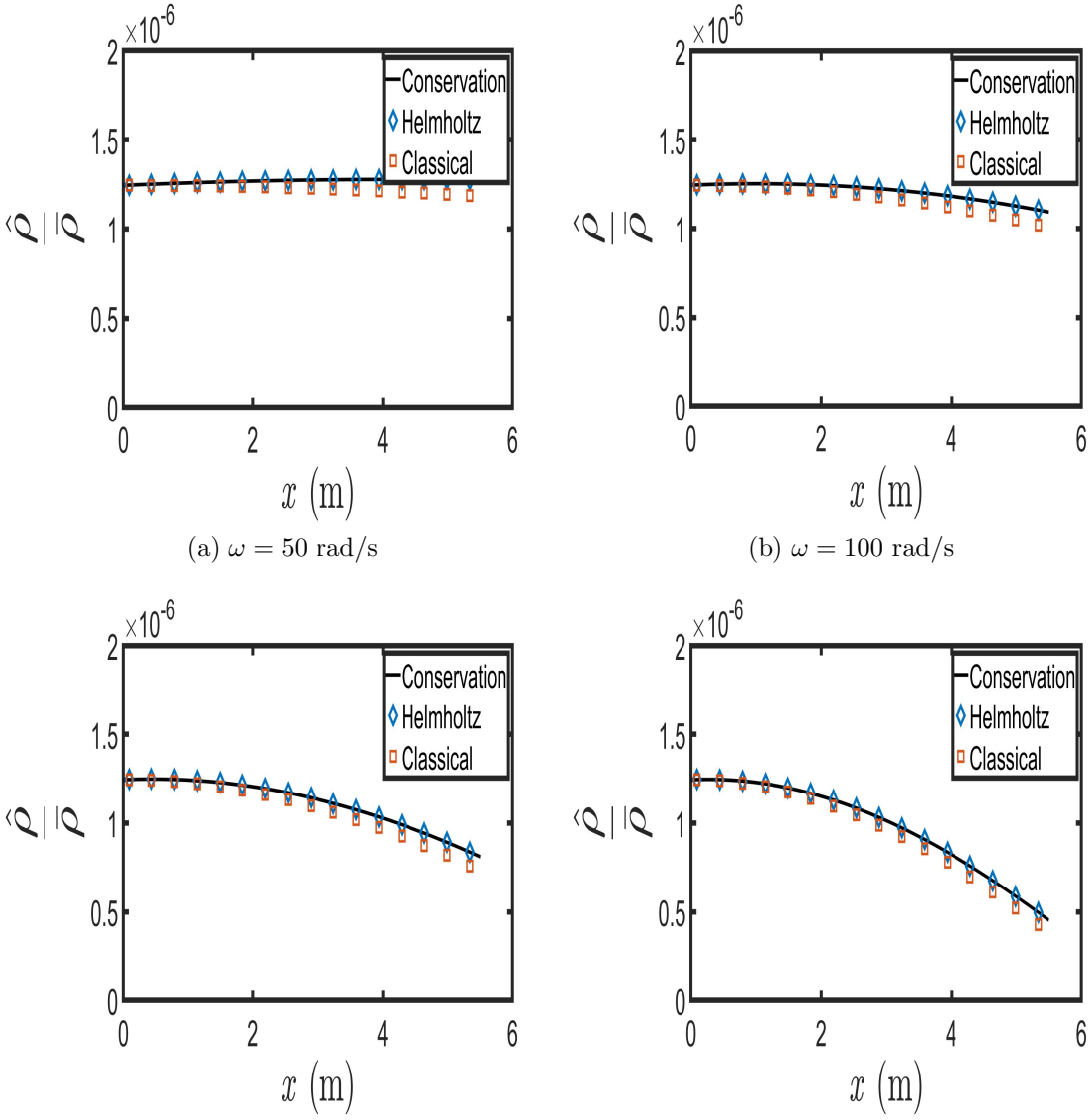

(a) $\omega = 50$ rad/s

(b) $\omega = 100$ rad/s

(c) $\omega = 150$ rad/s

(d) $\omega = 200$ rad/s

Figure A.2: Density Fluctuations for linear profile - case III

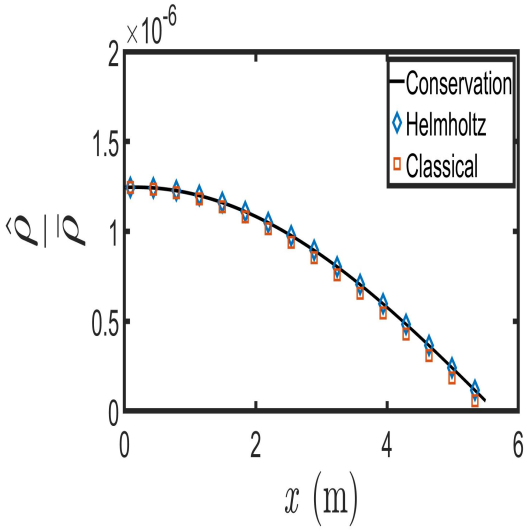

(e) $\omega = 250$ rad/s

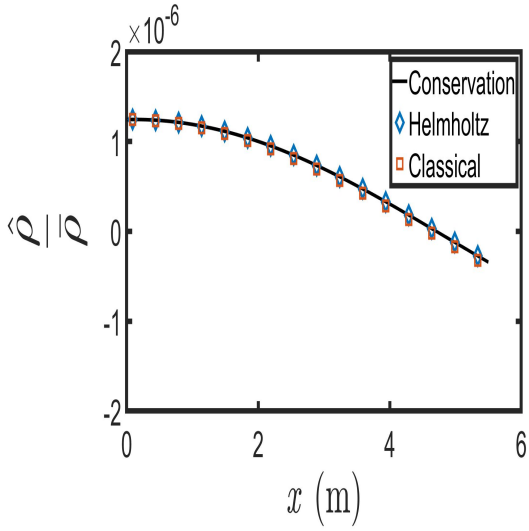

(f) $\omega = 300$ rad/s

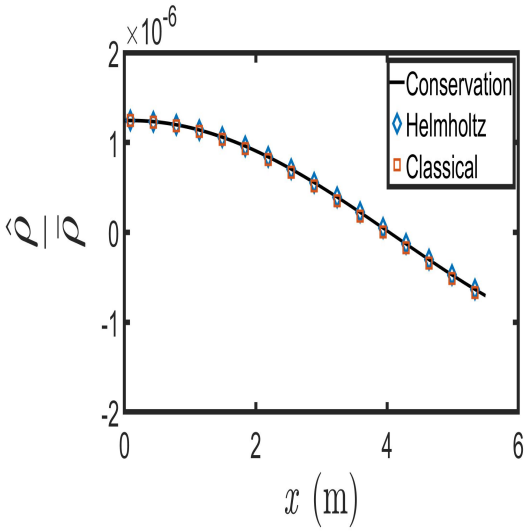

(g) $\omega = 350$ rad/s

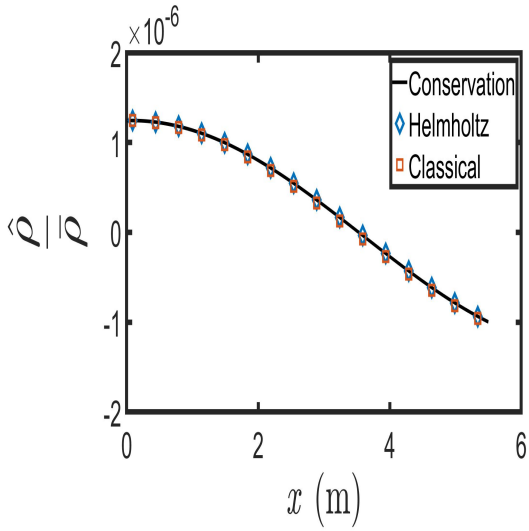

(h) $\omega = 400$ rad/s

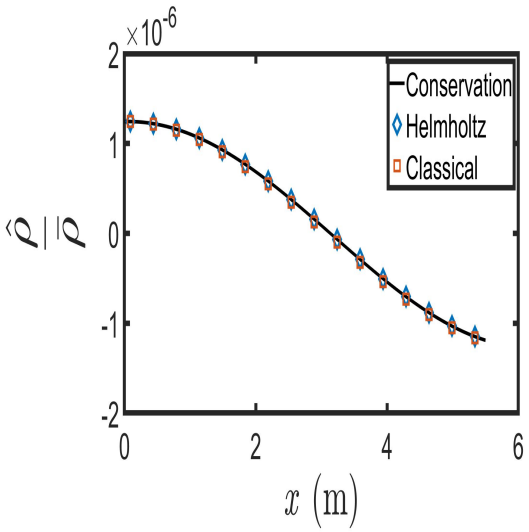

(i) $\omega = 450$ rad/s

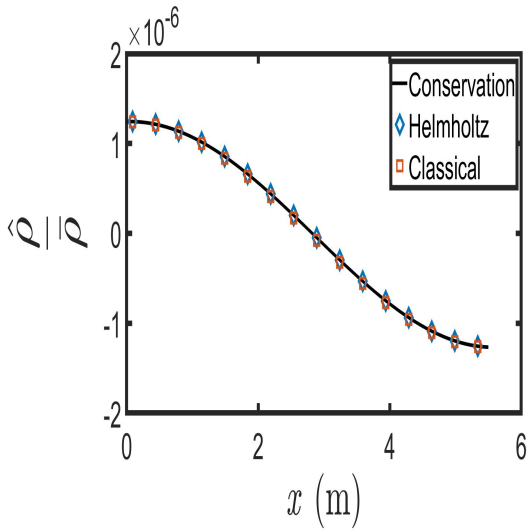

(j) $\omega = 500$ rad/s

Figure A.2: Density Fluctuations for linear profile - case III

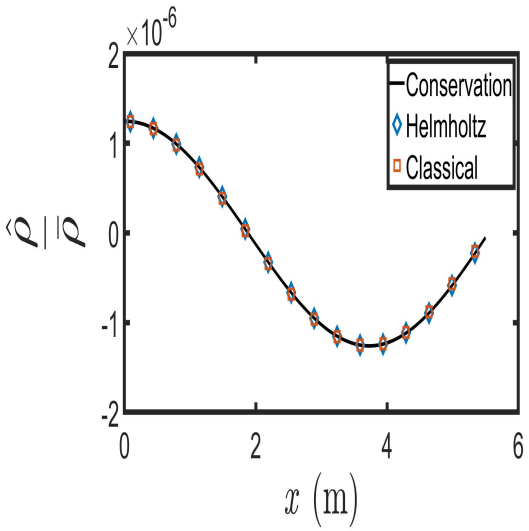

(k) $\omega = 750$ rad/s

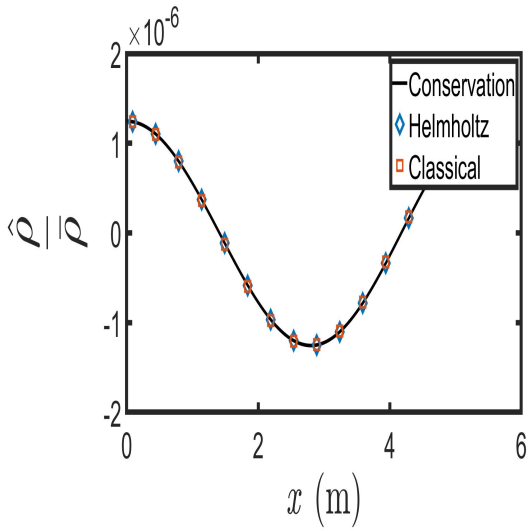

(l) $\omega = 1000$ rad/s

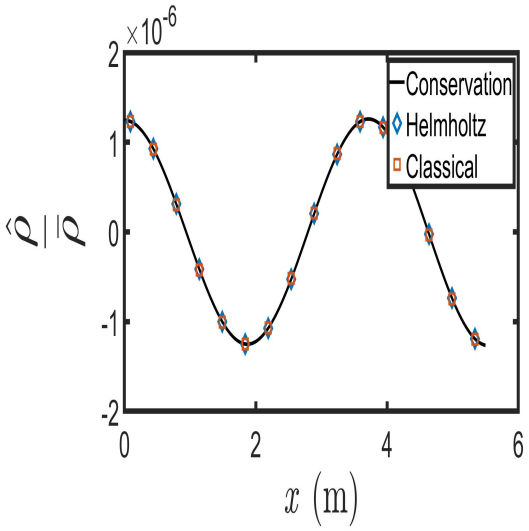

(m) $\omega = 1500$ rad/s

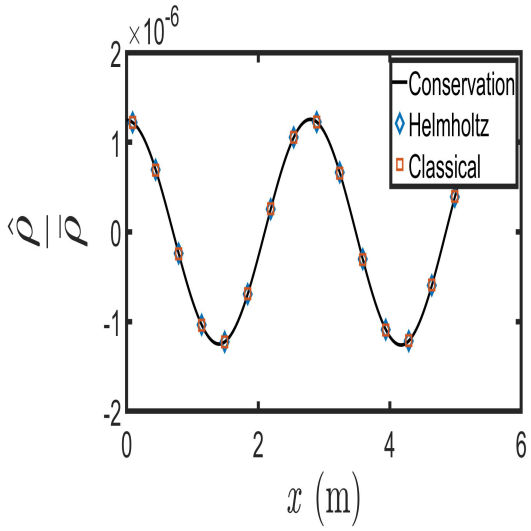

(n) $\omega = 2000$ rad/s

Figure A.2: Density Fluctuations for linear profile - case III

A.2 Four - Thirds Temperature Profile

A.2.1 Pressure fluctuations across the duct

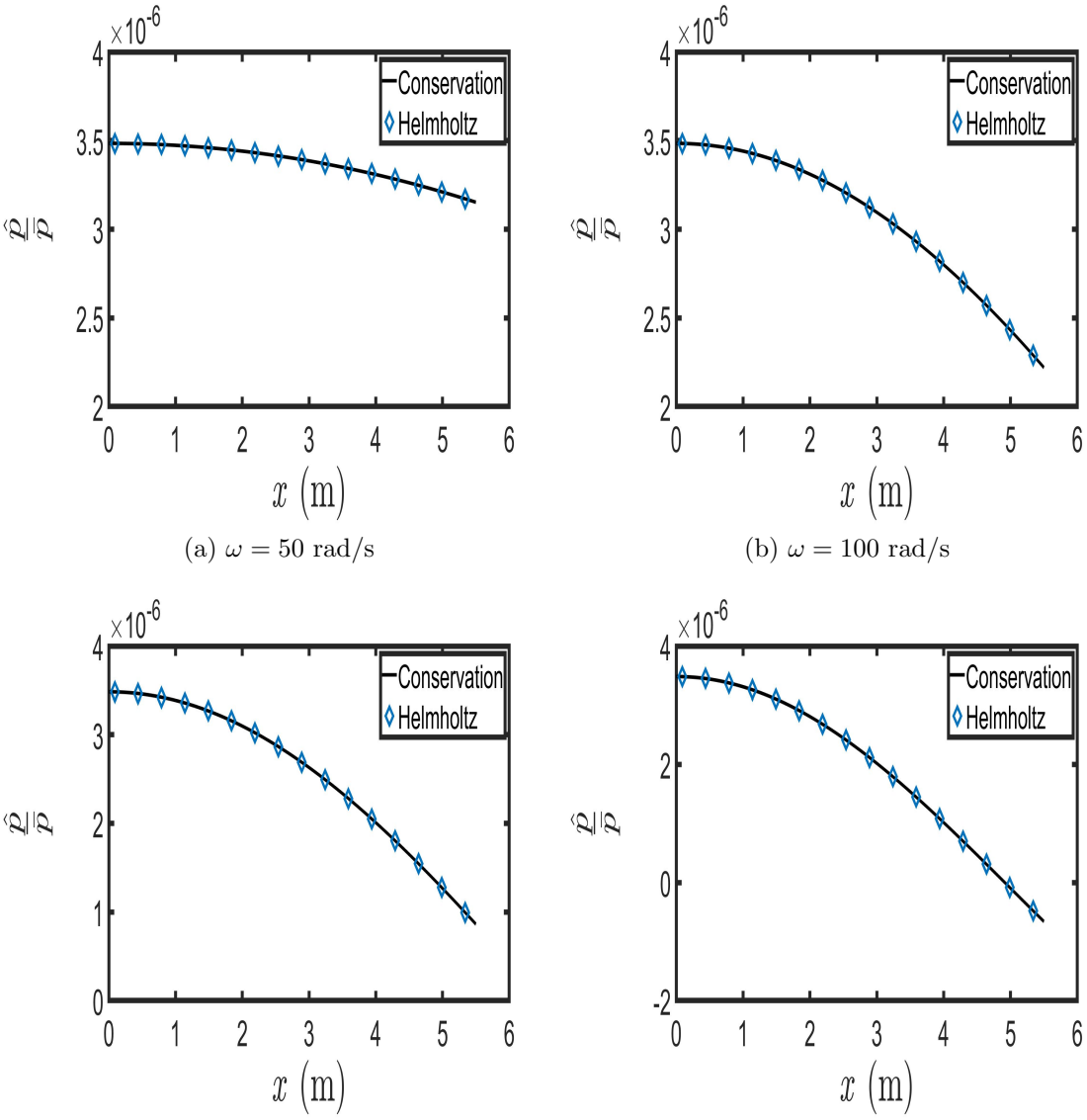

(a) $\omega = 50$ rad/s

(b) $\omega = 100$ rad/s

(c) $\omega = 150$ rad/s

(d) $\omega = 200$ rad/s

Figure A.3: Pressure Fluctuations for non-linear profile - case III

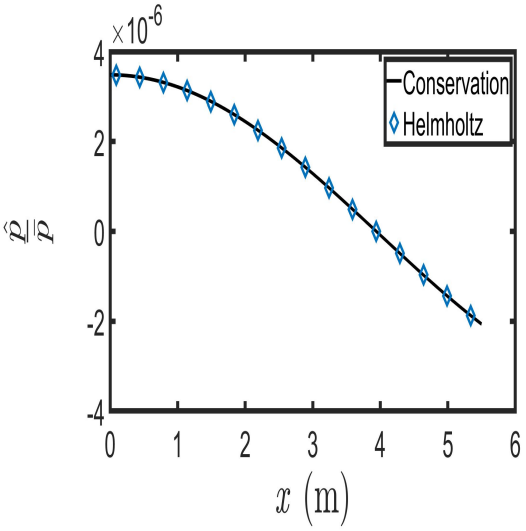

(e) $\omega = 250$ rad/s

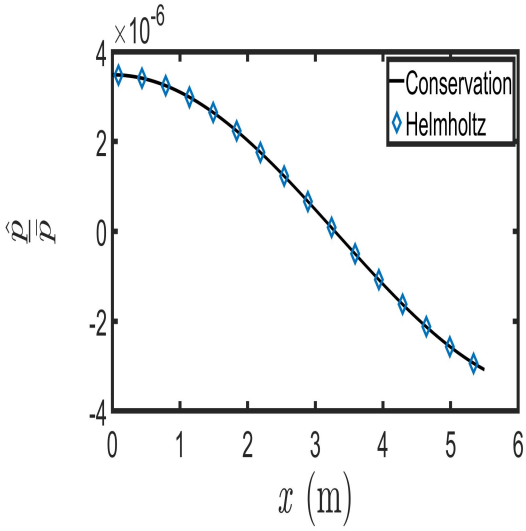

(f) $\omega = 300$ rad/s

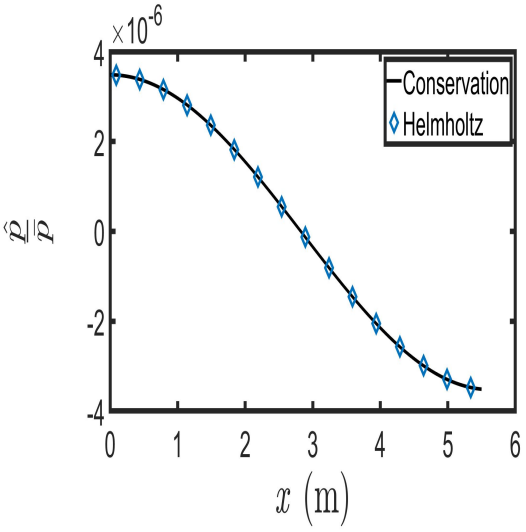

(g) $\omega = 350$ rad/s

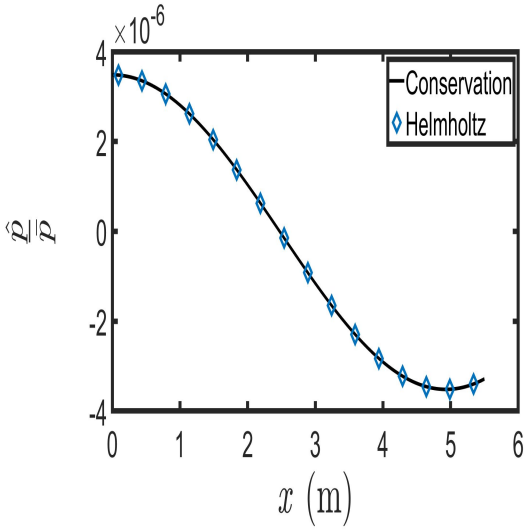

(h) $\omega = 400$ rad/s

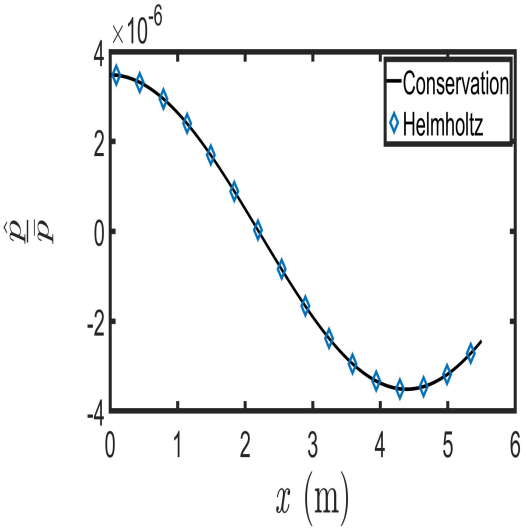

(i) $\omega = 450$ rad/s

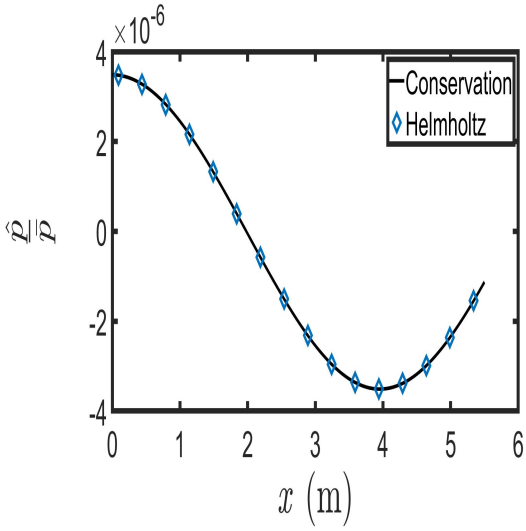

(j) $\omega = 500$ rad/s

Figure A.3: Pressure Fluctuations for non-linear profile - case III

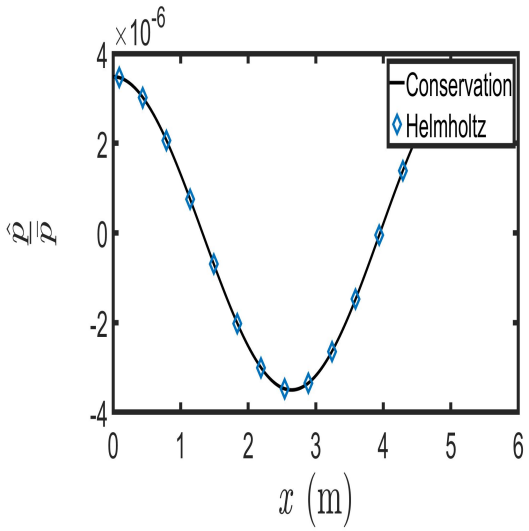

(k) $\omega = 750$ rad/s

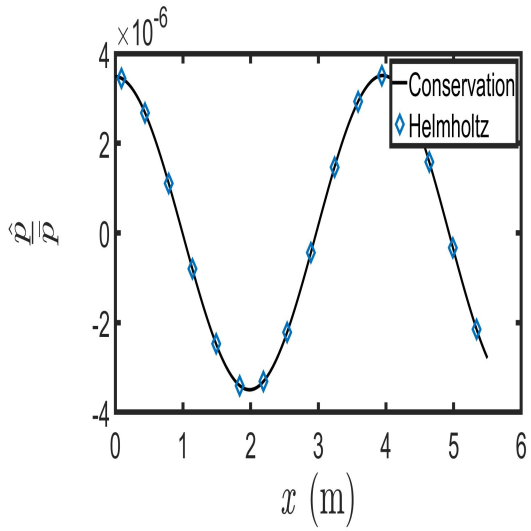

(l) $\omega = 1000$ rad/s

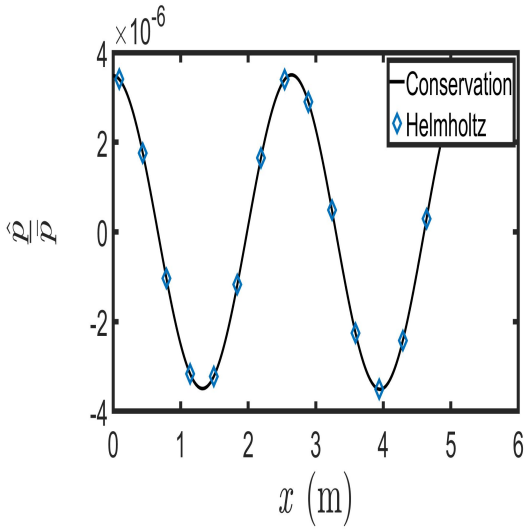

(m) $\omega = 1500$ rad/s

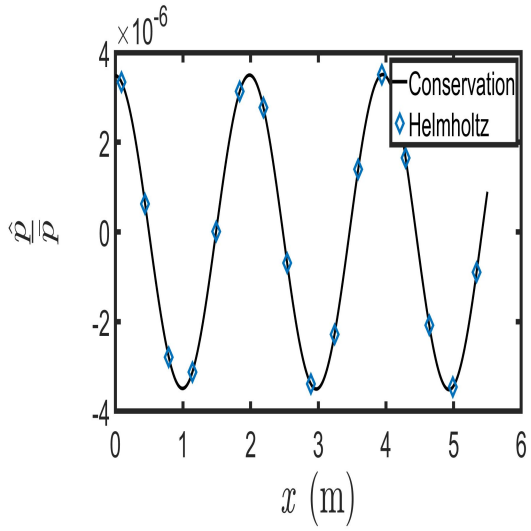

(n) $\omega = 2000$ rad/s

Figure A.3: Pressure Fluctuations for non-linear profile - case III

A.2.2 Density fluctuations across the duct

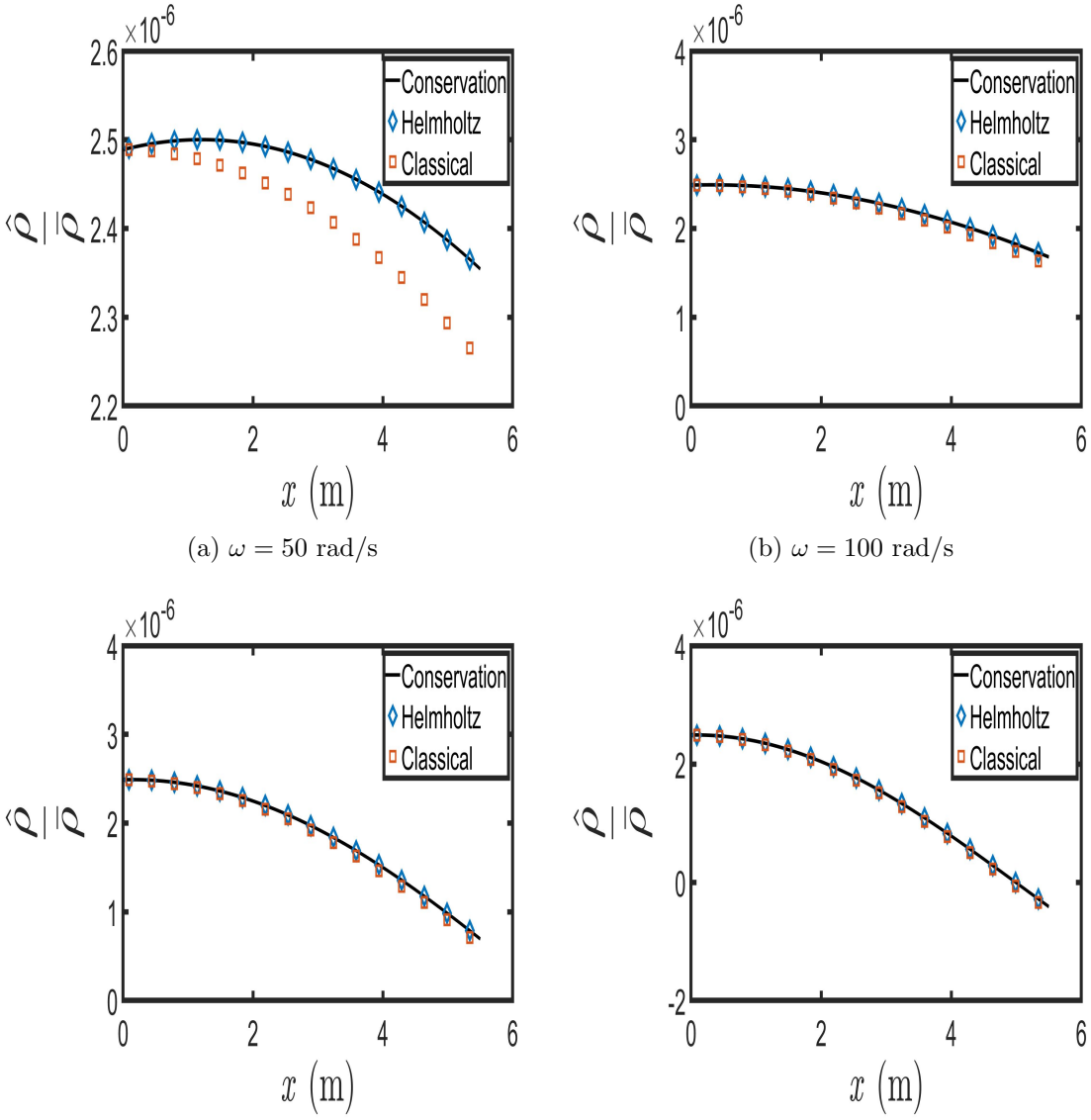

(a) $\omega = 50$ rad/s

(b) $\omega = 100$ rad/s

(c) $\omega = 150$ rad/s

(d) $\omega = 200$ rad/s

Figure A.4: Density Fluctuations for non-linear profile - case III

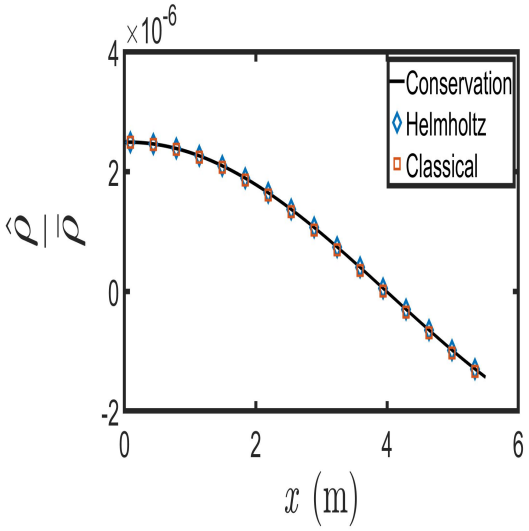

(e) $\omega = 250$ rad/s

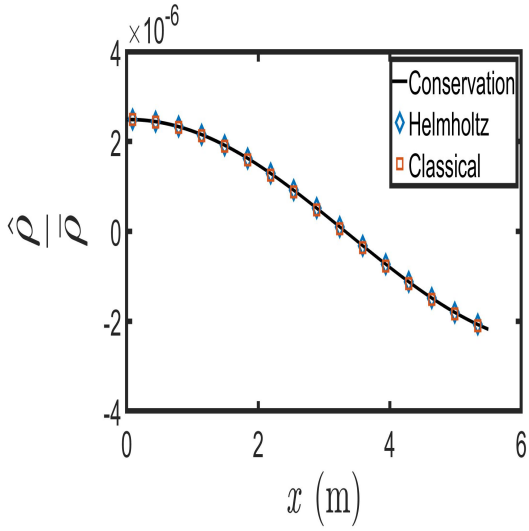

(f) $\omega = 300$ rad/s

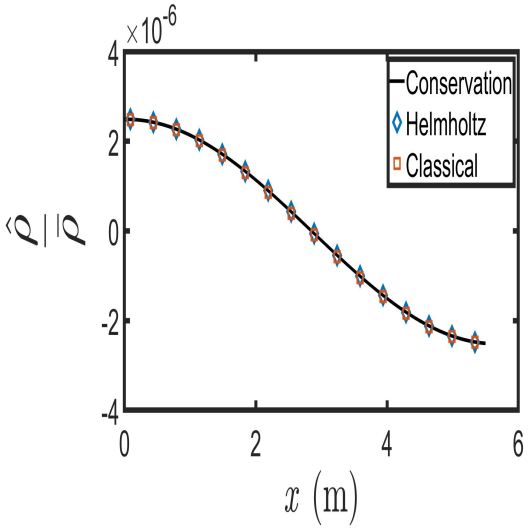

(g) $\omega = 350$ rad/s

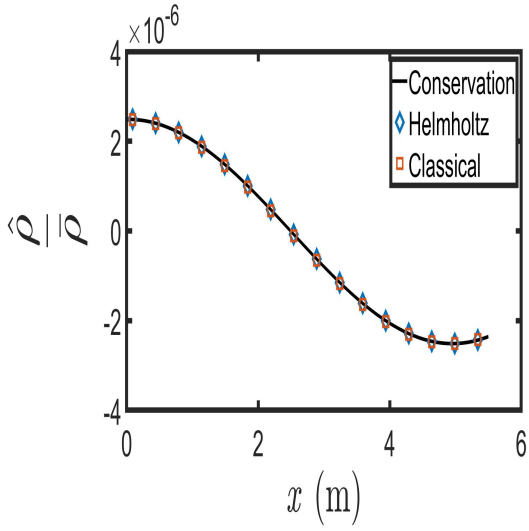

(h) $\omega = 400$ rad/s

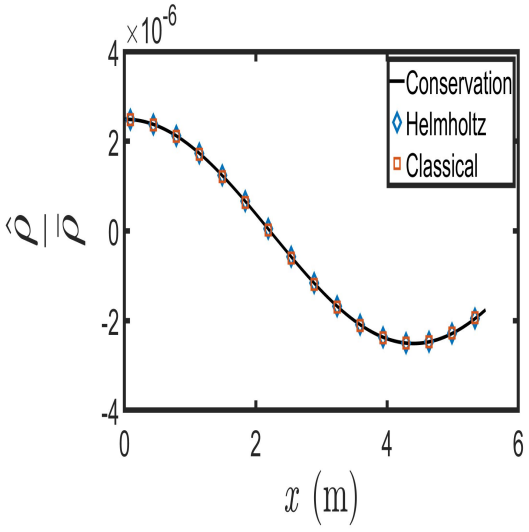

(i) $\omega = 450$ rad/s

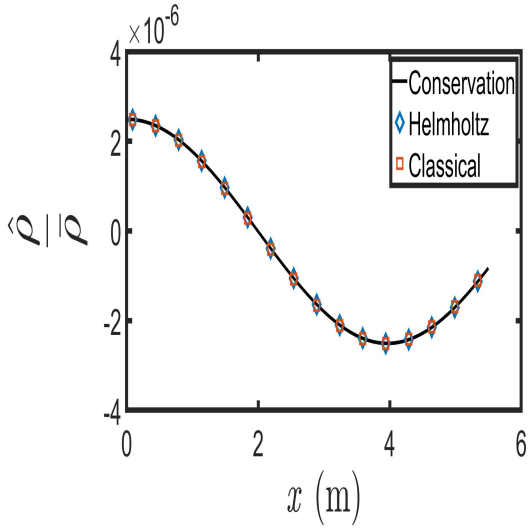

(j) $\omega = 500$ rad/s

Figure A.4: Density Fluctuations for non-linear profile - case III

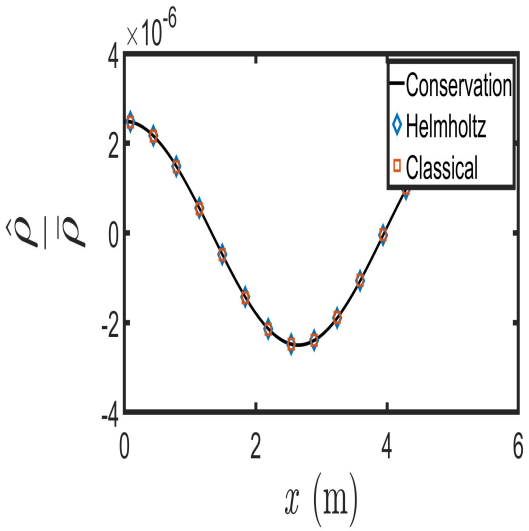

(k) $\omega = 750$ rad/s

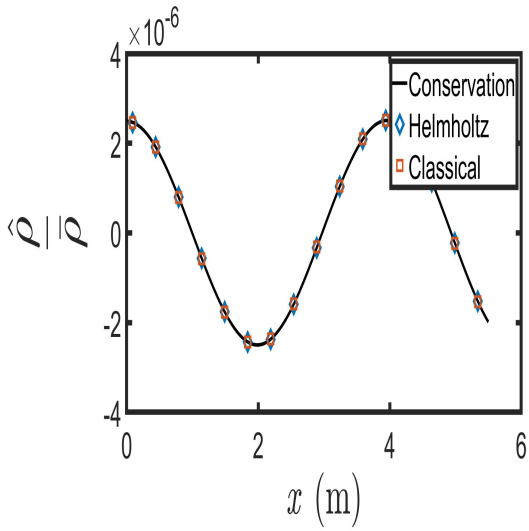

(l) $\omega = 1000$ rad/s

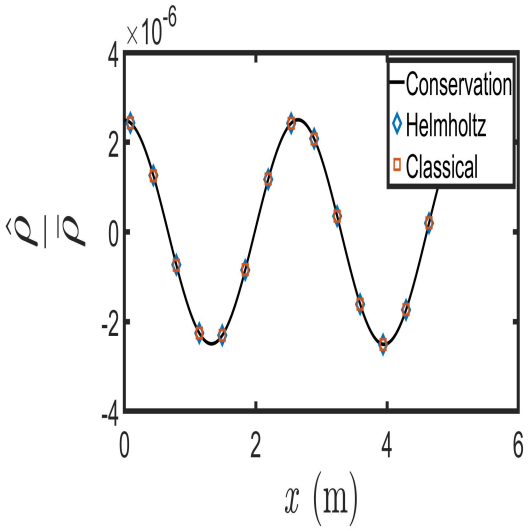

(m) $\omega = 1500$ rad/s

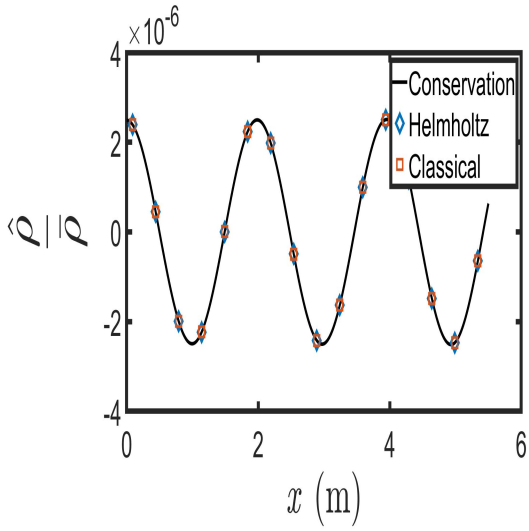

(n) $\omega = 2000$ rad/s

Figure A.4: Density Fluctuations for non-linear profile - case III

Appendix B

Supporting Plots for CASE IV

B.1 Linear Temperature Profile

B.1.1 Pressure fluctuations across the duct

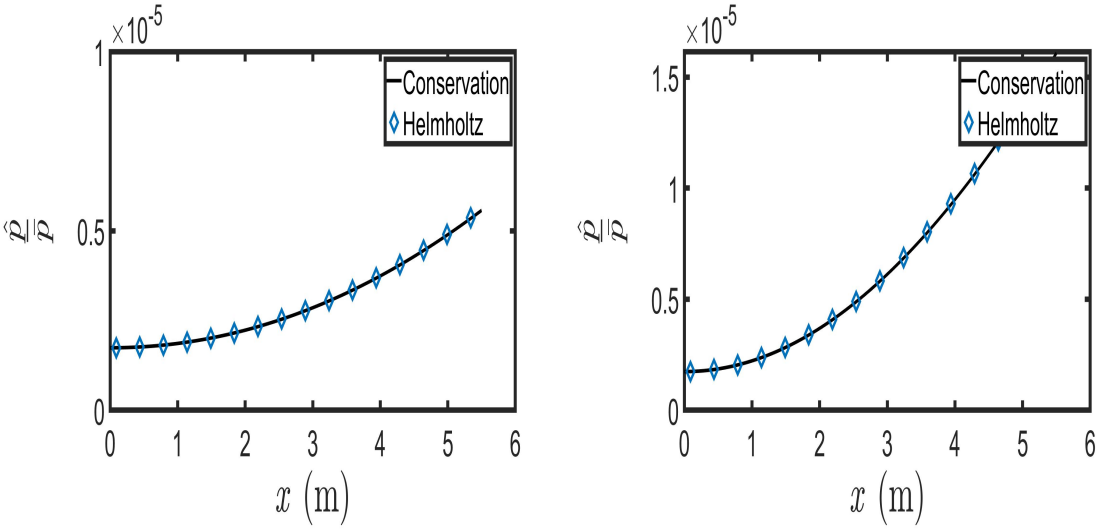

(a) $\omega = 50$ rad/s (b) $\omega = 100$ rad/s

Figure B.1: Pressure Fluctuations for linear profile - case IV

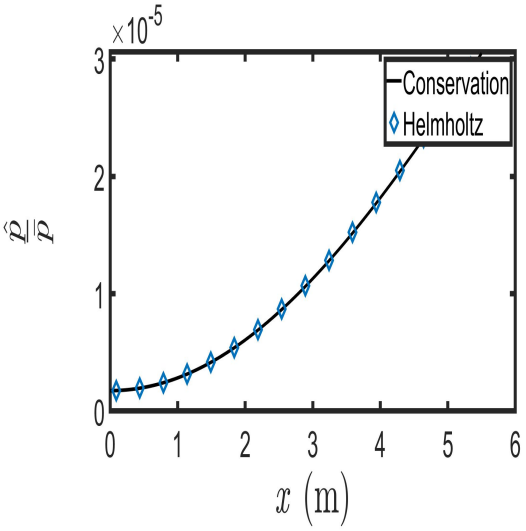

(c) $\omega = 150$ rad/s

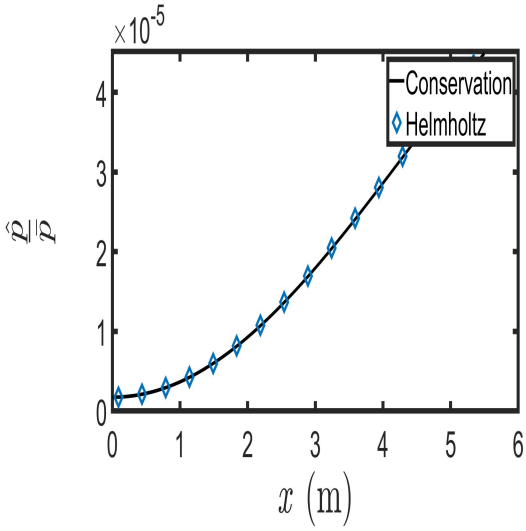

(d) $\omega = 200$ rad/s

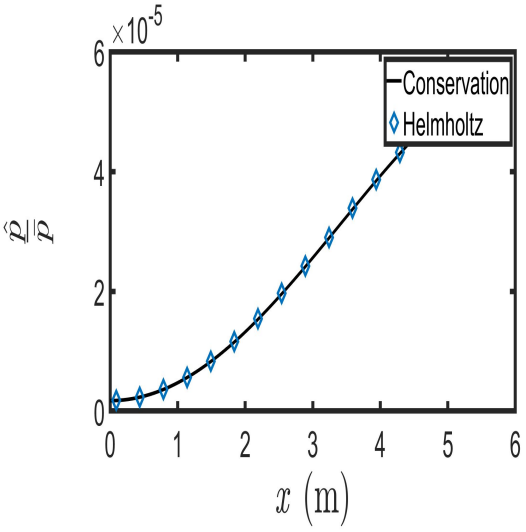

(e) $\omega = 250$ rad/s

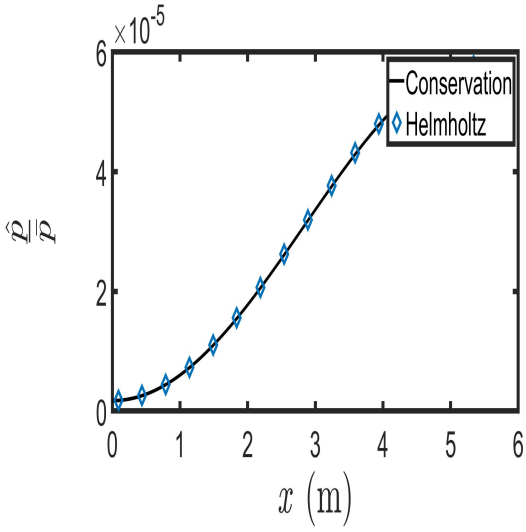

(f) $\omega = 300$ rad/s

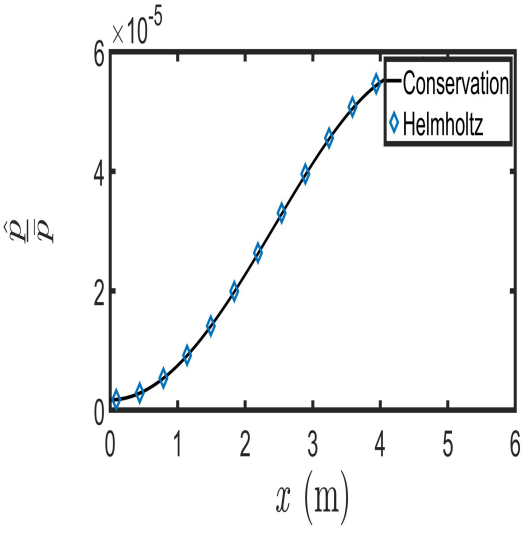

(g) $\omega = 350$ rad/s

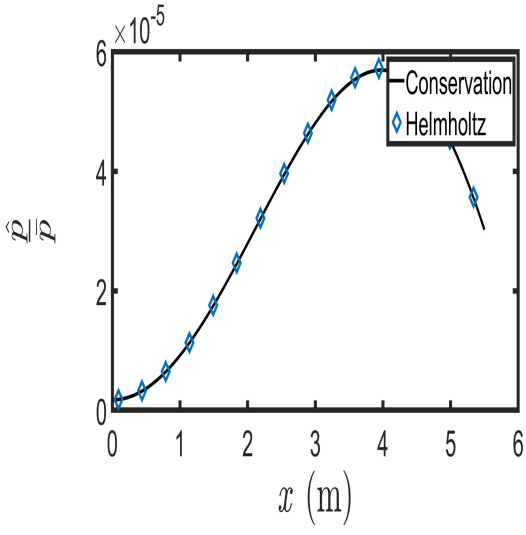

(h) $\omega = 400$ rad/s

Figure B.1: Pressure Fluctuations for linear profile - case IV

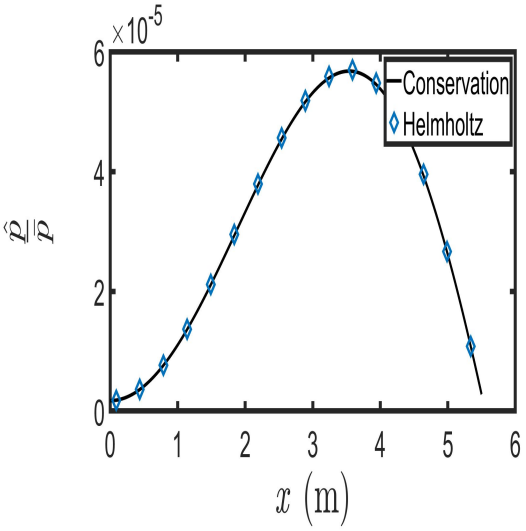

(i) $\omega = 450$ rad/s

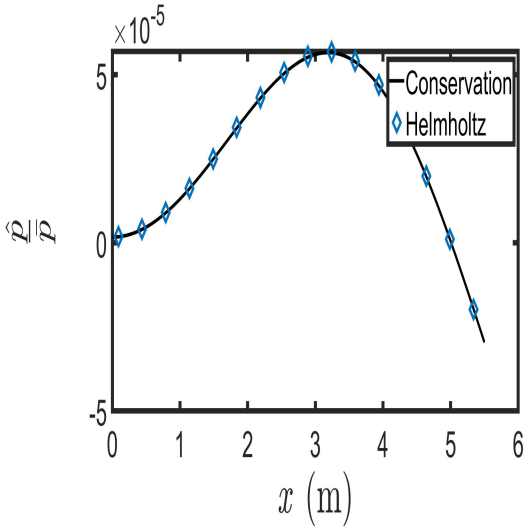

(j) $\omega = 500$ rad/s

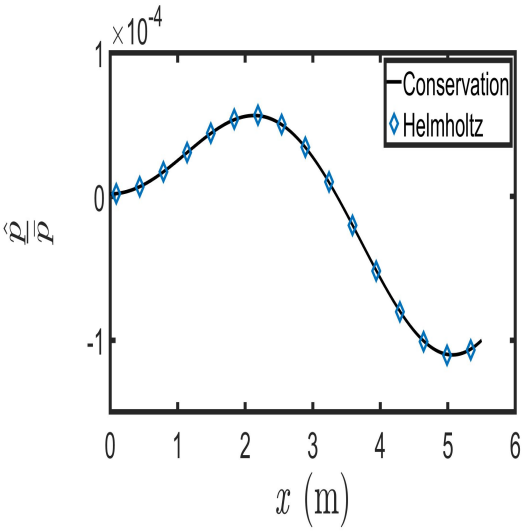

(k) $\omega = 750$ rad/s

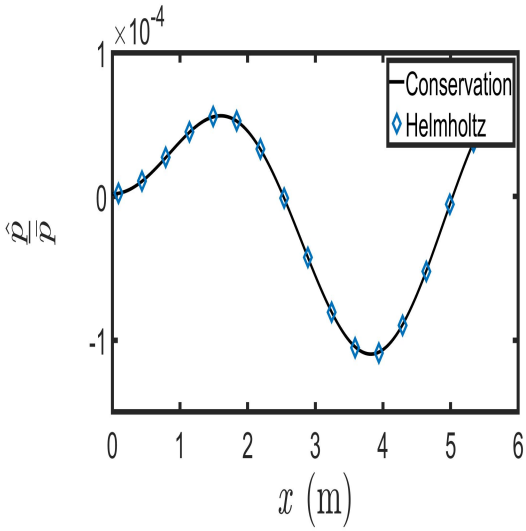

(l) $\omega = 1000$ rad/s

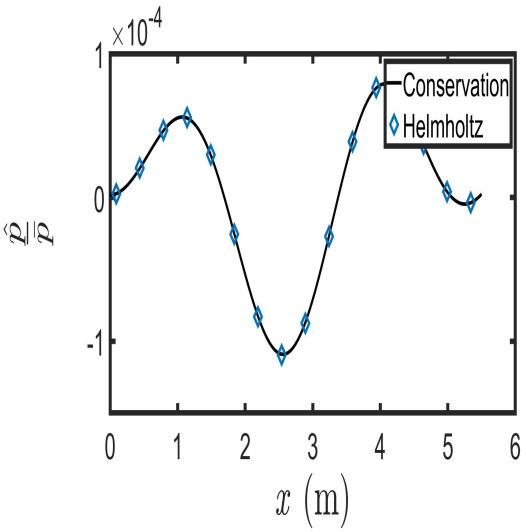

(m) $\omega = 1500$ rad/s

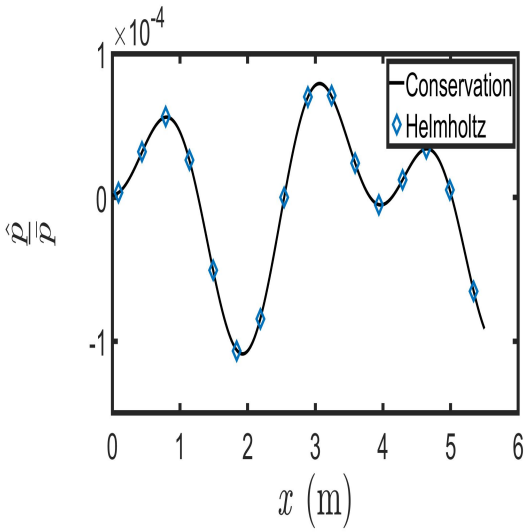

(n) $\omega = 2000$ rad/s

Figure B.1: Pressure Fluctuations for linear profile - case IV

B.1.2 Density fluctuations across the duct

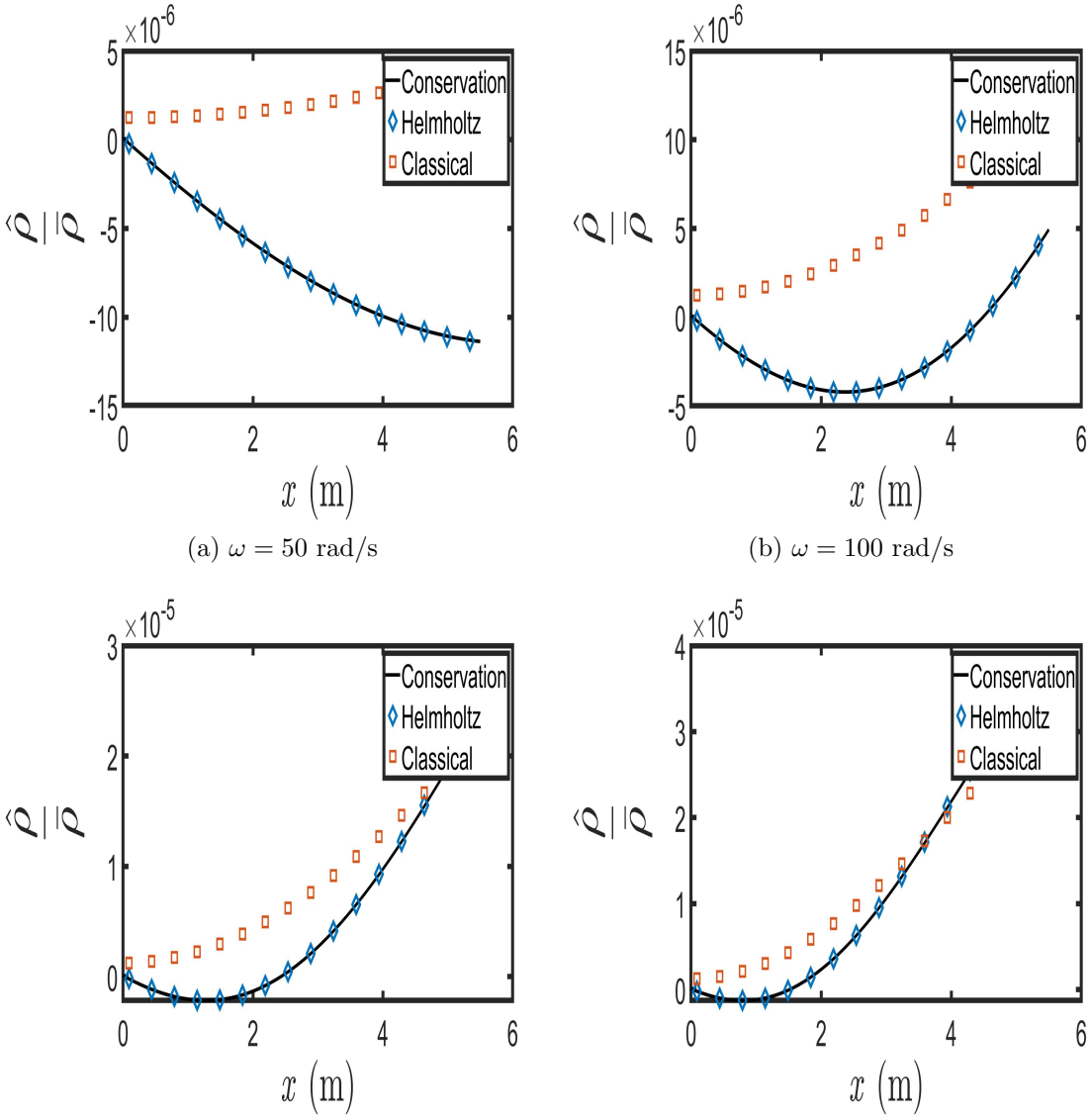

(a) $\omega = 50$ rad/s

(b) $\omega = 100$ rad/s

(c) $\omega = 150$ rad/s

(d) $\omega = 200$ rad/s

Figure B.2: Density Fluctuations for linear profile - case IV

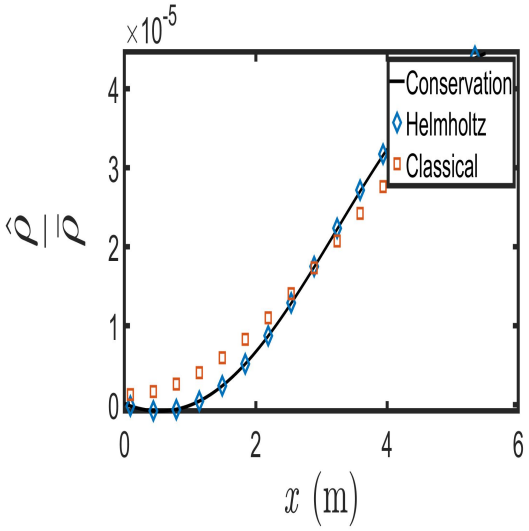

(e) $\omega = 250$ rad/s

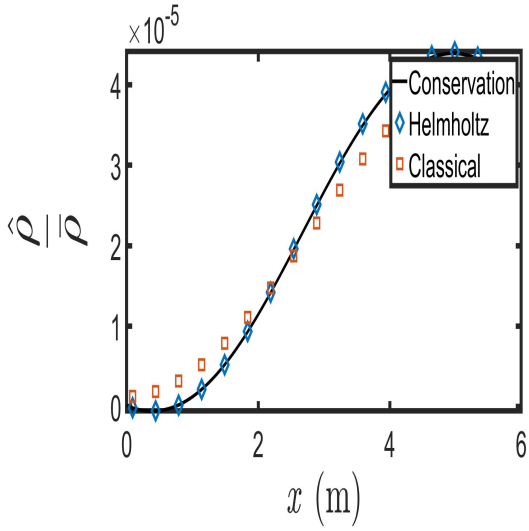

(f) $\omega = 300$ rad/s

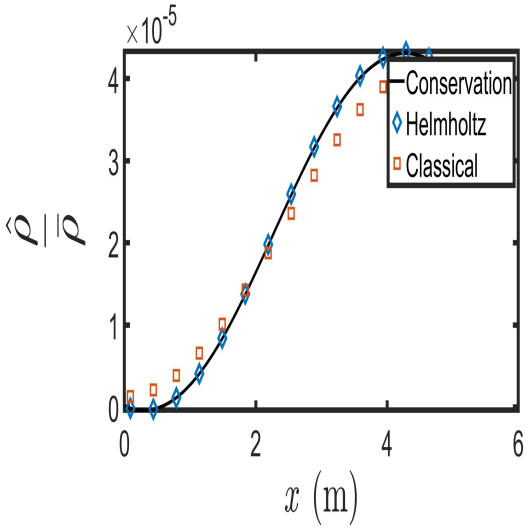

(g) $\omega = 350$ rad/s

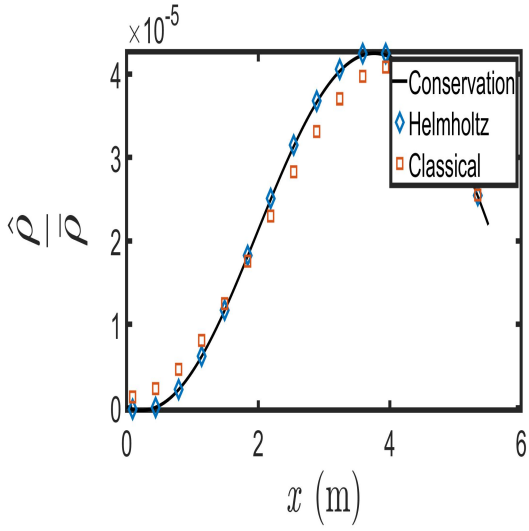

(h) $\omega = 400$ rad/s

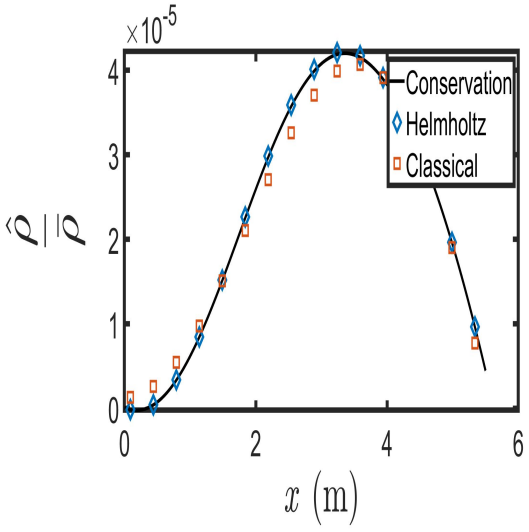

(i) $\omega = 450$ rad/s

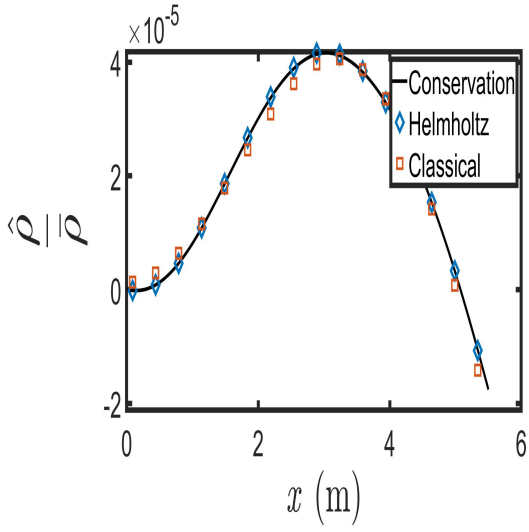

(j) $\omega = 500$ rad/s

Figure B.2: Density Fluctuations for linear profile - case IV

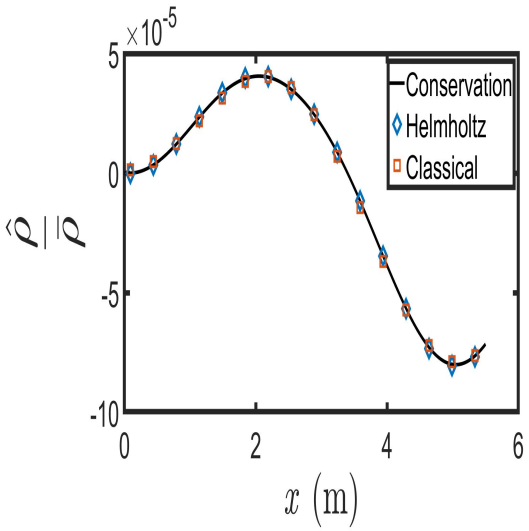

(k) $\omega = 750$ rad/s

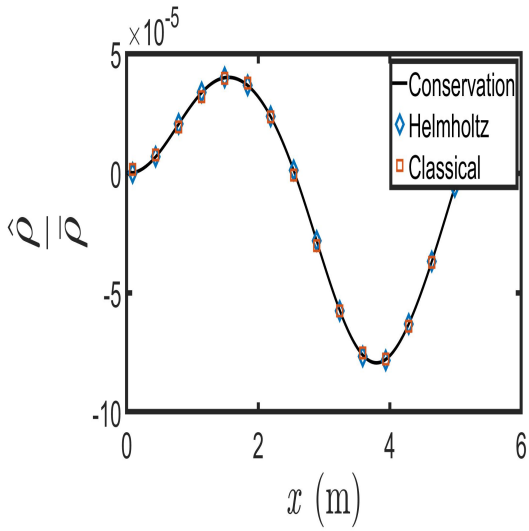

(l) $\omega = 1000$ rad/s

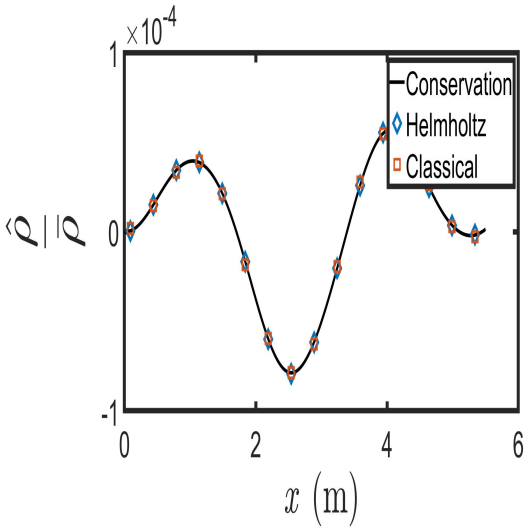

(m) $\omega = 1500$ rad/s

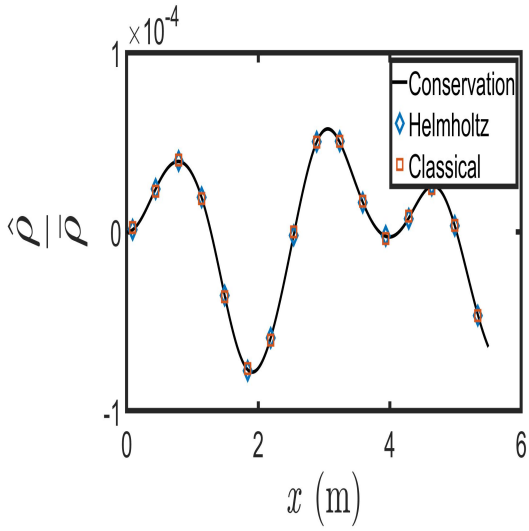

(n) $\omega = 2000$ rad/s

Figure B.2: Density Fluctuations for linear profile - case IV

B.2 Four - Thirds Temperature Profile

B.2.1 Pressure fluctuations across the duct

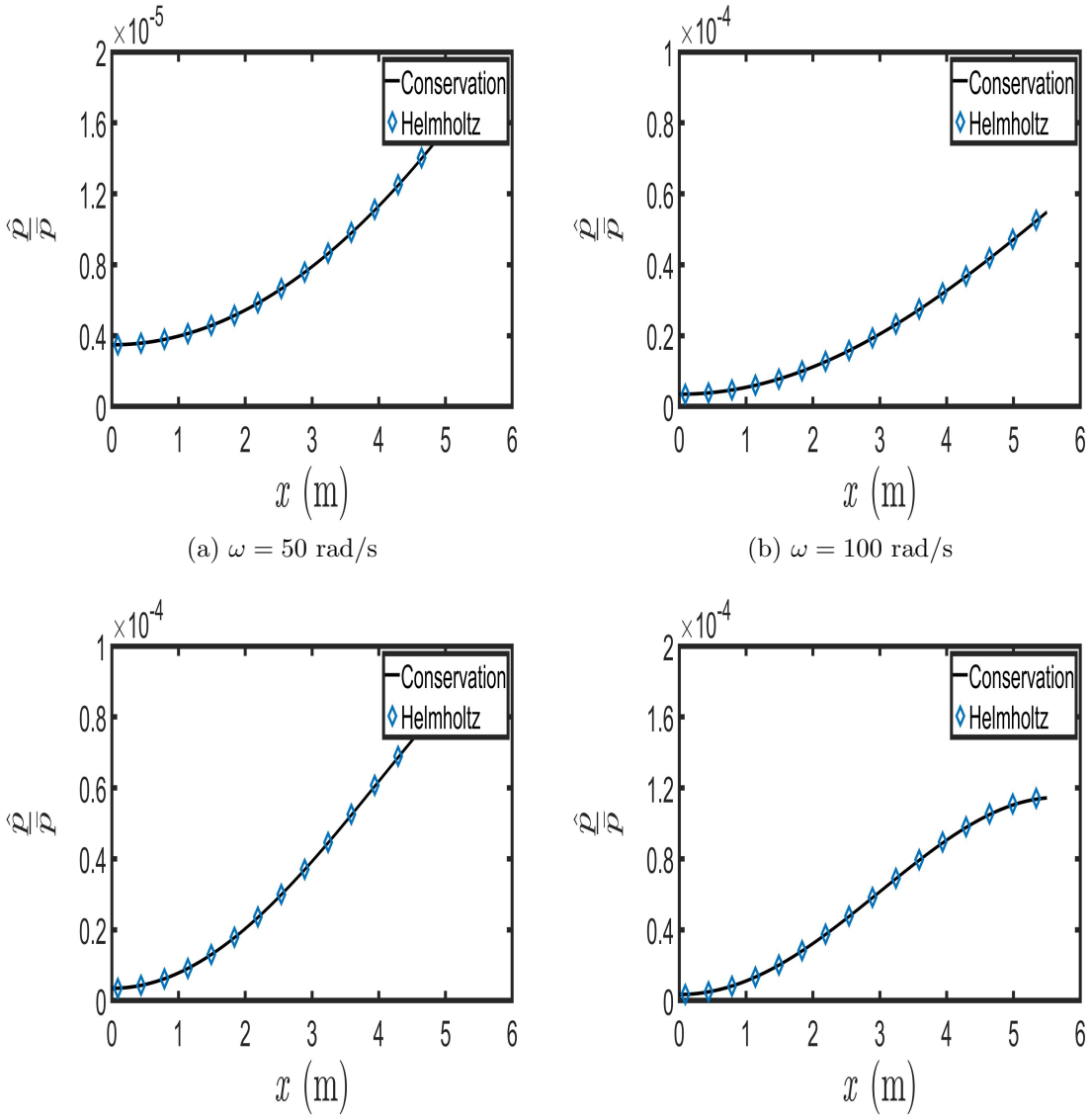

(a) $\omega = 50$ rad/s

(b) $\omega = 100$ rad/s

(c) $\omega = 150$ rad/s

(d) $\omega = 200$ rad/s

Figure B.3: Pressure Fluctuations for non-linear profile - case IV

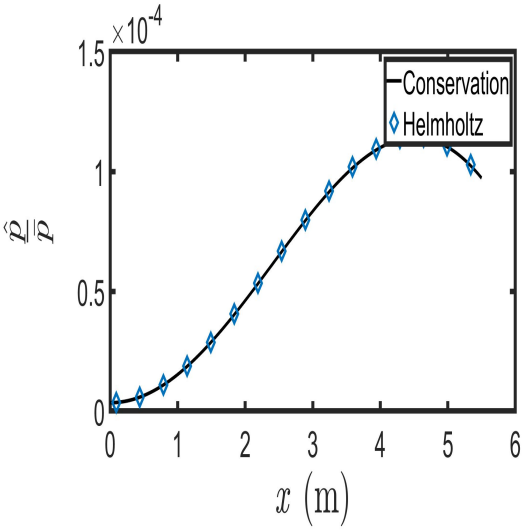

(e) $\omega = 250$ rad/s

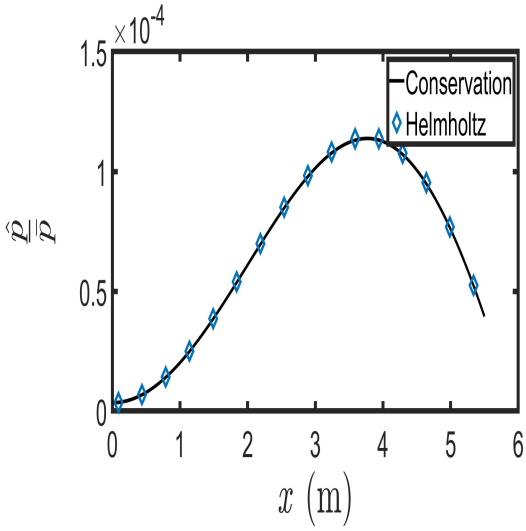

(f) $\omega = 300$ rad/s

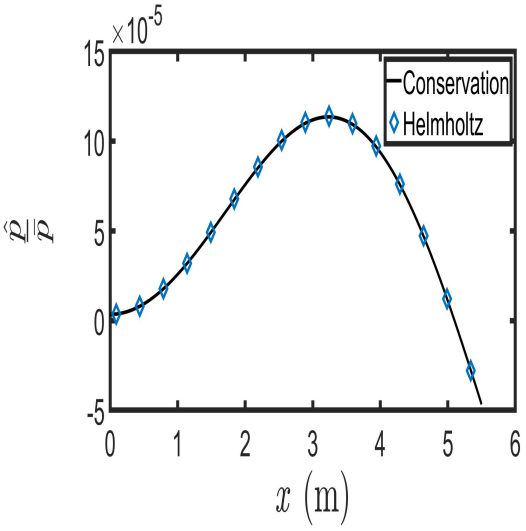

(g) $\omega = 350$ rad/s

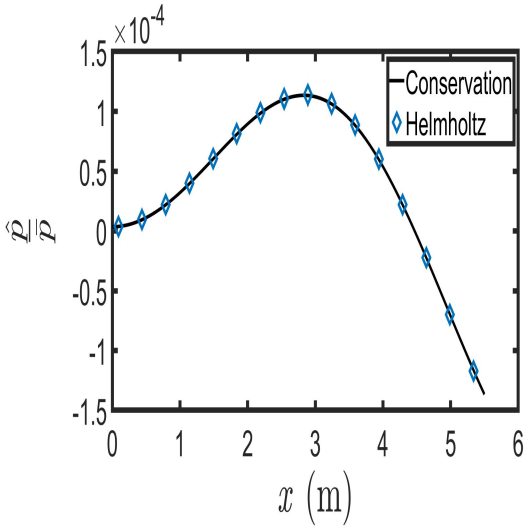

(h) $\omega = 400$ rad/s

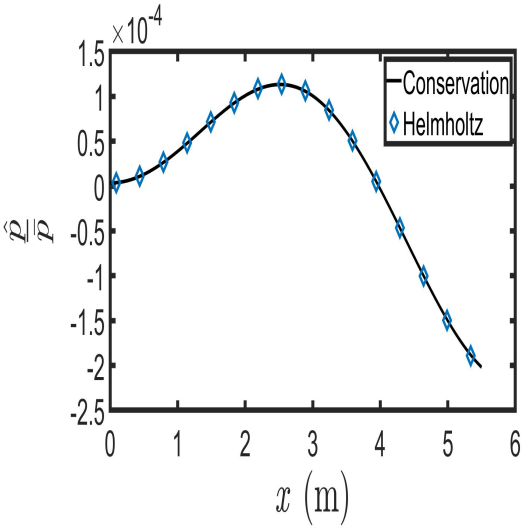

(i) $\omega = 450$ rad/s

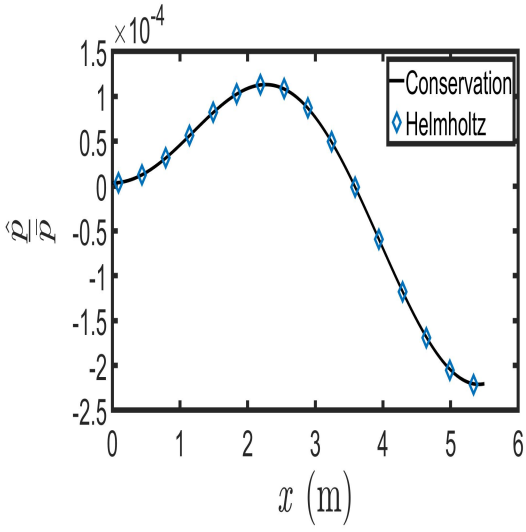

(j) $\omega = 500$ rad/s

Figure B.3: Pressure Fluctuations for non-linear profile - case IV

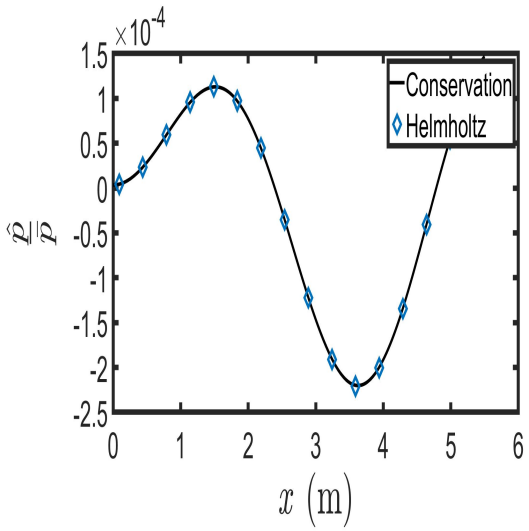

(k) $\omega = 750$ rad/s

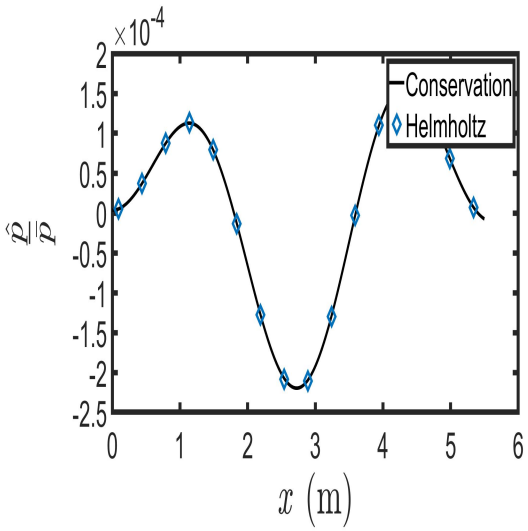

(l) $\omega = 1000$ rad/s

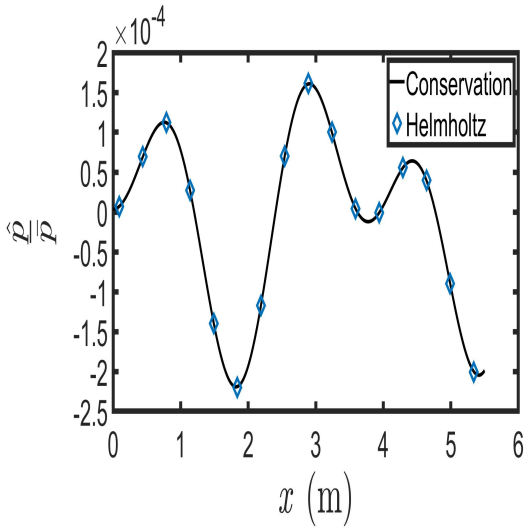

(m) $\omega = 1500$ rad/s

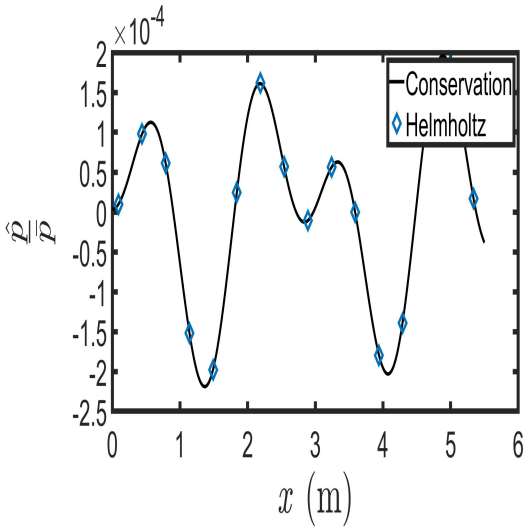

(n) $\omega = 2000$ rad/s

Figure B.3: Pressure Fluctuations for non-linear profile - case IV

B.2.2 Density fluctuations across the duct

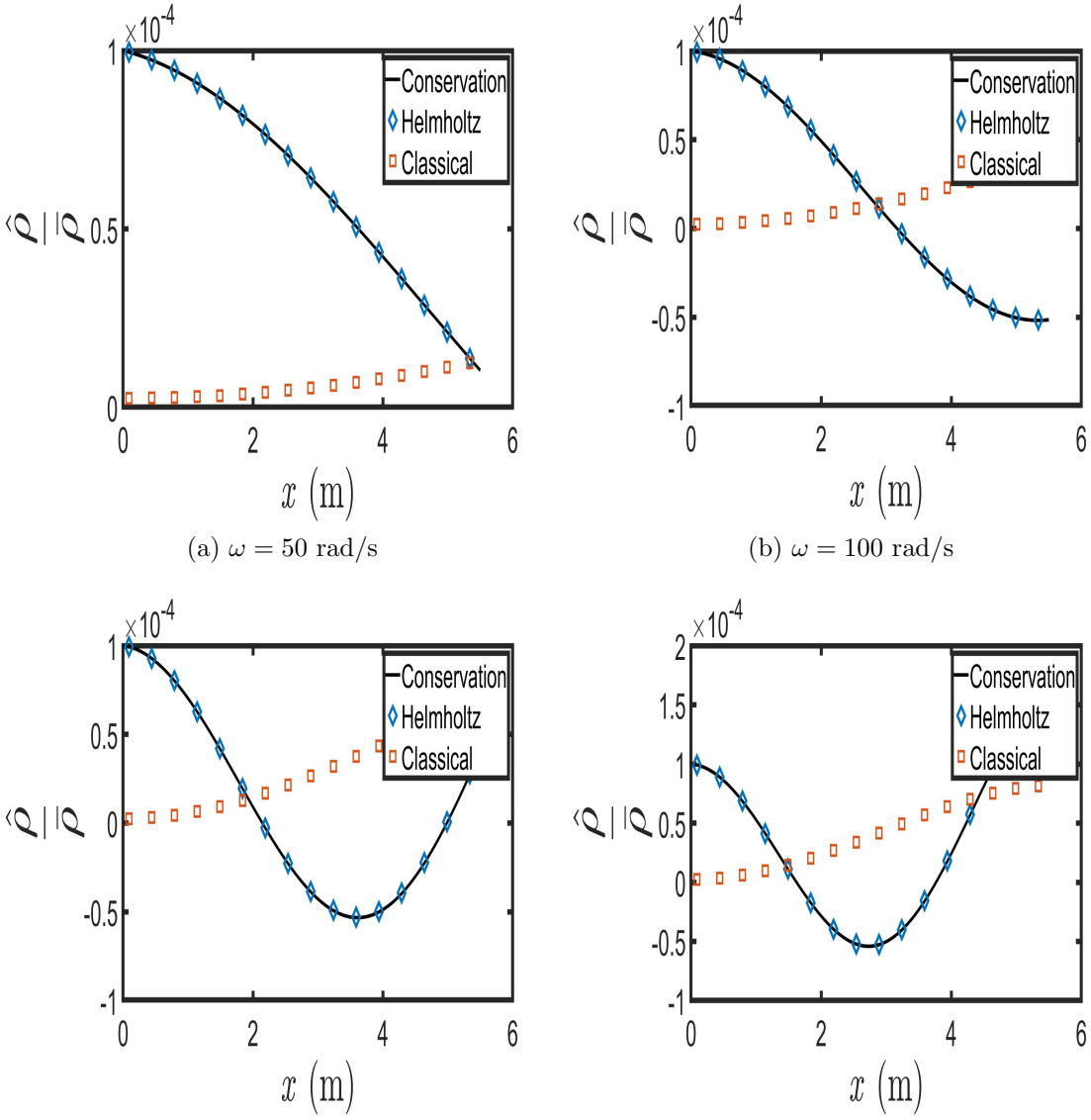

(a) $\omega = 50$ rad/s

(b) $\omega = 100$ rad/s

(c) $\omega = 150$ rad/s

(d) $\omega = 200$ rad/s

Figure B.4: Density Fluctuations for non-linear profile - case IV

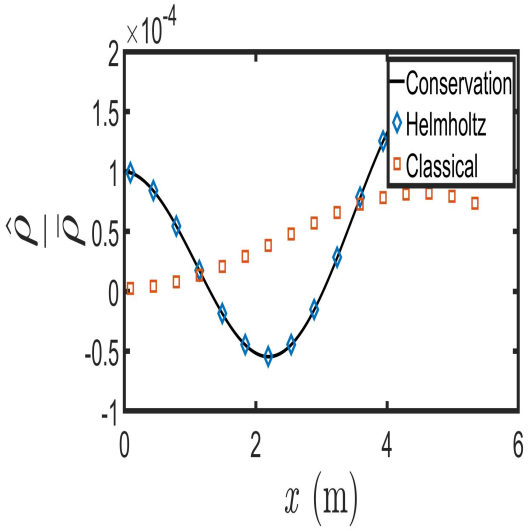

(e) $\omega = 250$ rad/s

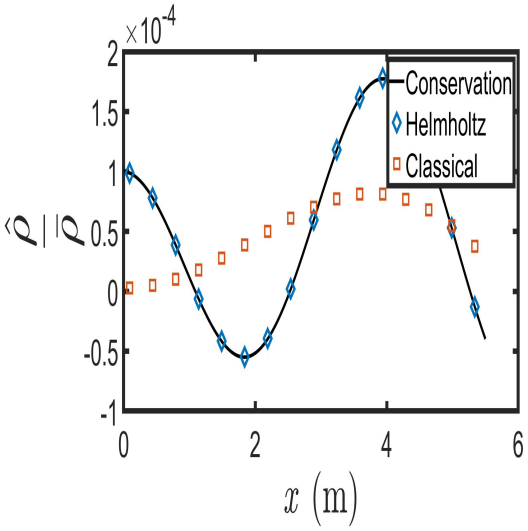

(f) $\omega = 300$ rad/s

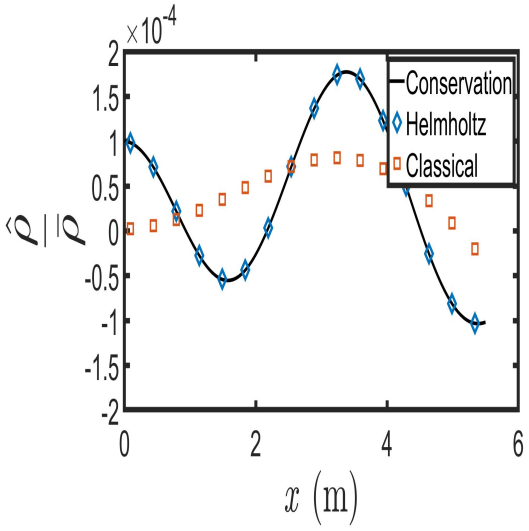

(g) $\omega = 350$ rad/s

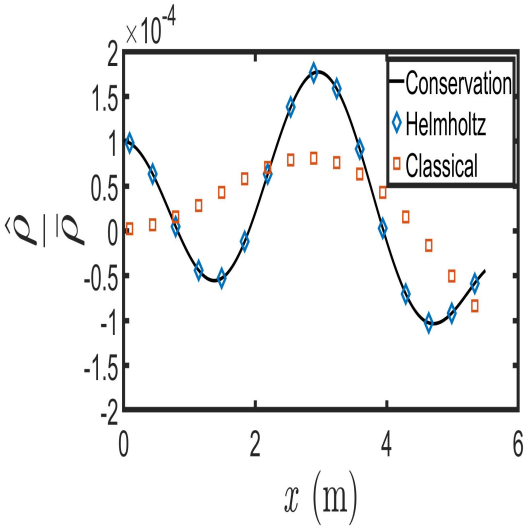

(h) $\omega = 400$ rad/s

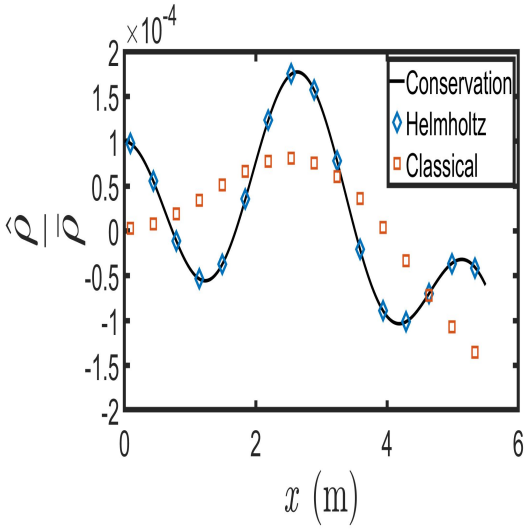

(i) $\omega = 450$ rad/s

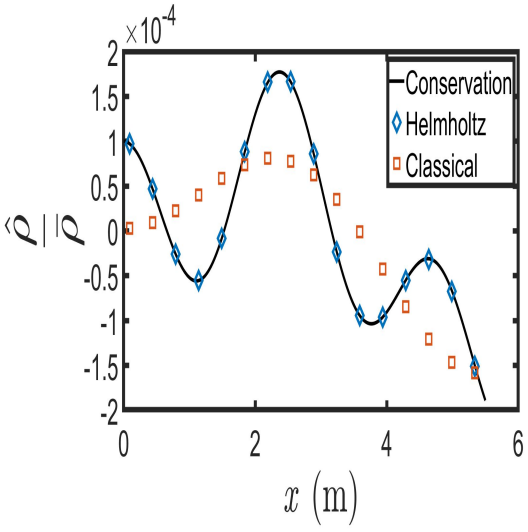

(j) $\omega = 500$ rad/s

Figure B.4: Density Fluctuations for non-linear profile - case IV

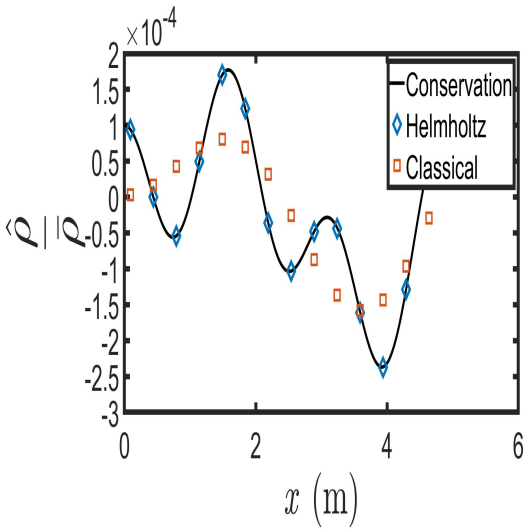

(k) $\omega = 750$ rad/s

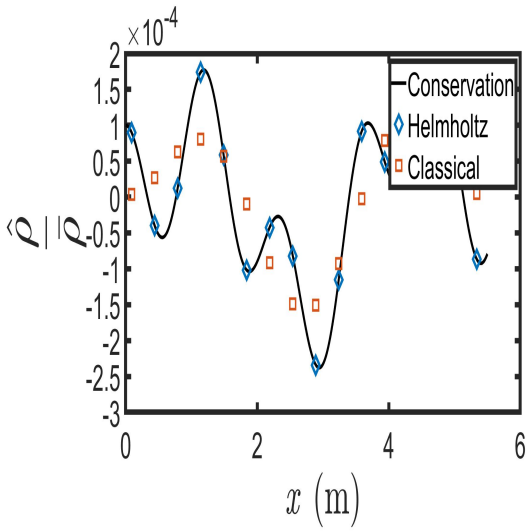

(l) $\omega = 1000$ rad/s

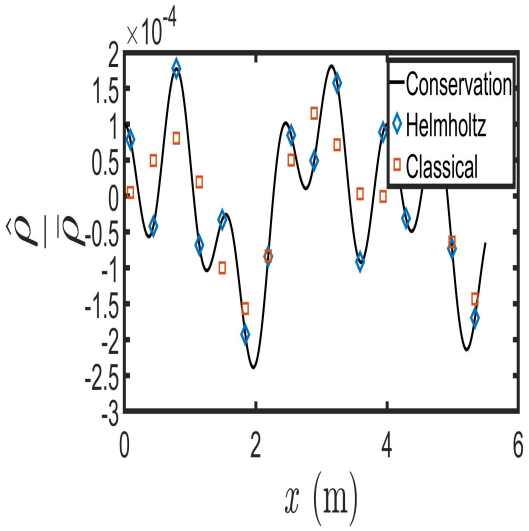

(m) $\omega = 1500$ rad/s

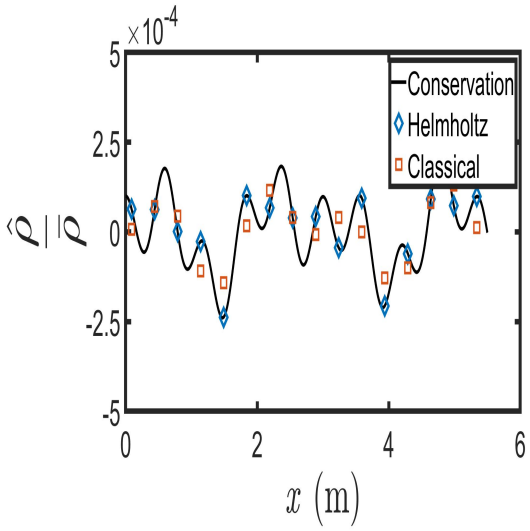

(n) $\omega = 2000$ rad/s

Figure B.4: Density Fluctuations for non-linear profile - case IV

Appendix C

Supporting Plots for CASE V

C.1 Linear Temperature Profile

C.1.1 Pressure fluctuations across the duct

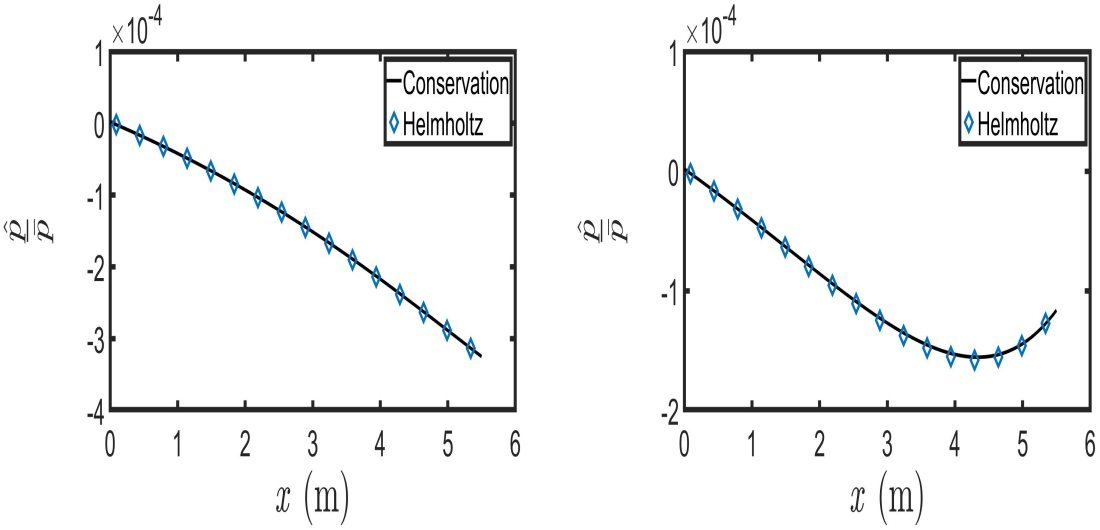

(a) $\omega = 50$ rad/s (b) $\omega = 100$ rad/s

Figure C.1: Pressure Fluctuations for linear profile - case V

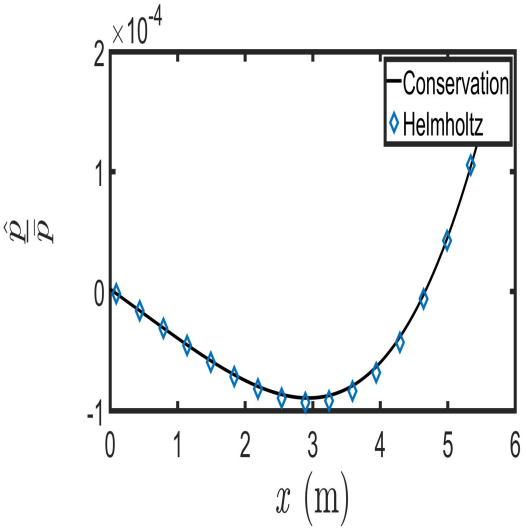

(c) $\omega = 150$ rad/s

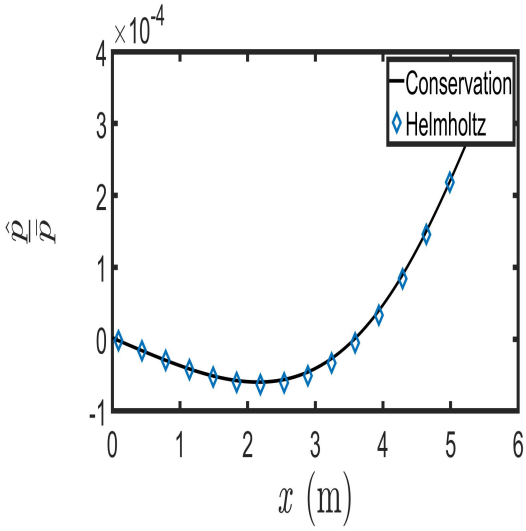

(d) $\omega = 200$ rad/s

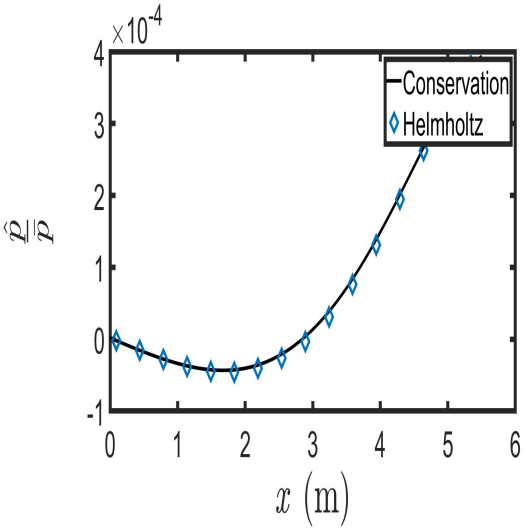

(e) $\omega = 250$ rad/s

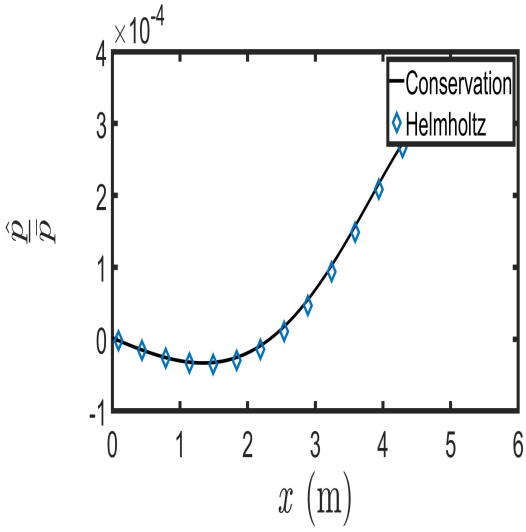

(f) $\omega = 300$ rad/s

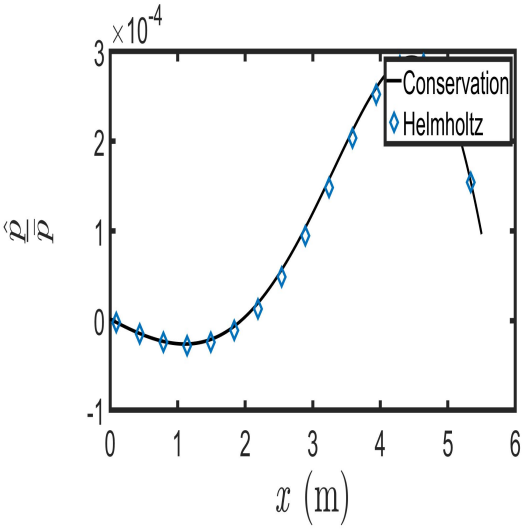

(g) $\omega = 350$ rad/s

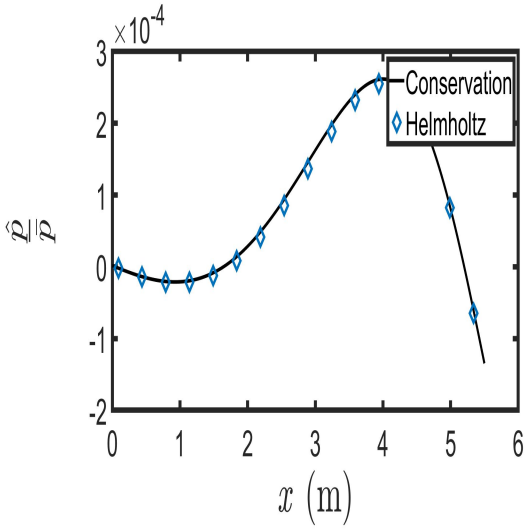

(h) $\omega = 400$ rad/s

Figure C.1: Pressure Fluctuations for linear profile - case V

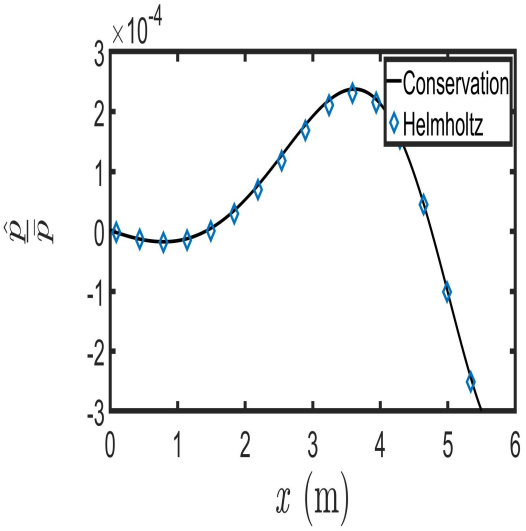

(i) $\omega = 450$ rad/s

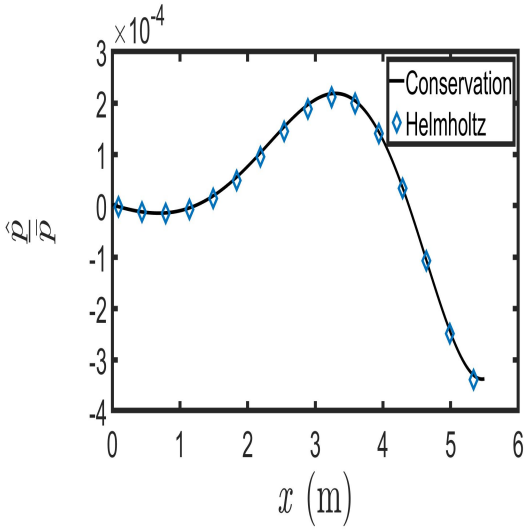

(j) $\omega = 500$ rad/s

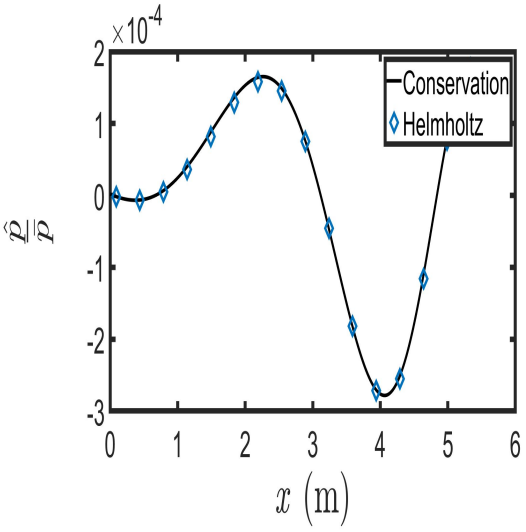

(k) $\omega = 750$ rad/s

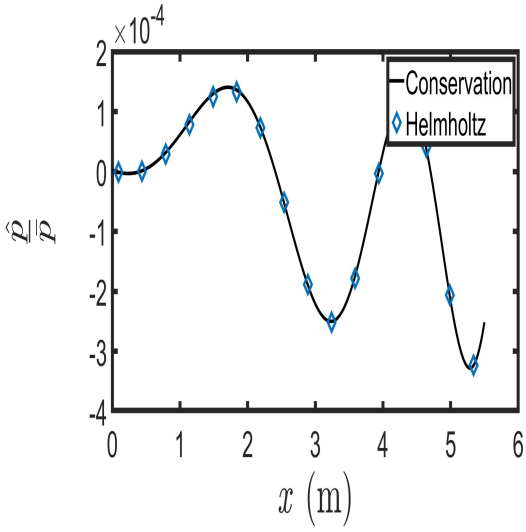

(l) $\omega = 1000$ rad/s

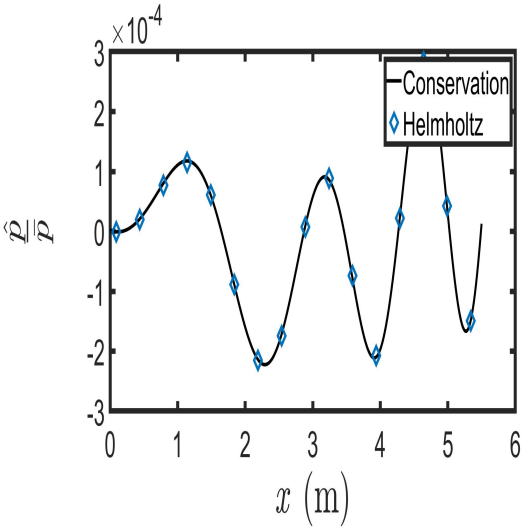

(m) $\omega = 1500$ rad/s

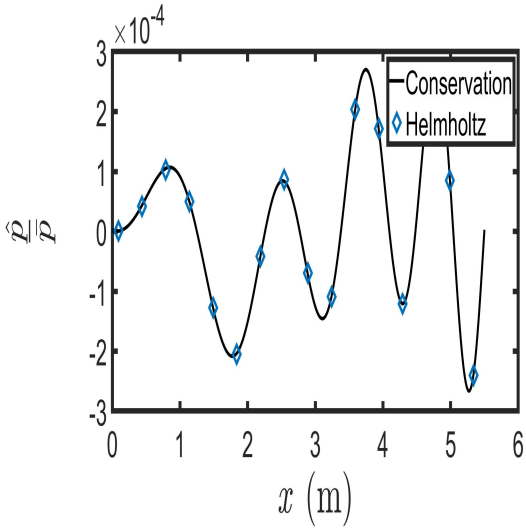

(n) $\omega = 2000$ rad/s

Figure C.1: Pressure Fluctuations for linear profile - case V

C.1.2 Density fluctuations across the duct

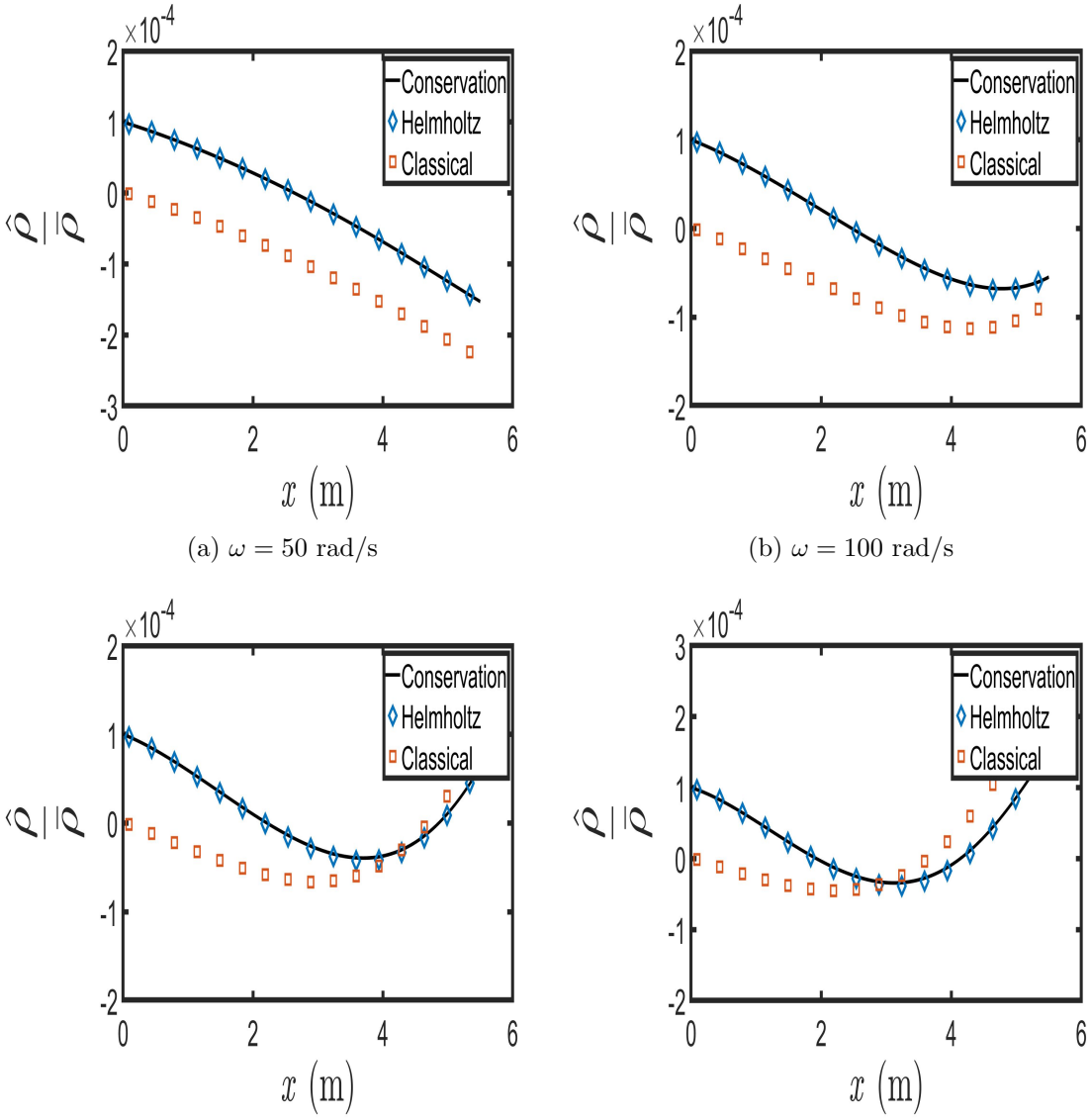

(a) $\omega = 50$ rad/s

(b) $\omega = 100$ rad/s

(c) $\omega = 150$ rad/s

(d) $\omega = 200$ rad/s

Figure C.2: Density Fluctuations for linear profile - case V

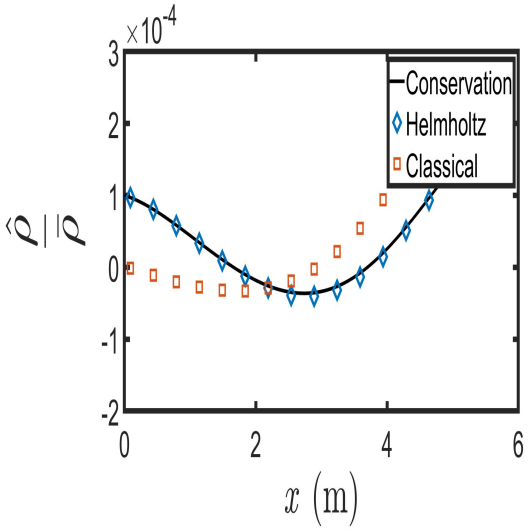

(e) $\omega = 250$ rad/s

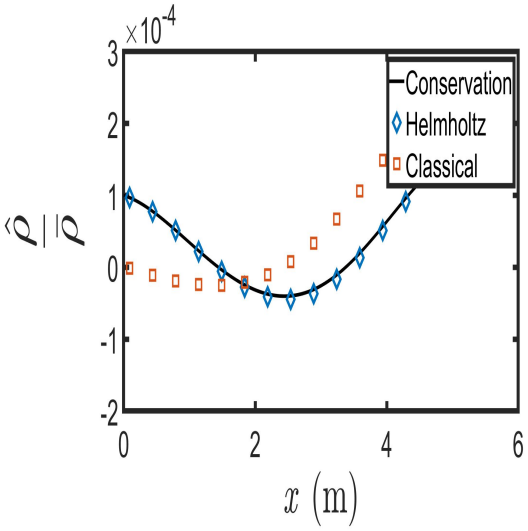

(f) $\omega = 300$ rad/s

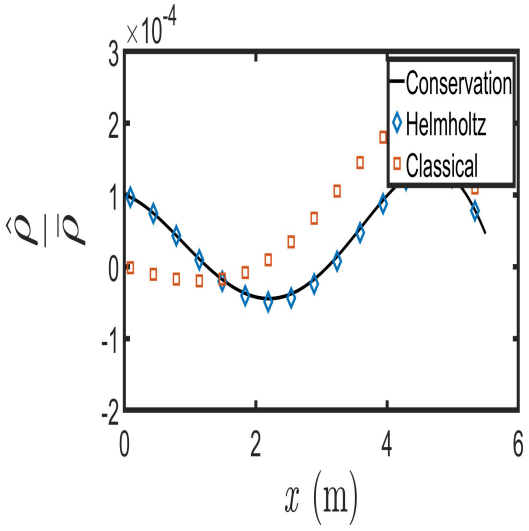

(g) $\omega = 350$ rad/s

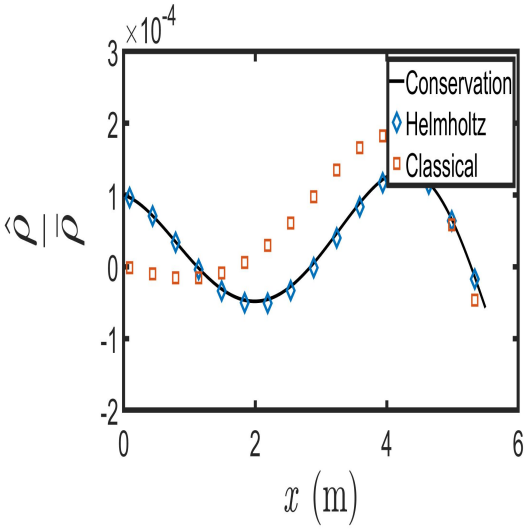

(h) $\omega = 400$ rad/s

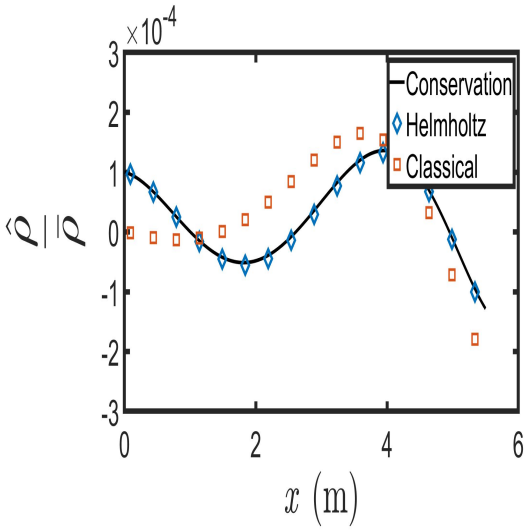

(i) $\omega = 450$ rad/s

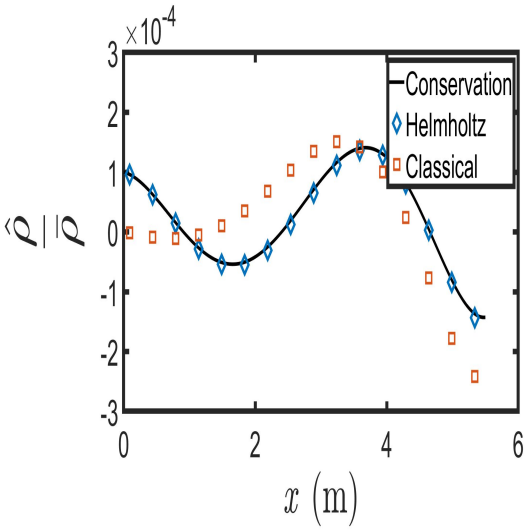

(j) $\omega = 500$ rad/s

Figure C.2: Density Fluctuations for linear profile - case V

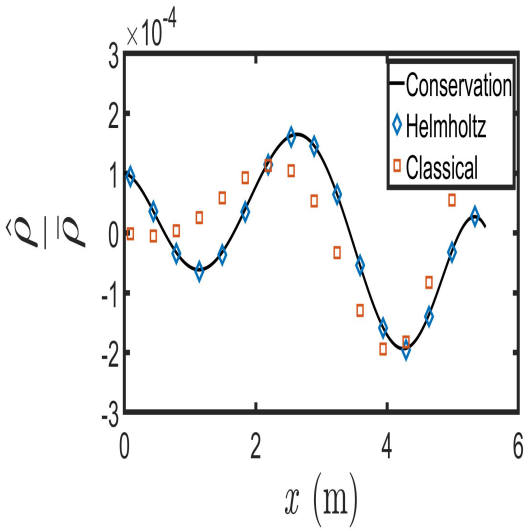

(k) $\omega = 750$ rad/s

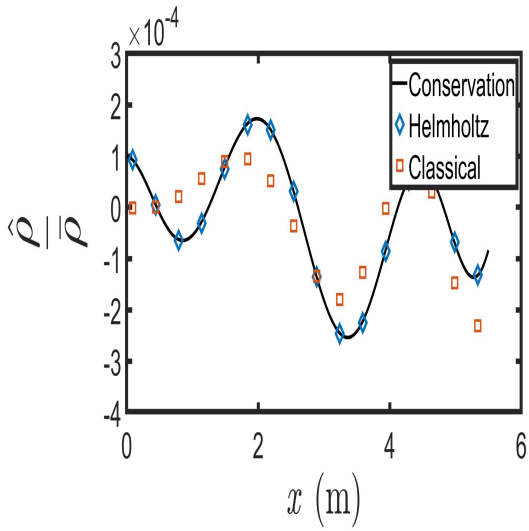

(l) $\omega = 1000$ rad/s

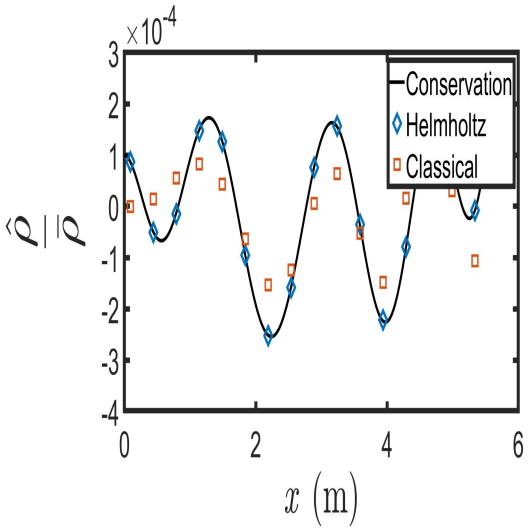

(m) $\omega = 1500$ rad/s

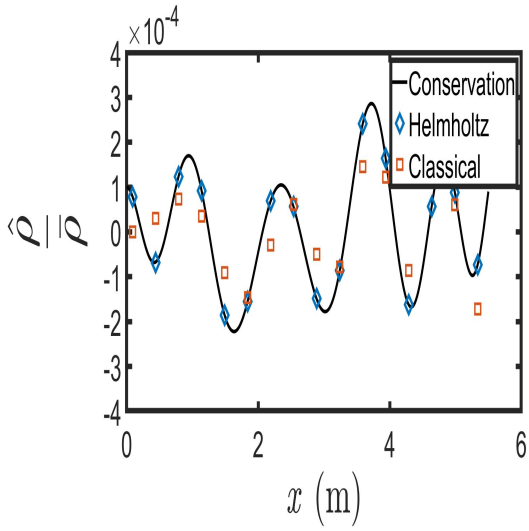

(n) $\omega = 2000$ rad/s

Figure C.2: Density Fluctuations for linear profile - case V

C.2 Four - Thirds Temperature Profile

C.2.1 Pressure fluctuations across the duct

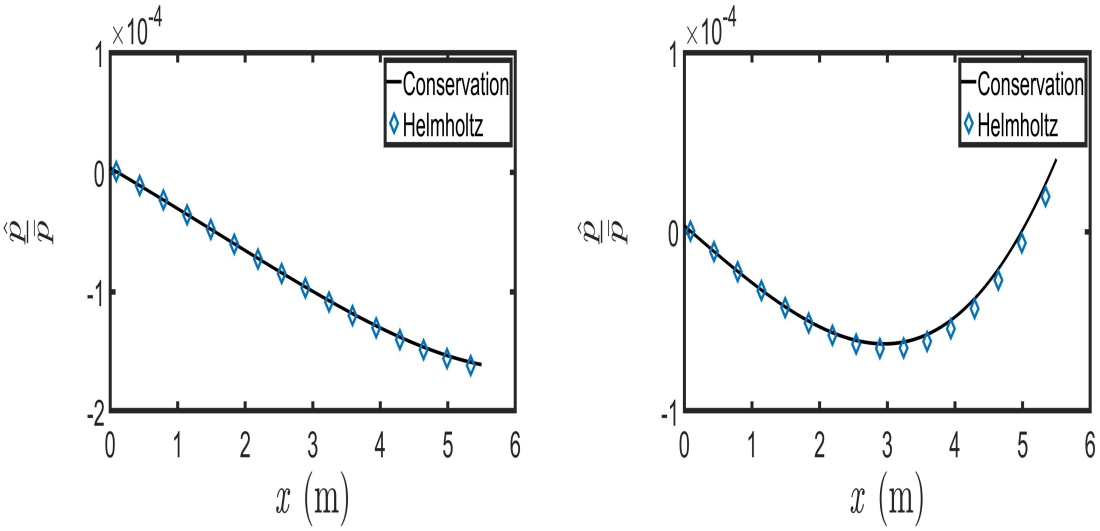

(a) $\omega = 50$ rad/s

(b) $\omega = 100$ rad/s

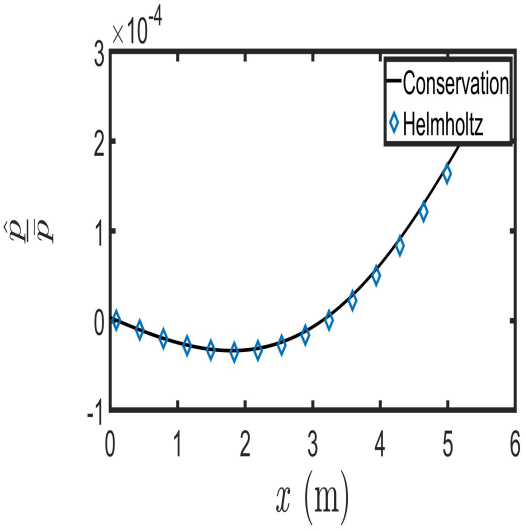

(c) $\omega = 150$ rad/s

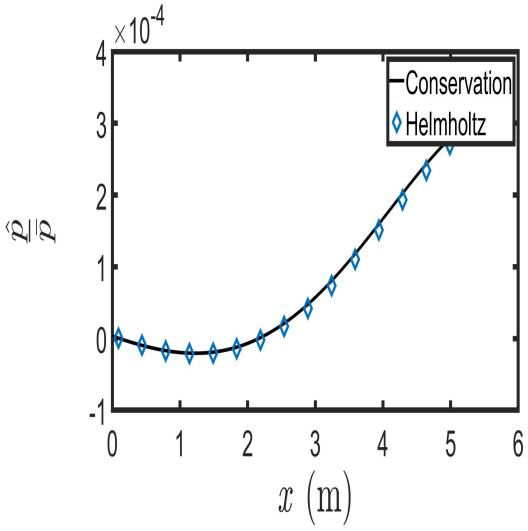

(d) $\omega = 200$ rad/s

Figure C.3: Pressure Fluctuations for non-linear profile - case V

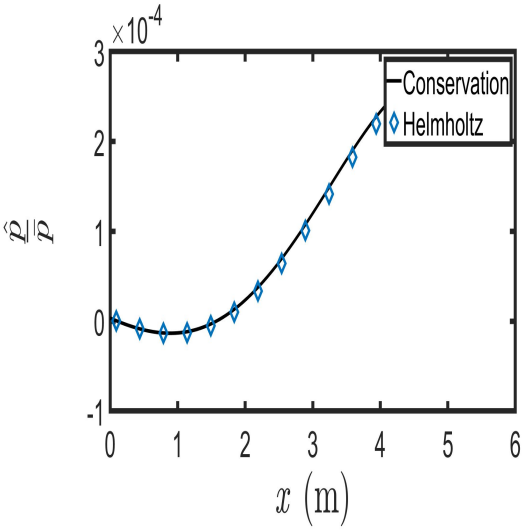

(e) $\omega = 250$ rad/s

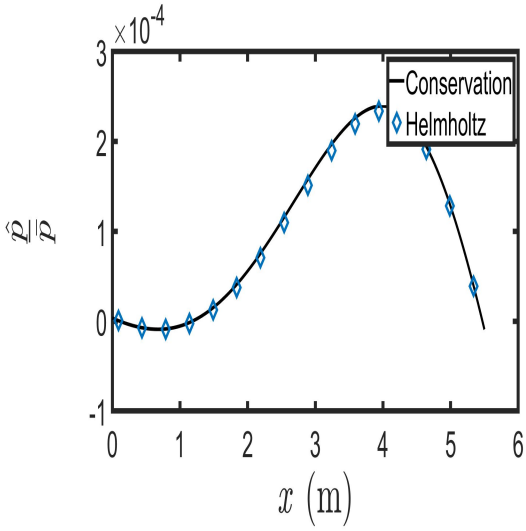

(f) $\omega = 300$ rad/s

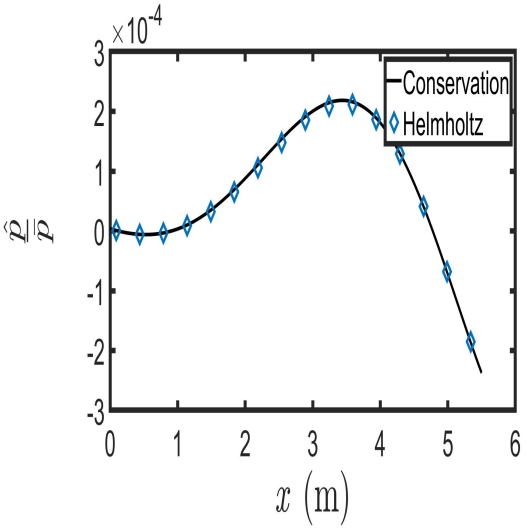

(g) $\omega = 350$ rad/s

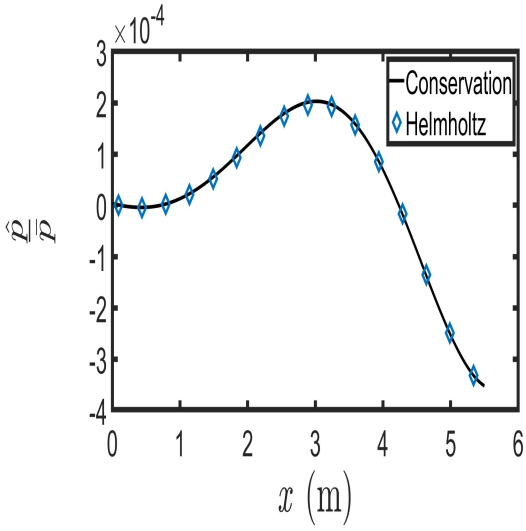

(h) $\omega = 400$ rad/s

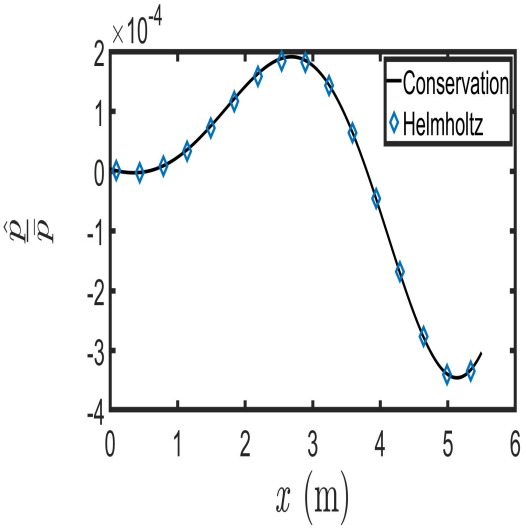

(i) $\omega = 450$ rad/s

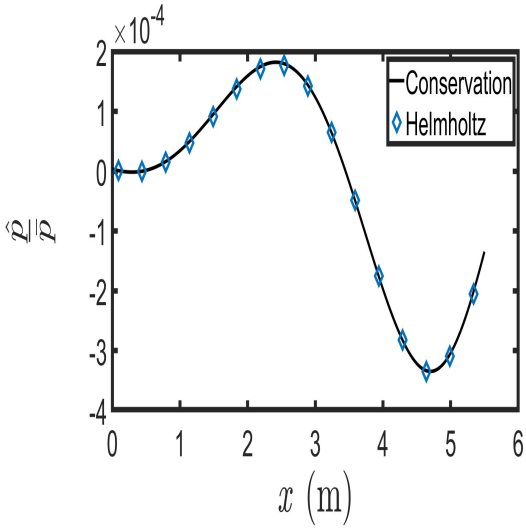

(j) $\omega = 500$ rad/s

Figure C.3: Pressure Fluctuations for non-linear profile - case V

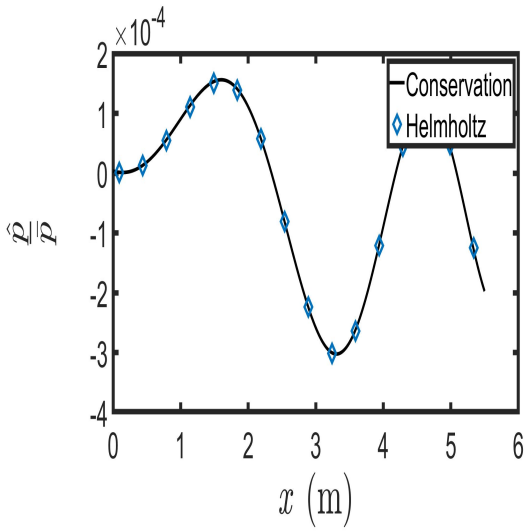

(k) $\omega = 750$ rad/s

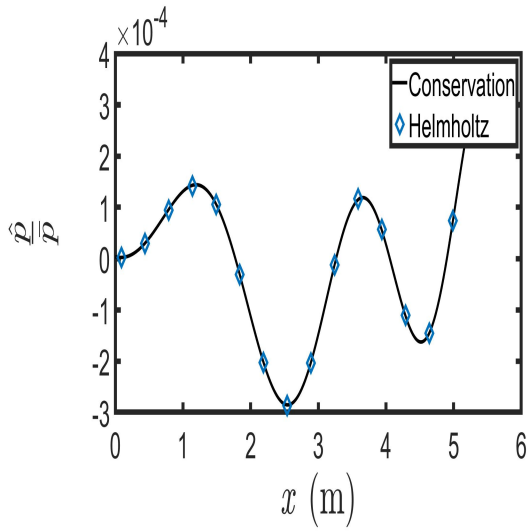

(l) $\omega = 1000$ rad/s

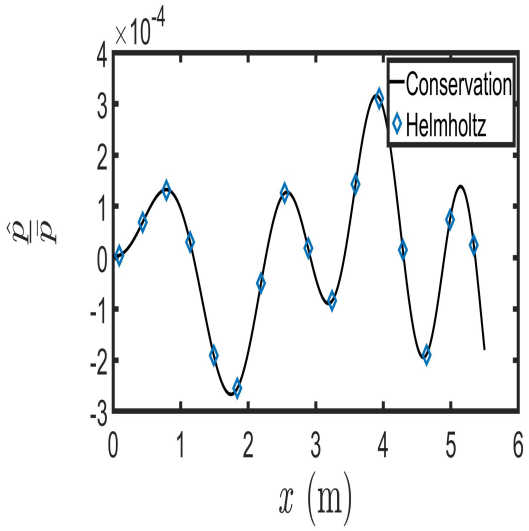

(m) $\omega = 1500$ rad/s

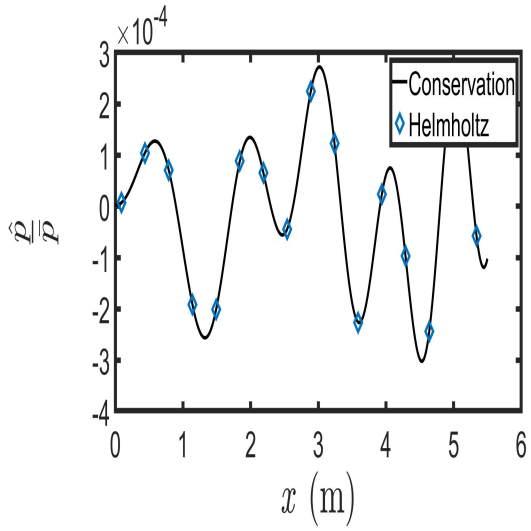

(n) $\omega = 2000$ rad/s

Figure C.3: Pressure Fluctuations for non-linear profile - case V

C.2.2 Density fluctuations across the duct

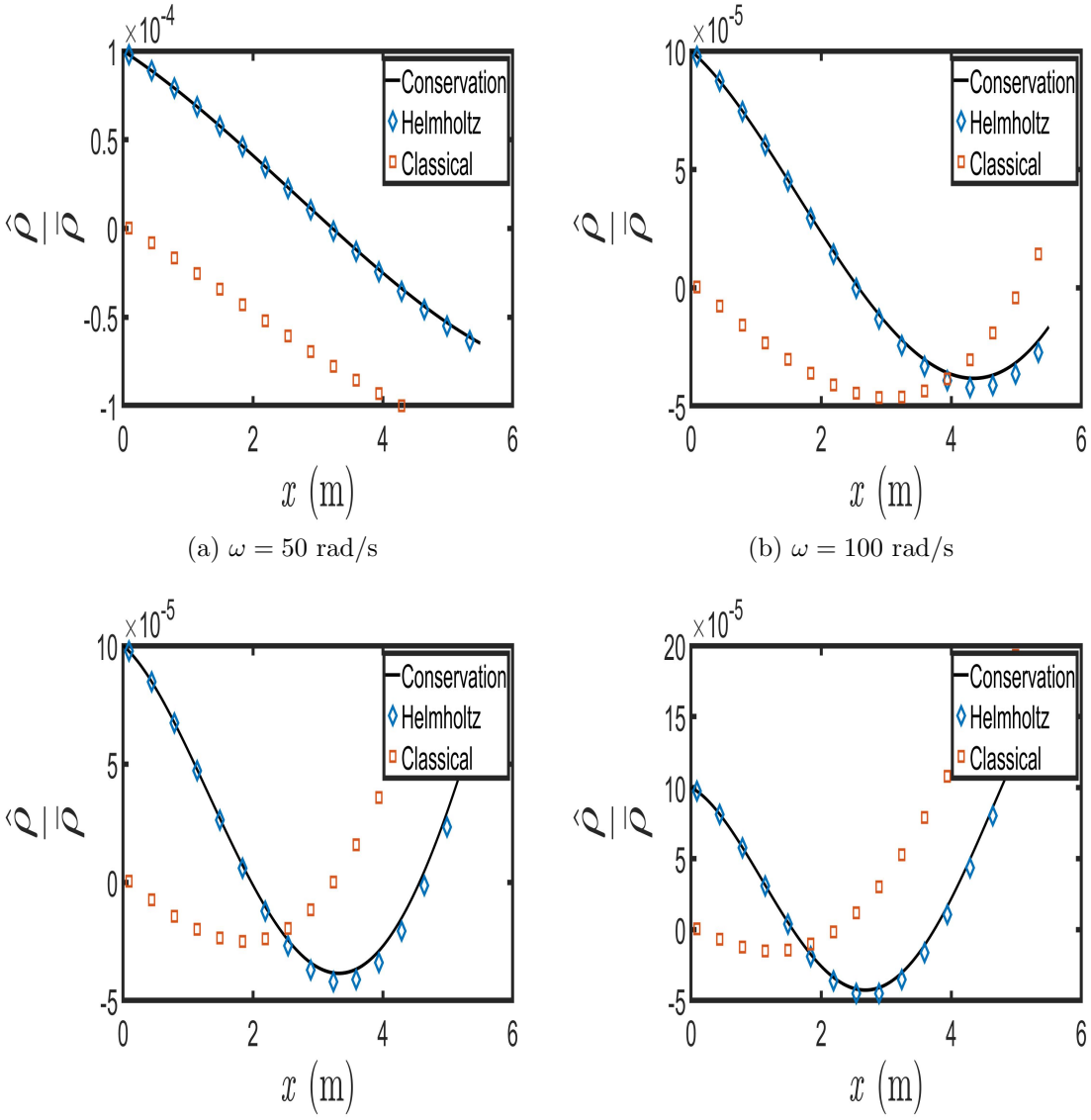

(a) $\omega = 50$ rad/s

(b) $\omega = 100$ rad/s

(c) $\omega = 150$ rad/s

(d) $\omega = 200$ rad/s

Figure C.4: Density Fluctuations for non-linear profile - case V

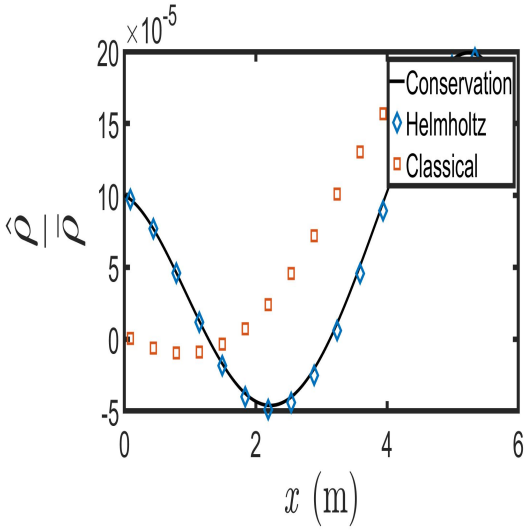

(e) $\omega = 250$ rad/s

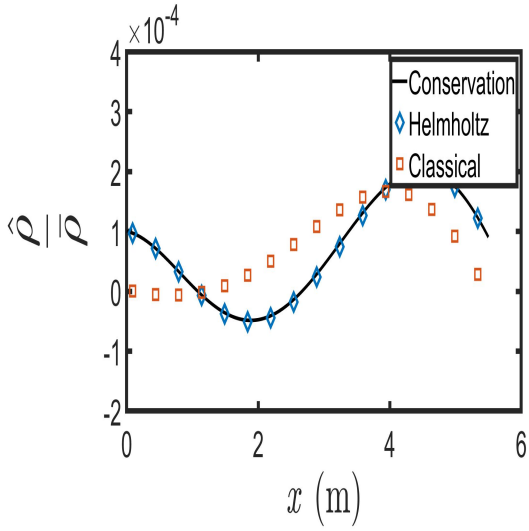

(f) $\omega = 300$ rad/s

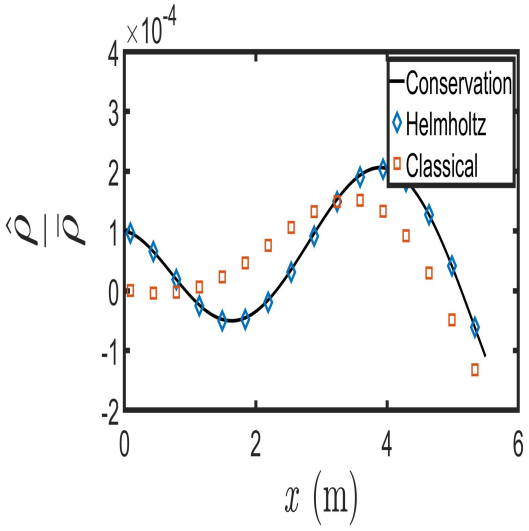

(g) $\omega = 350$ rad/s

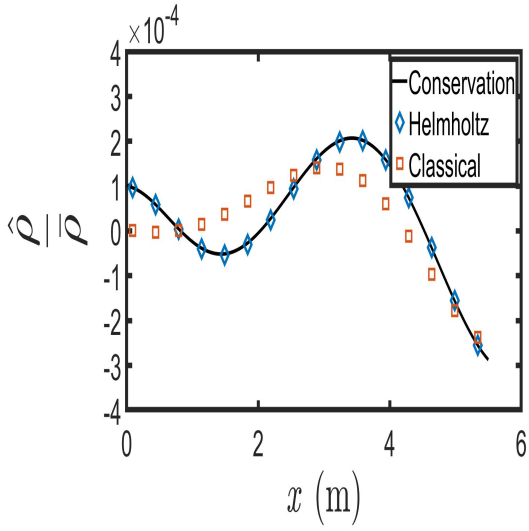

(h) $\omega = 400$ rad/s

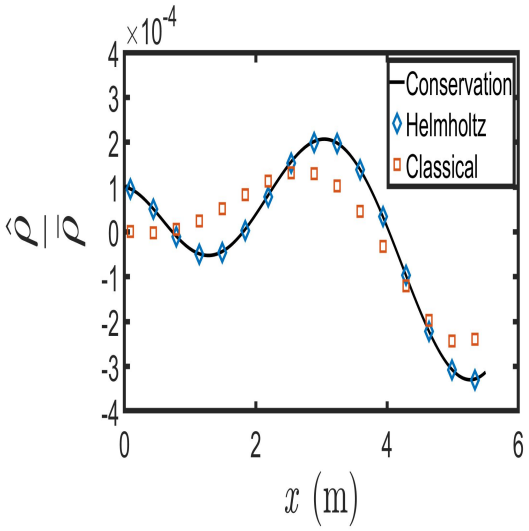

(i) $\omega = 450$ rad/s

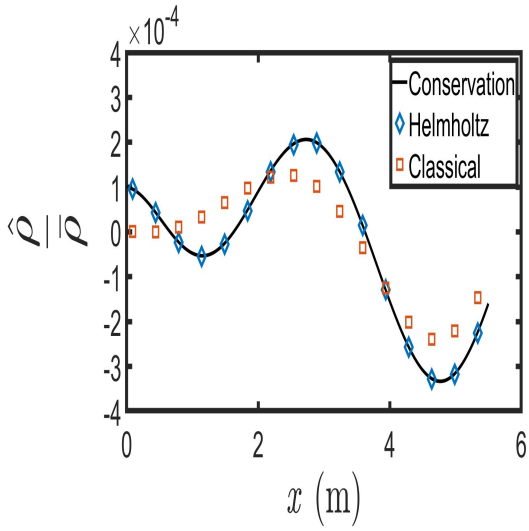

(j) $\omega = 500$ rad/s

Figure C.4: Density Fluctuations for non-linear profile - case V

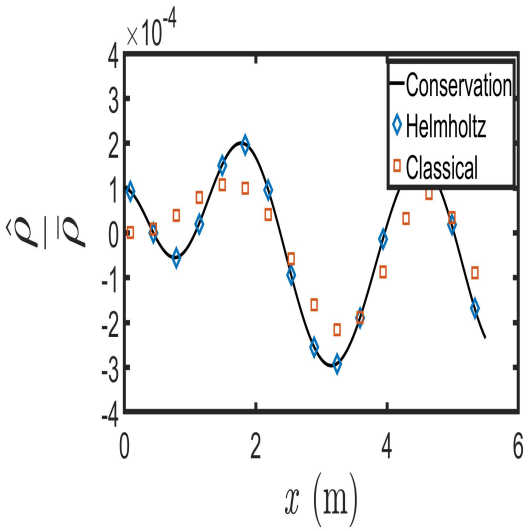

(k) $\omega = 750$ rad/s

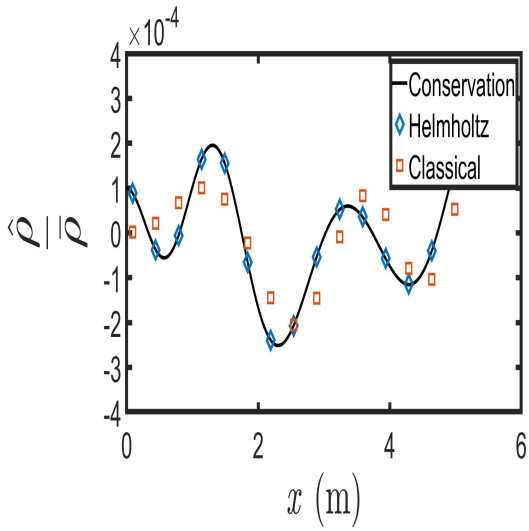

(l) $\omega = 1000$ rad/s

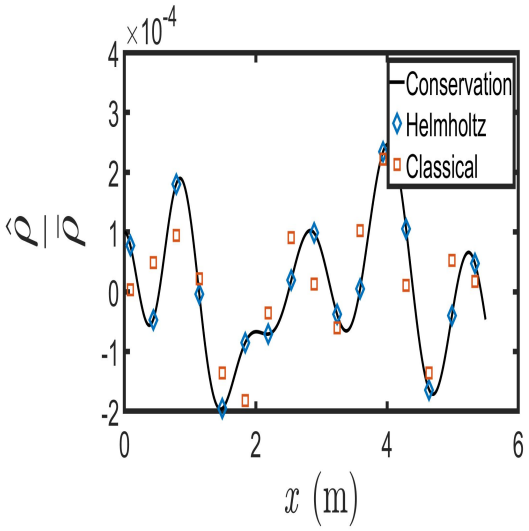

(m) $\omega = 1500$ rad/s

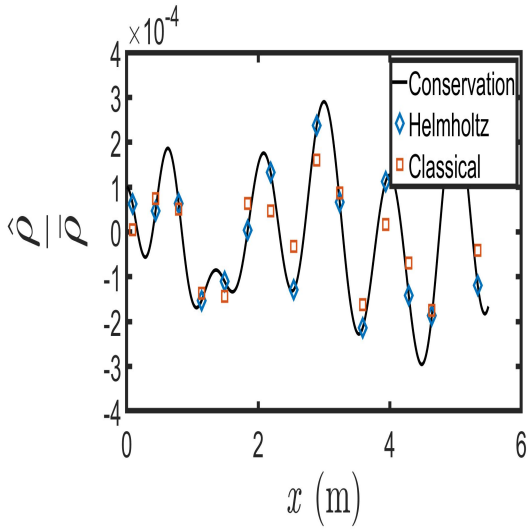

(n) $\omega = 2000$ rad/s

Figure C.4: Density Fluctuations for non-linear profile - case V

Bibliography

[1] Manchar Lal Munjal. *Acoustics of ducts and mufflers with application to exhaust and ventilation system design*. John Wiley & Sons, 1987.

[2] RI Sujith, GA Waldherr, and BT Zinn. An exact solution for one-dimensional acoustic fields in ducts with an axial temperature gradient. *Journal of Sound and Vibration*, 184(3):389–402, 1995.

[3] Vijaya Krishna Rani and Sarma L Rani. Wkb solutions to the quasi 1-d acoustic wave equation in ducts with non-uniform cross-section and inhomogeneous mean flow properties–acoustic field and combustion instability. *Journal of Sound and Vibration*, 436:183–219, 2018.

[4] John William Strutt Baron Rayleigh. *The theory of sound*, volume 2. Macmillan, 1896.

[5] Lawrence E Kinsler, Austin R Frey, Alan B Coppens, and James V Sanders. Fundamentals of acoustics. *Fundamentals of Acoustics, 4th Edition, by Lawrence E. Kinsler, Austin R. Frey, Alan B. Coppens, James V. Sanders, pp. 560. ISBN 0-471-84789-5. Wiley-VCH, December 1999.*, page 560, 1999.

[6] Allan D Pierce and Robert T Beyer. *Acoustics: An Introduction to Its Physical Principles and Applications. 1989 Edition*. ASA, 1990.

[7] Paul Filippi, Aime Bergassoli, Dominique Habault, and Jean Pierre Lefebvre. *Acoustics: basic physics, theory, and methods*. Elsevier, 1998.

[8] Ann P Dowling and Simon R Stow. Acoustic analysis of gas turbine combustors. *Journal of propulsion and power*, 19(5):751–764, 2003.

[9] Osman K Mawardi. On the generalization of the concept of impedance in acoustics. *The Journal of the Acoustical Society of America*, 23(5):571–576, 1951.

[10] ML Munjal and MG Prasad. On plane-wave propagation in a uniform pipe in the presence of a mean flow and a temperature gradient. *The Journal of the Acoustical Society of America*, 80(5):1501–1506, 1986.

[11] KS Peat. A first aproximation to the effects of mean flow on sound propagation through cylindrical capillary tubes. *Journal of Sound and Vibration*, 175(4):475–489, 1994.

[12] M Bednarik, M Cervenka, P Lotton, and G Penelet. Behavior of plane waves propagating through a temperature-inhomogeneous region. *Journal of Sound and Vibration*, 362:292–304, 2016.

[13] Alvin J Robins. Exact solutions of the helmholtz equation for plane wave propagation in a medium with variable density and sound speed. *The Journal of the Acoustical Society of America*, 93(3):1347–1352, 1993.

[14] Tobias Holzinger, Alejandro Cardenas, and Wolfgang Polifke. An analytical solution for acoustic wave propagation in a narrow duct with mean temperature gradient. In *16th AIAA/CEAS Aeroacoustics Conference*, page 3891, 2010.

[15] B Karthik, B Manoj Kumar, and RI Sujith. Exact solutions to one-dimensional acoustic fields with temperature gradient and mean flow. *The Journal of the Acoustical Society of America*, 108(1):38–43, 2000.

[16] P Bala Subrahmanyam, RI Sujith, and Tim C Lieuwen. A family of exact transient solutions for acoustic wave propagation in inhomogeneous, non-uniform area ducts. *Journal of sound and vibration*, 240(4):705–715, 2001.

[17] A Cummings. Ducts with axial temperature gradients: an approximate solution for sound transmission and generation. *Journal of Sound and Vibration*, 51(1):55–67, 1977.

[18] Jingxuan Li and Aimee S Morgans. The one-dimensional acoustic field in a duct with arbitrary mean axial temperature gradient and mean flow. *Journal of Sound and Vibration*, 400:248–269, 2017.